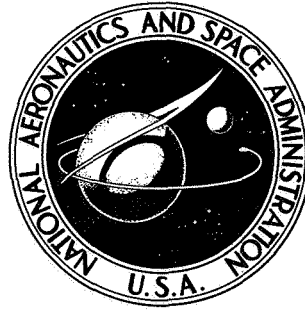


N71-31055

NASA TECHNICAL NOTE



NASA TN D-6365

NASA TN D-6365

**CASE FILE
COPY**

**THE UTILIZATION OF HALO ORBITS
IN ADVANCED LUNAR OPERATIONS**

by Robert W. Farquhar

Goddard Space Flight Center

Greenbelt, Md. 20771

NATIONAL AERONAUTICS AND SPACE ADMINISTRATION • WASHINGTON, D. C. • JULY 1971

1. Report No. NASA TN D-6365	2. Government Accession No.	3. Recipient's Catalog No.	
4. Title and Subtitle The Utilization of Halo Orbits in Advanced Lunar Operations		5. Report Date July 1971	
		6. Performing Organization Code	
7. Author(s) Robert W. Farquhar		8. Performing Organization Report No. G-1025	
9. Performing Organization Name and Address Goddard Space Flight Center Greenbelt, Maryland 20771		10. Work Unit No.	
		11. Contract or Grant No.	
		13. Type of Report and Period Covered Technical Note	
12. Sponsoring Agency Name and Address National Aeronautics and Space Administration Washington, D. C. 20546		14. Sponsoring Agency Code	
		15. Supplementary Notes	
16. Abstract <p>Flight mechanics and control problems associated with the stationing of spacecraft in halo orbits about the translunar libration point are discussed in some detail. Practical procedures for the implementation of the control techniques are described, and it is shown that these procedures can be carried out with very small ΔV costs.</p> <p>The possibility of using a relay satellite in a halo orbit to obtain a continuous communications link between the earth and the far side of the moon is also discussed. Several advantages of this type of lunar far-side data link over more conventional relay-satellite systems are cited. It is shown that, with a halo relay satellite, it would be possible to continuously control an unmanned lunar roving vehicle on the moon's far side. Backside tracking of lunar orbiters could also be realized.</p> <p>The desirability of locating a lunar space station in a halo orbit instead of a lunar polar orbit as recommended in the current NASA Integrated Program Plan is investigated. It is found that the halo-orbit location is superior in almost every respect. Of particular significance is the finding that the performance of a reusable lunar shuttle transportation system using halo-orbit rendezvous is better than that of one using lunar-orbit rendezvous.</p>			
17. Key Words Suggested by Author Halo Orbit Lunar Communications Lunar Shuttle Lunar Space Station		18. Distribution Statement Unclassified - Unlimited	
19. Security Classif. (of this report) Unclassified	20. Security Classif. (of this page) Unclassified	21. No. of Pages 101	22. Price * 3.00

* For sale by the National Technical Information Service, Springfield, Virginia 22151

FOREWORD

It is the policy of the National Aeronautics and Space Administration to employ, in all formal publications, the international metric units known collectively as the *Système Internationale d'Unités* and designated SI in all languages. In certain cases, however, utility requires that other systems of units be retained in addition to the SI units.

This document contains data so expressed because the use of the SI equivalents alone would impair communication. The non-SI units, given in parentheses following their computed SI equivalents, are the basis of the measurements and calculations reported here.

CONTENTS

	Page
Abstract	i
Foreword	ii
List of Acronyms	v
I. INTRODUCTION	1
II. MECHANICS OF HALO SATELLITES	3
A. Motion in the Vicinity of the Translunar Libration Point	3
B. Orbit Control	5
C. Transfer Trajectories	23
III. LUNAR FAR-SIDE COMMUNICATIONS LINK	29
A. Synchronous Halo Monitor (SHALOM)	29
B. Importance in Anticipated Unmanned Lunar Program	30
C. Spacecraft Considerations	32
D. Complete Lunar Communications Network	35
IV. HALO-ORBIT SPACE STATION IN SUPPORT OF AN EXPANDED LUNAR EXPLORATION PROGRAM	41
A. Elements of Expanded Lunar Program	41
B. Role of Halo-Orbit Space Station (HOSS)	42
C. Lunar Transportation System Performance	49
D. Use of HOSS as a Launching Platform for Unmanned Planetary Probes	61
V. CONCLUSIONS AND RECOMMENDATIONS	73
ACKNOWLEDGMENT	73
References	75

CONTENTS-continued

	Page
Appendix A—Nonlinear Equations of Motion	77
Appendix B—Analytical Solution for Lissajous Nominal Path	83
Appendix C—Fuel Cost for z-Axis Period Control	89
Appendix D—Derivation of Performance Function for a Two-Stage Space Tug . . .	91
Appendix E—Derivation of Performance Function for a Two-Stage Lunar Shuttle System	95
Appendix F—Derivation of Performance Function for a Lunar Shuttle System With a Two-Stage COOS	99

List of Acronyms

SHALOM	Synchronous halo monitor
HOSS	Halo-orbit space station
LOSS	Lunar-orbit space station
PSD	Propellant storage depot
OOS	Orbit-to-orbit shuttle
COOS	Chemical orbit-to-orbit shuttle
NOOS	Nuclear orbit-to-orbit shuttle

THE UTILIZATION OF HALO ORBITS IN ADVANCED LUNAR OPERATIONS

by

Robert W. Farquhar
Goddard Space Flight Center

CHAPTER I INTRODUCTION

The fact that the moon always presents the same hemisphere towards the earth both aids and hinders lunar exploration. Near-side lunar missions have been simplified because they have had direct access to at least one of the earth-based control centers. However, far-side lunar operations will continue to be rather awkward until an uninterrupted communications link with the earth is established. In 1966, an unusual relay-satellite scheme that would eliminate far-side communications blackout periods was presented (Reference 1). With this technique, a single relay satellite that is forced to follow a so-called halo orbit would provide continuous communications coverage for most of the moon's far side. The halo-satellite relay concept is illustrated in Figure 1. A comparison of this concept with another proposal that calls for two or more relay satellites in a lunar polar orbit will be given in this paper.

In the initial planning phase for the Apollo program, two rendezvous locations were considered. One was in earth orbit, and the other was in a low-altitude lunar orbit. As is well known, the lunar-orbit rendezvous mode was finally selected. Therefore, it is understandable that when the reusable lunar shuttle transportation system was first proposed, the lunar-orbit rendezvous technique was readily accepted. However, other rendezvous modes should receive some consideration before a final choice is made. In this paper, a new lunar shuttle mode that uses halo-orbit rendezvous will be investigated. The relative merits of the lunar-orbit and halo-orbit rendezvous concepts will be discussed at length.

Up to now, the usefulness of halo orbits has been overlooked in planning a future lunar exploration program. It is the purpose of this paper to exhibit the unique importance of halo orbits for both manned and unmanned lunar operations.

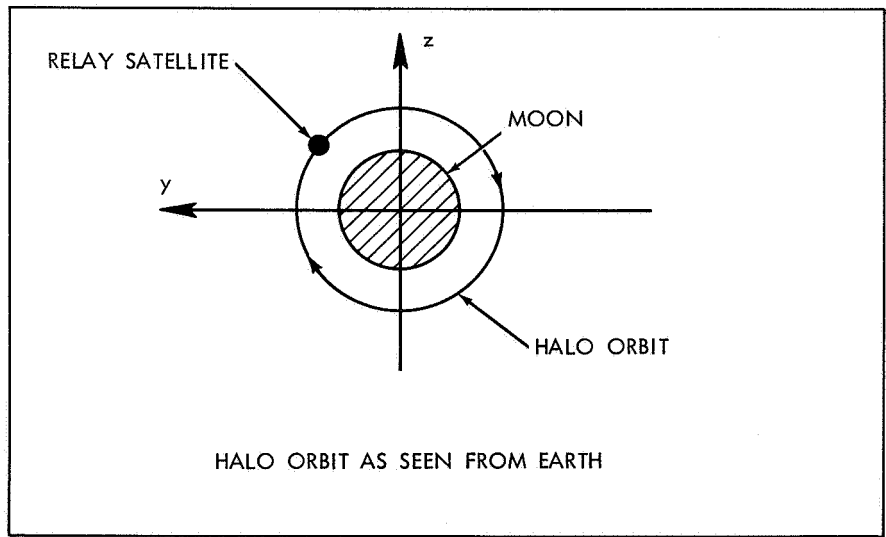
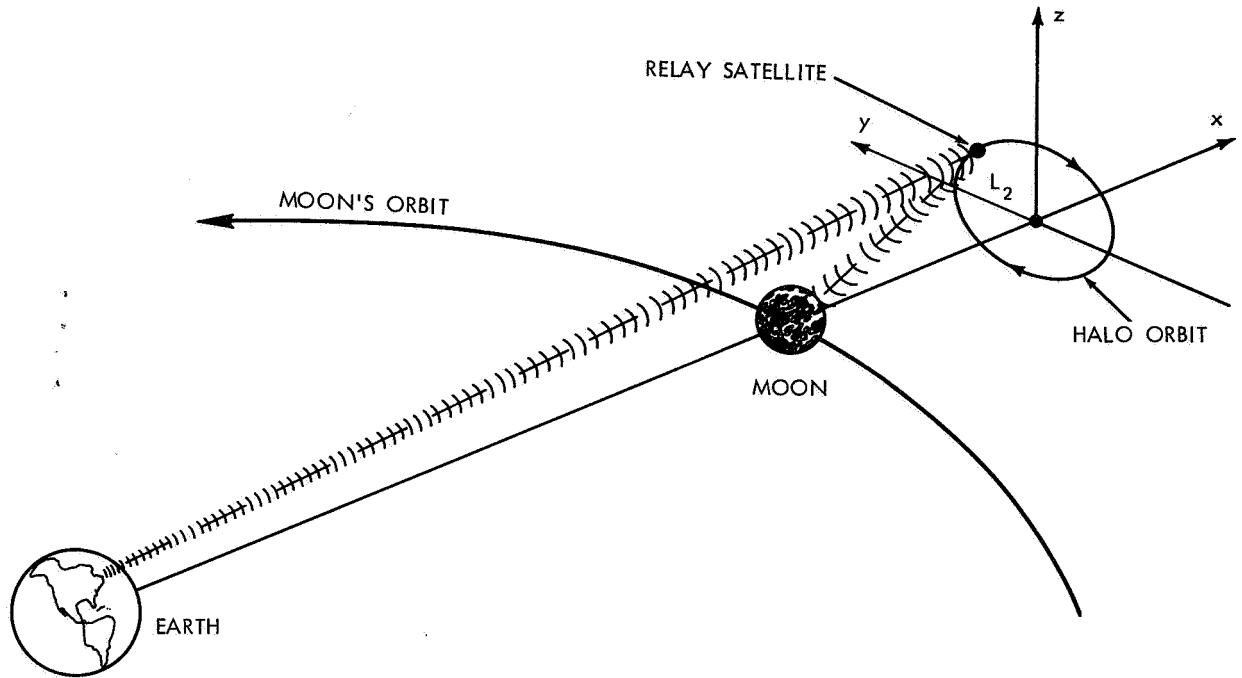


Figure 1—Lunar far-side communications with halo satellite.

CHAPTER II

MECHANICS OF HALO SATELLITES

Before the utility of halo satellites in future lunar operations is discussed, a brief description of the flight mechanics associated with the placement and maintenance of satellites in halo orbits is in order. Therefore, an overview of the orbit-control techniques and the basic transfer trajectories for these satellites is presented here; most mathematical details are relegated to the appendices.

A. Motion in the Vicinity of the Translunar Libration Point

As was shown by Lagrange in 1772, there are five points in the earth-moon gravitational field with the interesting property that if a satellite were placed at one of them with the proper velocity, it would be in equilibrium because the gravitational accelerations acting on the satellite would be counterbalanced by its centripetal acceleration (i. e., accelerations are balanced in the rotating reference frame). These "libration points" are all located in the moon's orbital plane, and their general configuration is depicted in Figure 2. This paper will be primarily concerned with the translunar libration point L_2 .

1. Equations of Motion

It should be noted at the outset that the distance between L_2 and the moon is not constant. However, the ratio of this distance to the instantaneous earth-moon distance R is constant; that is,

$$\gamma_L = \frac{d_2}{R} = 0.1678331476 \quad (1)$$

Consider the motion of a satellite in the vicinity of the L_2 point. If a Cartesian coordinate system (x, y, z) is fixed at L_2 , it can be shown that the linearized equations of motion are* (Reference 2)

$$\ddot{x} - 2\dot{y} - (2B_L + 1)x = 0 \quad (2a)$$

$$\ddot{y} + 2\dot{x} + (B_L - 1)y = 0 \quad (2b)$$

$$\ddot{z} + B_L z = 0 \quad (2c)$$

*The usual normalizations are employed, i.e., the following quantities are set equal to unity: (1) unperturbed mean earth-moon distance ($a = 384,748.91$ km); (2) mean angular rate of moon around earth ($n = 2.661699489 \times 10^{-6}$ rad/sec); (3) sum of the masses of the earth (M_\oplus) and of the moon (M_\ominus), where $M_\oplus/M_\ominus = 81.30$.

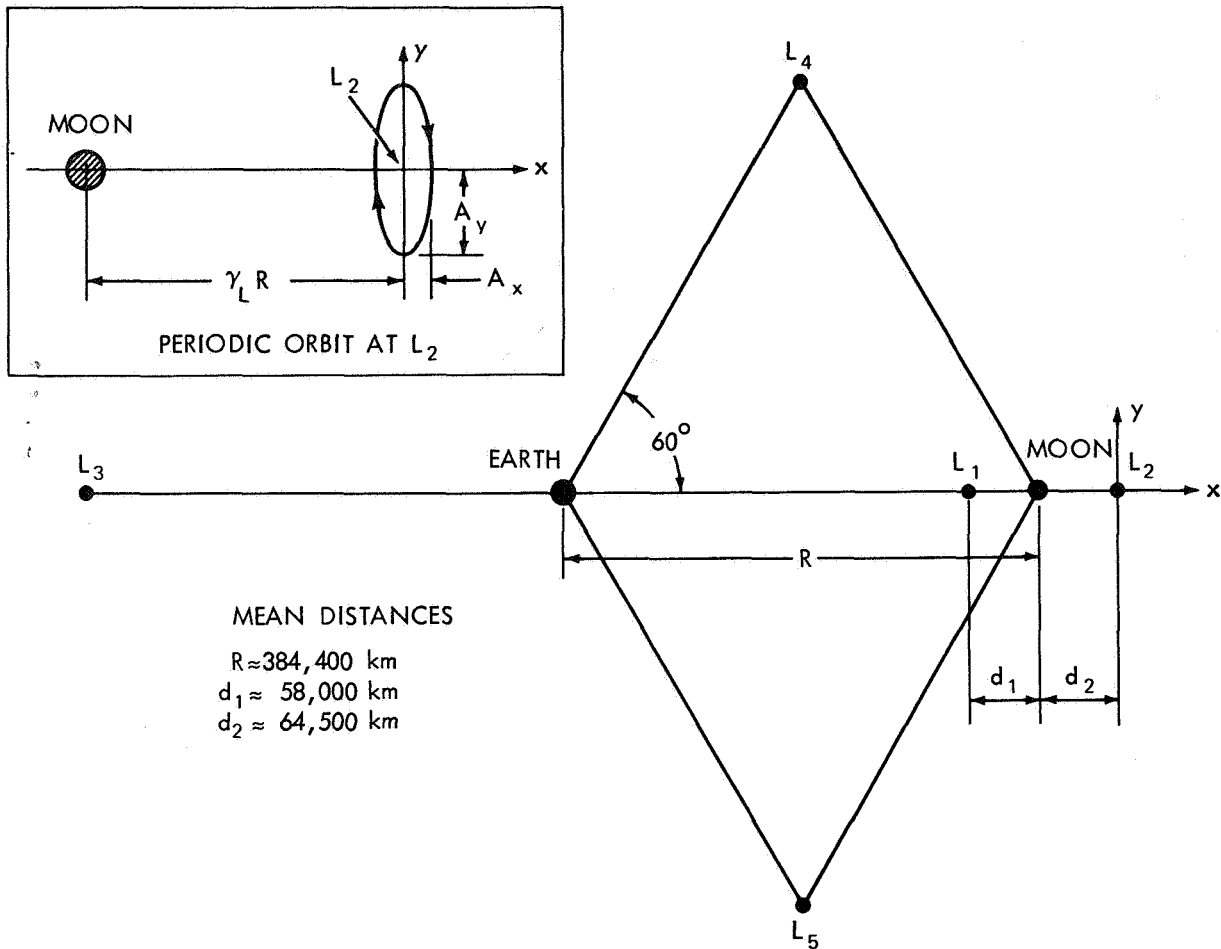


Figure 2—Libration points in the earth-moon system.

where $B_L = 3.19042$. It is immediately obvious that the motion along the z -axis is independent of the motion in the xy -plane and is simple harmonic. The motion in the xy -plane is coupled, and it can readily be shown (Reference 2) that this motion possesses an oscillatory mode as well as a divergent one. Because of the presence of this divergent mode, a satellite will require some stationkeeping if it is to remain near the L_2 point.

Although Equation 2 exhibits many of the principal features of motion in the vicinity of the L_2 point, it is an approximation that neglects the effects of nonlinearities, the eccentricity of the moon's orbit, and the influence of the sun's gravitational field.* The complexity introduced by these effects is illustrated by the more accurate set of equations given in Appendix A.

2. Periodic Orbits

If certain initial conditions are satisfied, it is possible for a satellite to follow a periodic orbit about the libration point, as shown in Figure 2. These initial conditions

*Solar radiation pressure could constitute another nonnegligible effect if the satellite had a large area-to-mass ratio.

are chosen so that only the oscillatory mode of the xy-motion is excited. However, the periodic orbit is unstable, and stationkeeping is necessary for the satellite to remain in this orbit.

A whole family of these orbits exist, and their equations are given by

$$\begin{aligned}x_n &= A_x \sin \omega_{xy} t \\y_n &= A_y \cos \omega_{xy} t\end{aligned}\tag{3}$$

where $\omega_{xy} = 1.86265$ and $A_x = 0.343336 A_y$. The periods of these periodic orbits are about 14.67 days.

B. Orbit Control

As noted above, the L_2 libration point and the periodic orbits around it are inherently unstable. Therefore, a satellite cannot remain in the vicinity of L_2 unless it is equipped with a stationkeeping system (e. g. , cold-gas jets). This question then arises: since some stationkeeping is required in any case, why isn't it just as easy to station the satellite at some other fixed point in the earth-moon system? The answer is that the stationkeeping fuel cost is significantly higher in the vicinity of a nonequilibrium point. In theory, the fuel cost at a libration point can be made arbitrarily small. The same arguments hold for the periodic orbits around the libration points.

In this section, some of the details of a promising stationkeeping technique for a satellite in the vicinity of the L_2 point are presented. Additional controls that are needed to maintain satellites in halo orbits are also discussed.

1. Stabilization

An extremely simple control law has been devised to suppress the divergent mode of Equations 2a and 2b. If the control acceleration $F_{cx} = -k_1 \dot{x} - k_2 x$ is added to the right-hand side of Equation 2a; asymptotic stability is achieved provided that $k_1 > 0$ and $k_2 > (2B_L + 1)$. This means that a satellite can remain at the L_2 point by using a control law that requires only range and range-rate measurements (i. e., x and \dot{x}). Moreover, the control acceleration is always directed along the same axis.

The aforementioned control scheme can also be used to maintain a satellite in a periodic orbit around L_2 . If the deviations from the periodic orbit of Equation 3 are denoted by $\xi = x - x_n$ and $\eta = y - y_n$, it can be shown that the linearized equations of motion relative to the orbit path are (Reference 2)

$$\begin{aligned} \ddot{\xi} - 2\dot{\eta} - [(2B_L + 1) - 6C_L A_x \sin \omega_{xy} t] \xi - (3C_L A_y \cos \omega_{xy} t) \eta &= F_{cx} \\ \ddot{\eta} + 2\dot{\xi} - (3C_L A_y \cos \omega_{xy} t) \xi + [(B_L - 1) - 3C_L A_x \sin \omega_{xy} t] \eta &= 0 \end{aligned} \quad (4)$$

where $F_{cx} = -k_1 \dot{\xi} - k_2 \xi$ and $C_L = 15.8451$. For values of $A_y < 10,000$ km (0.026 in normalized units), the satellite motion is stable so long as $k_2 > (2B_L + 1)$ and $k_1 > 3.5$. However, when A_y becomes too large, a more sophisticated control law is required for stabilization. *

2. Nominal Trajectories

Ideally, the fuel cost associated with the stabilization scheme described above could be made negligibly small; the only limitation is the noise in the range and range-rate measurements. However, it should be recalled that the periodic orbit of Equation 3 was obtained from the linearized equations of motion and is only a first approximation to accurate nominal trajectories around the L_2 point. The accurate nominal trajectories are actually quasi-periodic and can be obtained by finding particular solutions to equations of motion that include the effects of nonlinearities, lunar eccentricity, and the sun's gravitational field. If a satellite is forced to follow an inaccurate nominal path, the stationkeeping fuel expenditure can become quite high.

A nominal trajectory can be represented as a series of successive approximations of the form

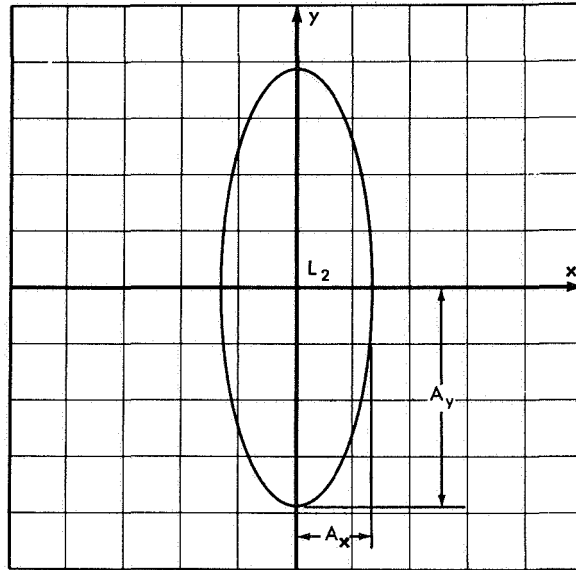
$$\begin{aligned} x_n &= x_1 + x_2 + x_3 + \dots \\ y_n &= y_1 + y_2 + y_3 + \dots \\ z_n &= z_1 + z_2 + z_3 + \dots \end{aligned} \quad (5)$$

where the subscript denotes the order of the term. With the use of a computer, to carry out the extensive algebraic manipulations, analytical nominal path solutions have been generated. * Some of these results are presented here.

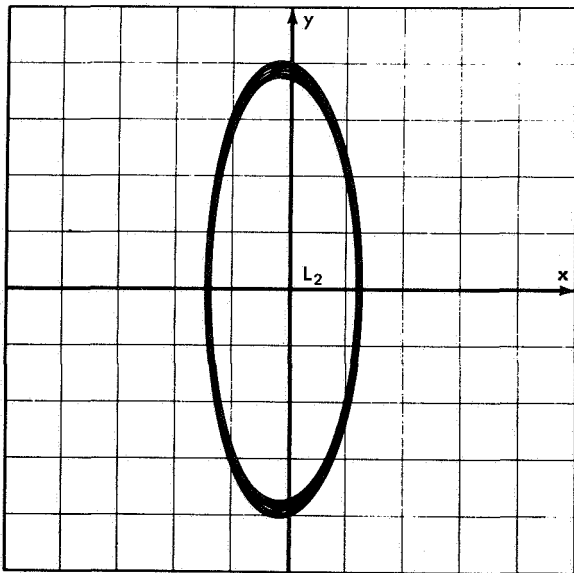
a. Lissajous Path

The third-order solution for the nominal path in the vicinity of L_2 is given in Appendix B. Traces of this solution for a one-year period are shown in Figures 3 and 4. Because the period of the oscillatory motion in the moon's orbital plane is 14.65 days, while the out-of-plane period is 15.23 days, the yz-projection of the nominal path is a Lissajous curve.

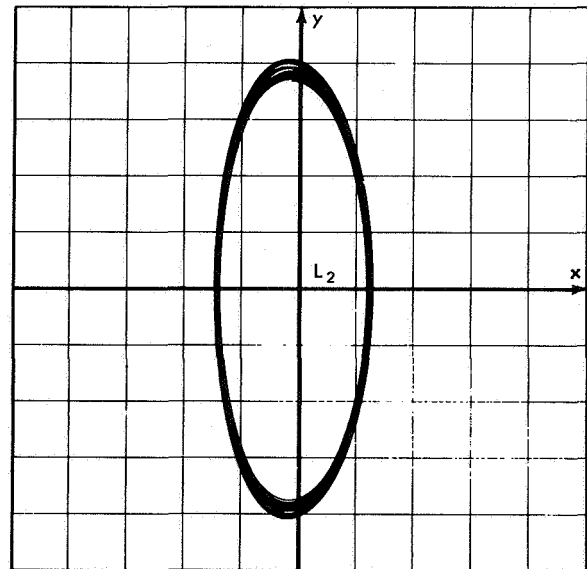
*Farquhar, R. W. and Kamel, A. A., "Satellite Stationkeeping in the Vicinity of the Translunar Libration Point", in preparation at National Aeronautics and Space Administration Goddard Space Flight Center, Greenbelt, Md. 20771.



FIRST ORDER

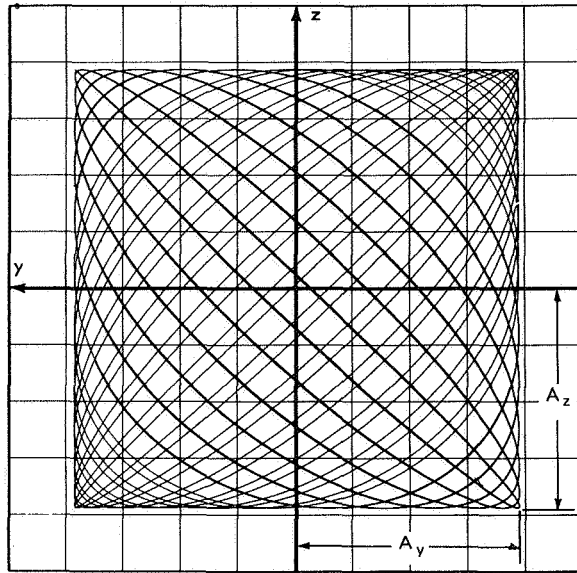


SECOND ORDER

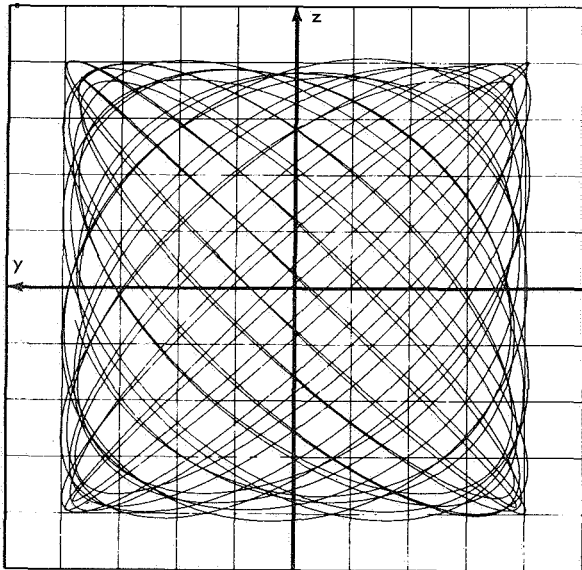


THIRD ORDER

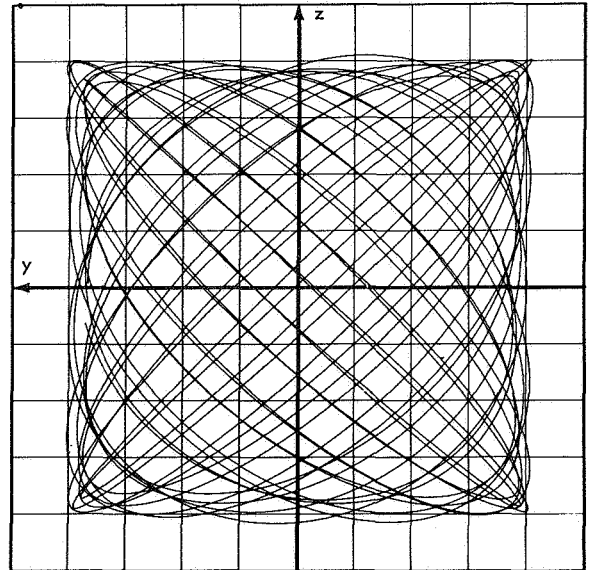
Figure 3—Lissajous nominal trajectory (projection in moon's orbital plane).
Grid size is 1290 km.



FIRST ORDER



SECOND ORDER



THIRD ORDER

Figure 4—Lissajous nominal trajectory (projection in plane perpendicular to earth-moon line). Grid size is 1290 km.

The effect of the accuracy of the nominal path on the stationkeeping fuel consumption has been tested with a computer simulation. For $A_y = A_z = 3500$ km, the average stationkeeping costs were as follows:

- (1) For the first-order nominal path, 571.8 mps/yr (1876 fps/yr);
- (2) For the second-order nominal path, 95.7 mps/yr (314 fps/yr);
- (3) For the third-order nominal path, 23.5 mps/yr (77 fps/yr).

These results dramatically illustrate the importance of an accurate nominal path.

b. Halo Path

For every value of $A_y > 32,871$ km, there is a corresponding value of A_z that will produce a nominal path where the fundamental periods of the y-axis and z-axis oscillations are equal. In this case, the nominal path as seen from the earth will never pass behind the moon. The exact relationship between A_y and A_z for this family of nominal paths is given in Figure 5.

It should be noted that the Lissajous nominal path solution of Appendix B is no longer valid in this instance, and that a new solution is required. The task of generating this halo nominal path has been completed* and traces for a typical trajectory for a one-year period are depicted in Figures 6-8. Because of the large values of A_y and A_z , the effects of the nonlinearities are quite pronounced. However, notice that the differences between the second-order and third-order solutions are barely distinguishable.

3. Period Control

For many applications, a small-amplitude satellite trajectory about L_2 is preferred. Unfortunately, the nominal trajectory for this case is a Lissajous path that will occasionally be hidden from the earth, as shown in Figure 9.** However, it is possible to use thrust control to alter the period of the z-axis oscillation so that it will be synchronized with that of the y-axis oscillation. When this is done, the nominal path is transformed into a halo orbit, as illustrated in Figure 10.

A simple control scheme to bring about this synchronization is to apply a thrust impulse along the z-axis every 7.32 days (Reference 3). The phase-plane representation of this technique is given in Figure 11. Although the main idea is diagrammed in Figure 11, it should be noted that the control logic is somewhat more complicated in actual practice.*

For operational reasons, it may be desirable to impart the period-control pulses less frequently than every 7.32 days. In this case, the amplitude of the halo orbit A_H must be increased to insure nonoccultation, because the satellite will follow a Lissajous nominal path between impulses. Higher-order nominal path corrections will cause an additional enlargement of A_H . These increases in A_H will in turn cause the average cost

* Farquhar and Kamel, op. cit.

** When the satellite is outside of the occulted zone, it will be visible from any point on the earth facing the moon.

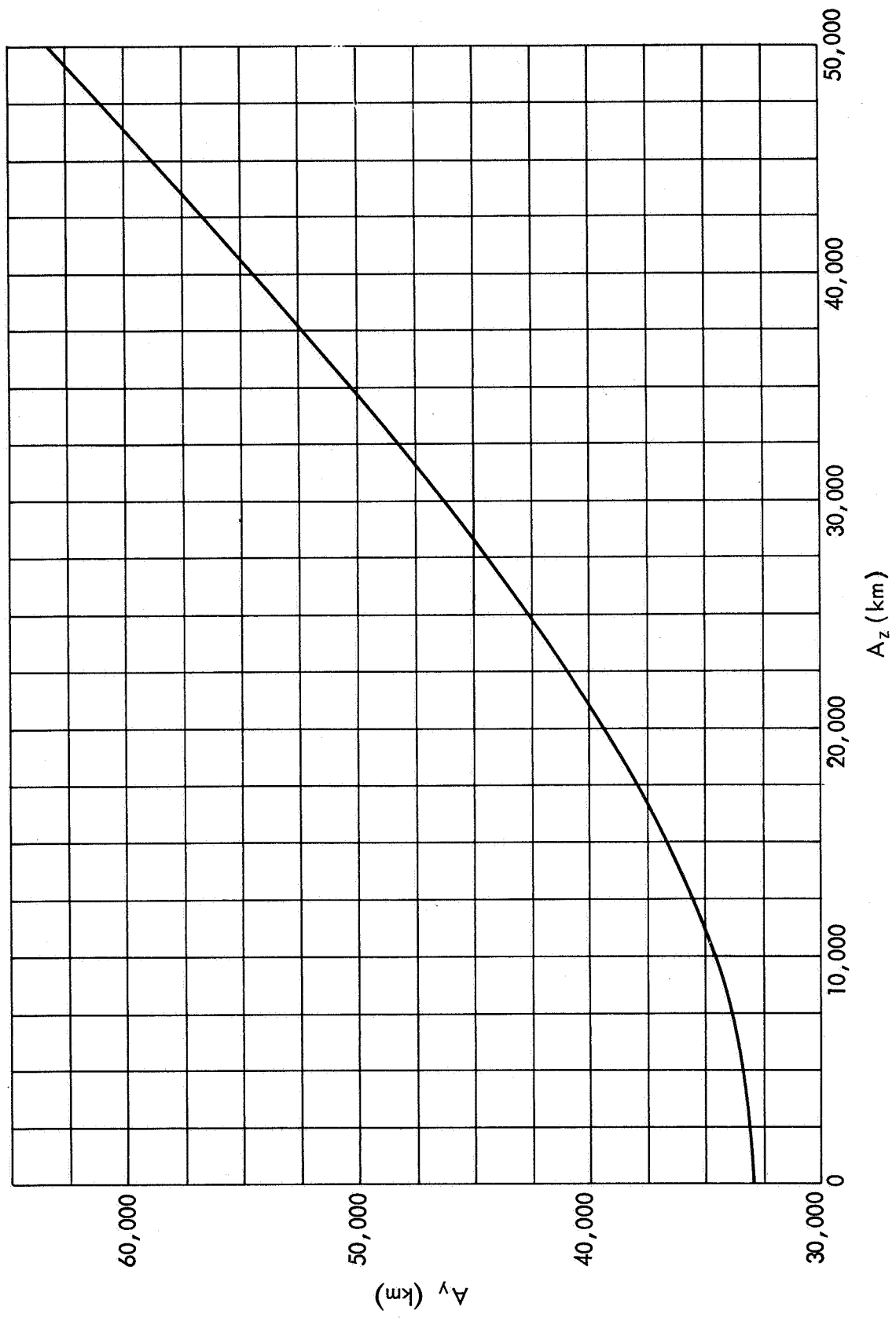
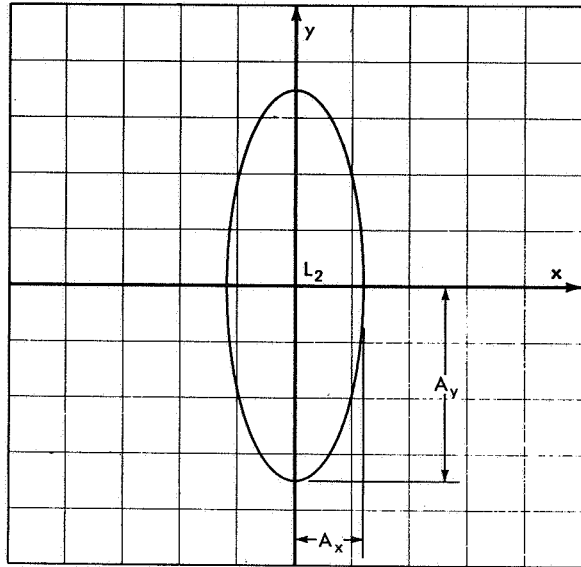
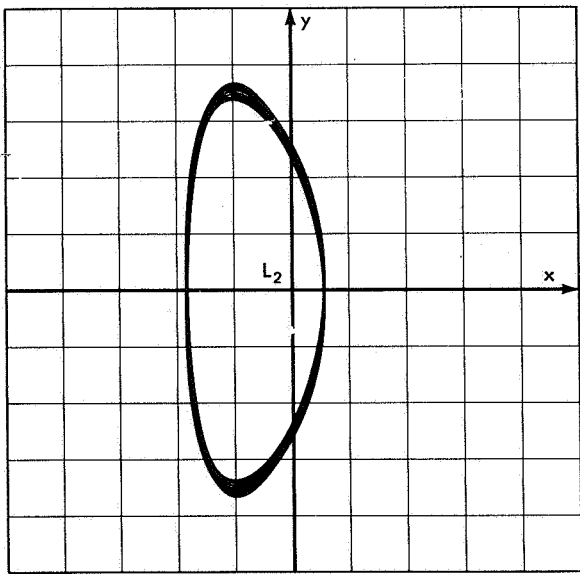


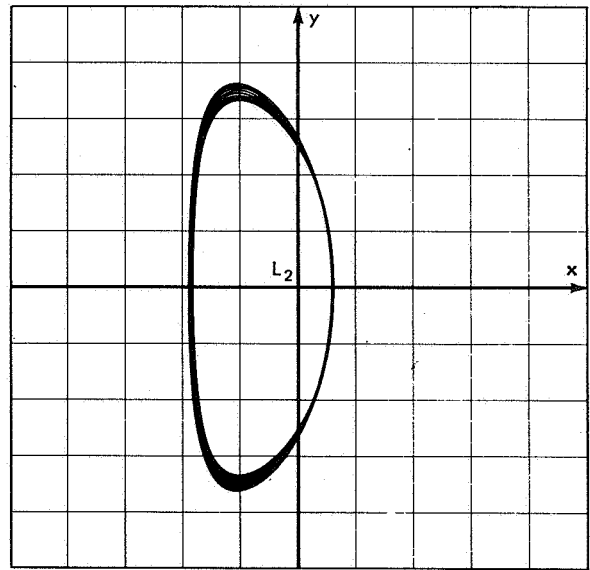
Figure 5--Amplitude relationship for halo nominal trajectories.



FIRST ORDER

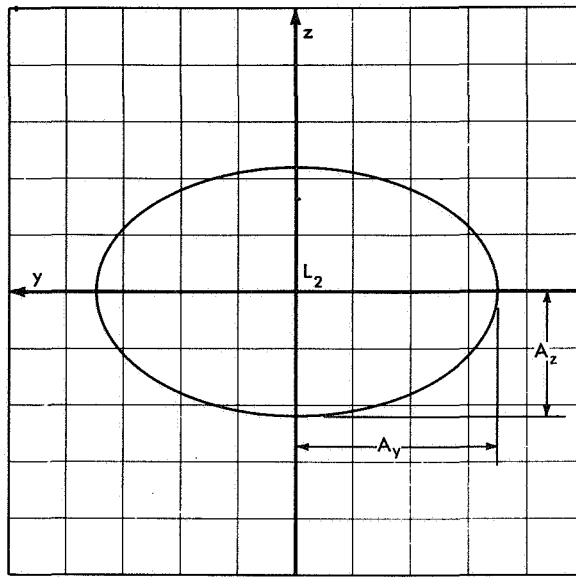


SECOND ORDER

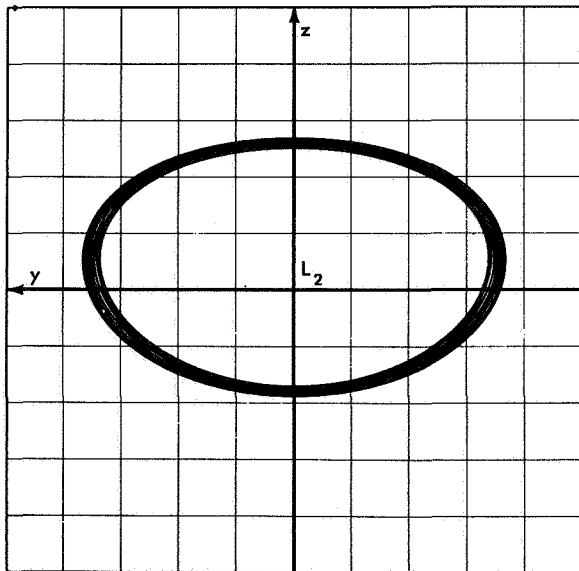


THIRD ORDER

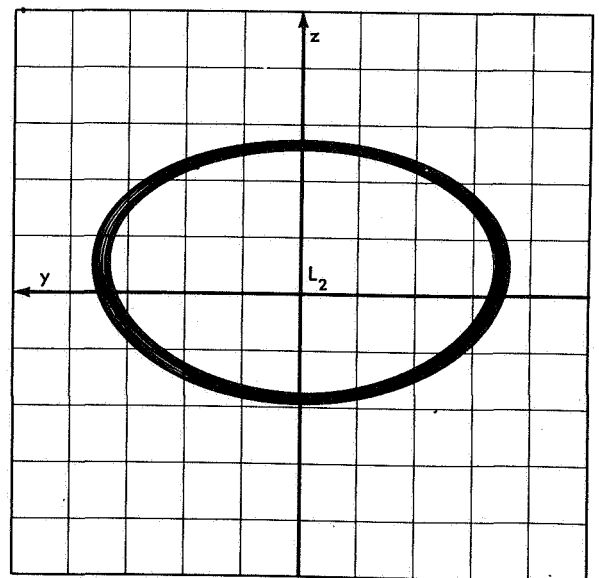
Figure 6—Halo nominal trajectory (projection in moon's orbital plane).
Grid size is 12,900 km.



FIRST ORDER

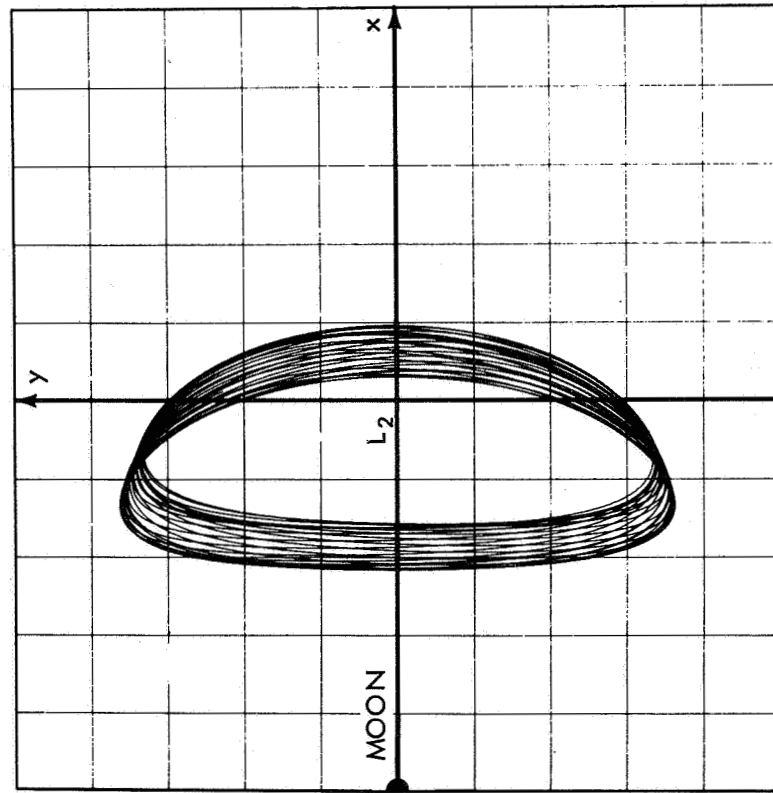


SECOND ORDER

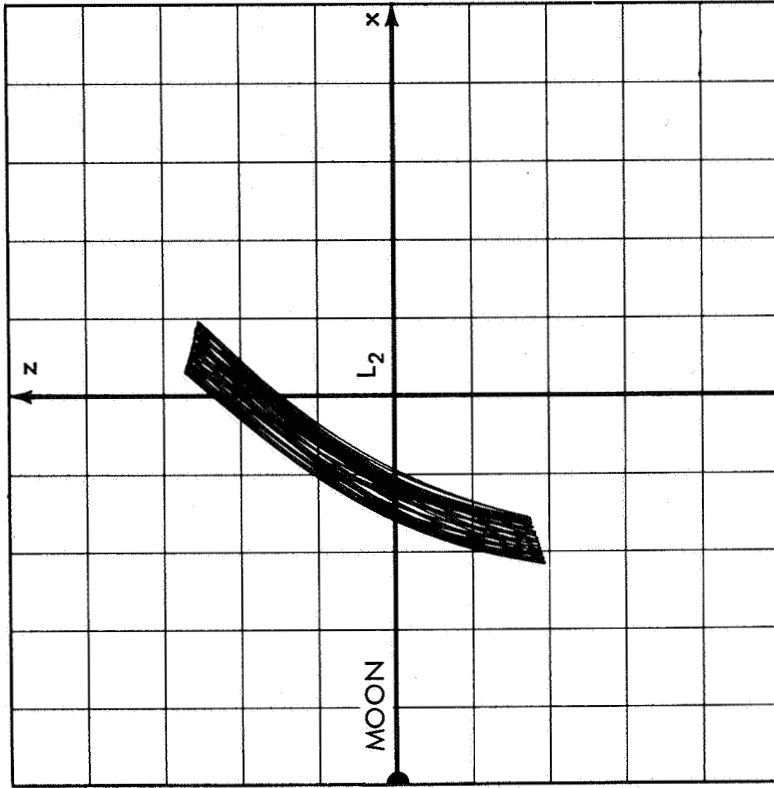


THIRD ORDER

Figure 7—Halo nominal trajectory (projection in plane perpendicular to earth-moon line). Grid size is 12,900 km.



PROJECTION IN MOON'S
ORBITAL PLANE



PROJECTION IN PLANE PERPENDICULAR
TO MOON'S ORBITAL PLANE

Figure 8—Halo nominal trajectory relative to mean L_2 point.
Grid size is 12,900 km.

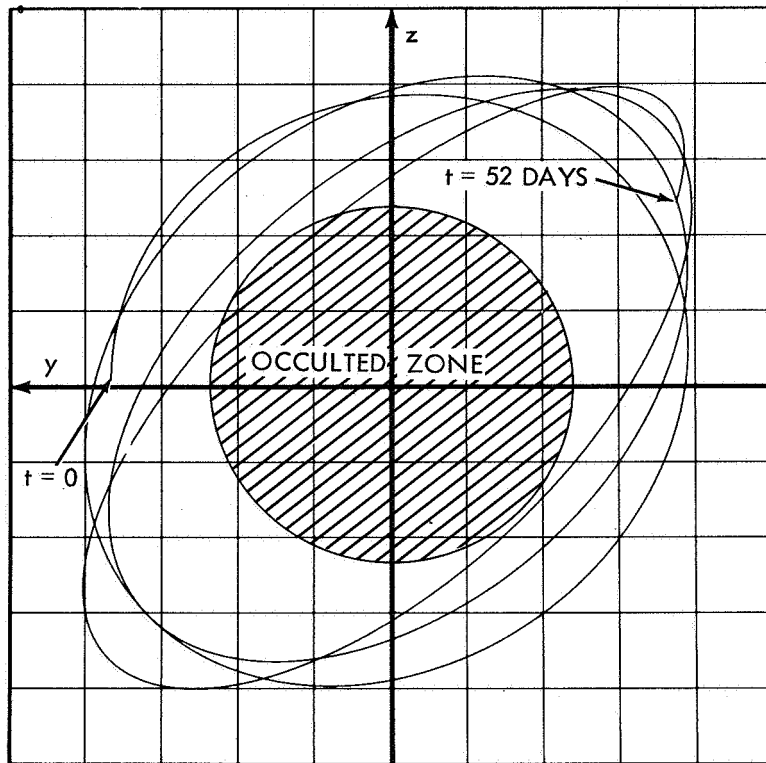


Figure 9—Nominal trajectory as seen from earth (without period control). Grid size is 1290 km.

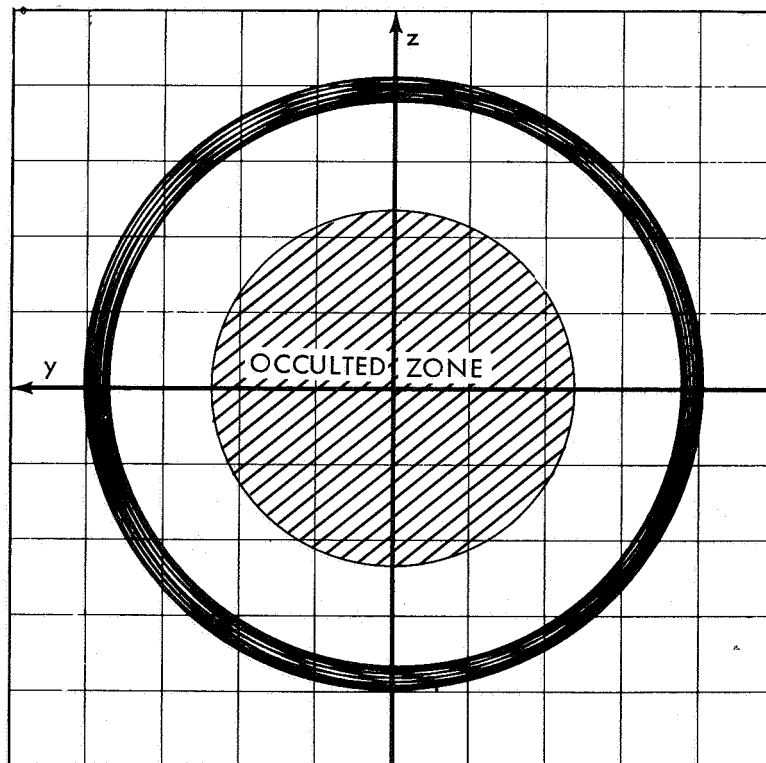


Figure 10—Nominal trajectory as seen from earth (with period control for 1 year). Grid size is 1290 km. Sinusoidal z-axis control is used (see Reference 2).

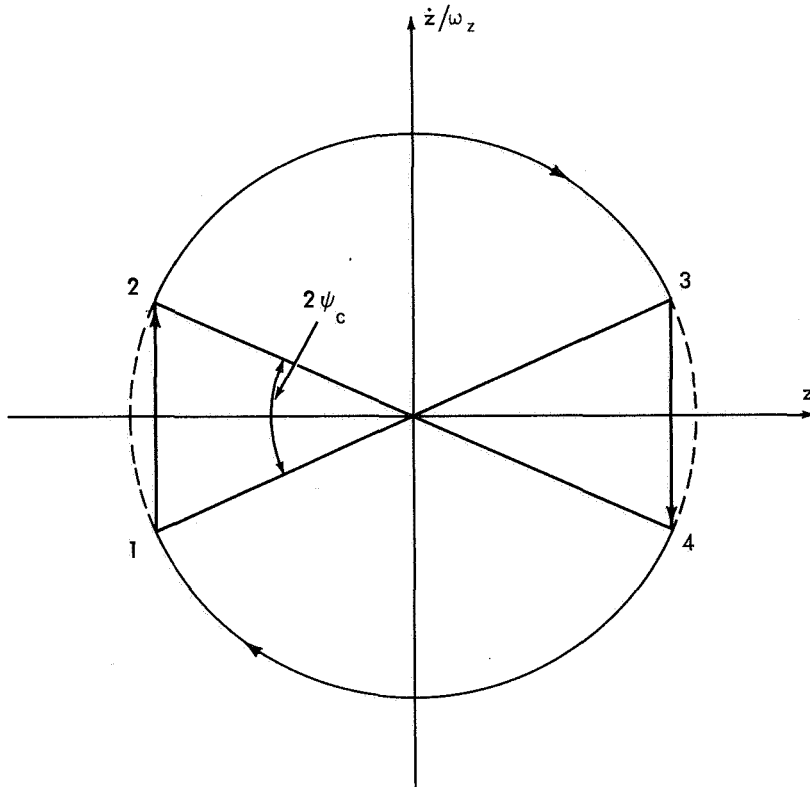


Figure 11—Phase-plane representation of z-axis period control (impulses applied at points 1 and 3).

for the period control $\overline{F_{cz}}$, to increase. The dependence of A_H and $\overline{F_{cz}}$ on the interval between control pulses Δt is shown in Figures 12 and 13. * A brief derivation of the relationships between A_H , $\overline{F_{cz}}$, and Δt is presented in Appendix C.

4. Practical Stationkeeping Technique

For a controlled satellite that is following a small-amplitude nominal path, the linearized equations of motion relative to the nominal path are approximately

$$\begin{aligned} \ddot{\xi} - 2\dot{\eta} - (2B_L + 1)\xi &= F_{cx} \\ \ddot{\eta} + 2\dot{\xi} + (B_L - 1)\eta &= F_{cy} \\ \ddot{\zeta} + B_L\zeta &= F_{cz} \end{aligned} \quad (6)$$

where $\xi = x - x_n$, $\eta = y - y_n$, $\zeta = z - z_n$, and F_{cx} , F_{cy} , and F_{cz} are control accelerations. As stated above, the divergent mode of the coupled motion in the $\xi \eta$ -plane can be eliminated by using the linear continuous control $F_{cx} = -k_1\dot{\xi} - k_2\xi$, $F_{cy} = 0$.

*Although continuous curves are shown, only the discrete values at $\Delta t = 7.32, 14.65$, etc., are meaningful.

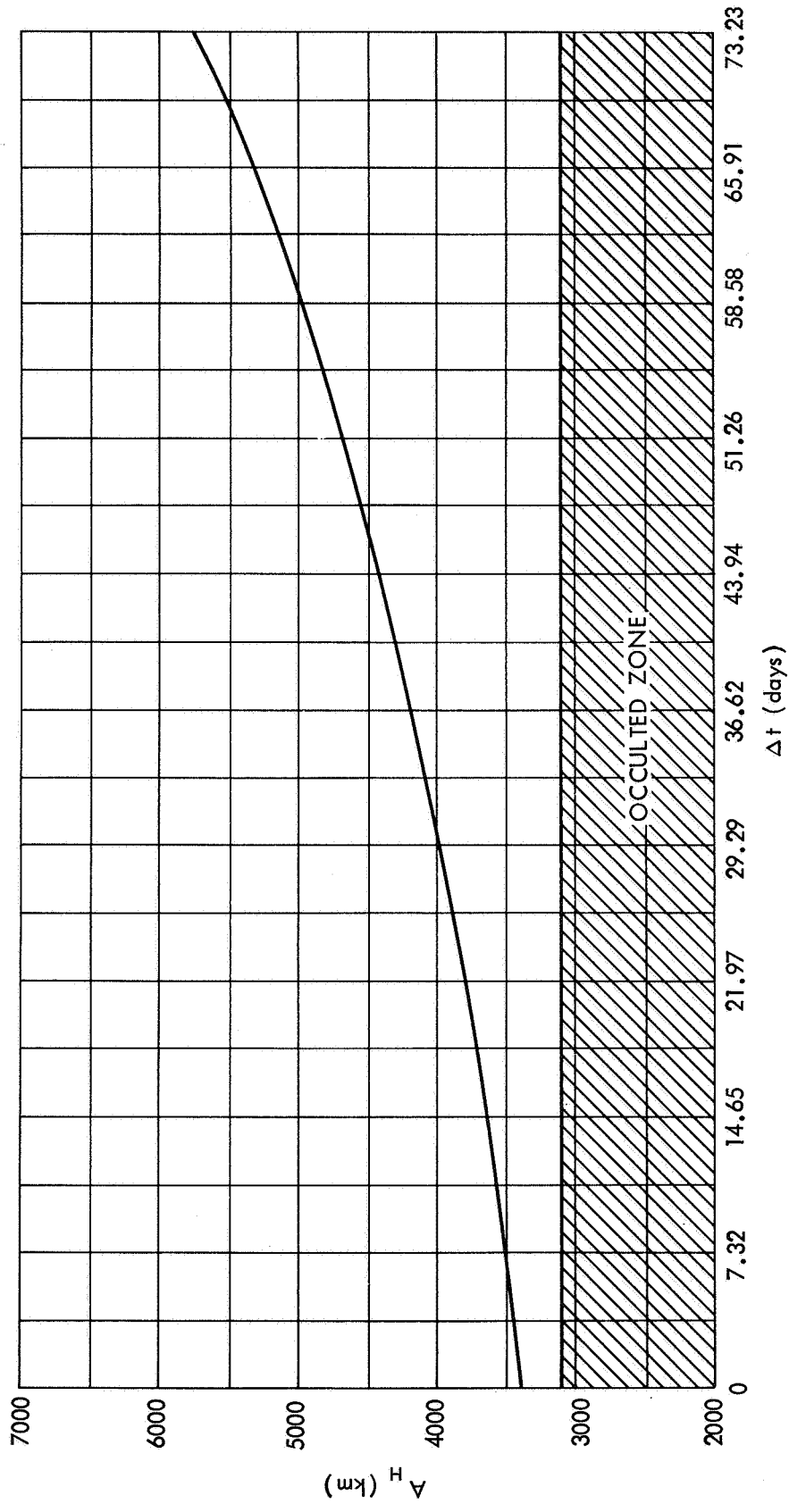


Figure 12—Amplitude of halo orbit vs. interval between control pulses.

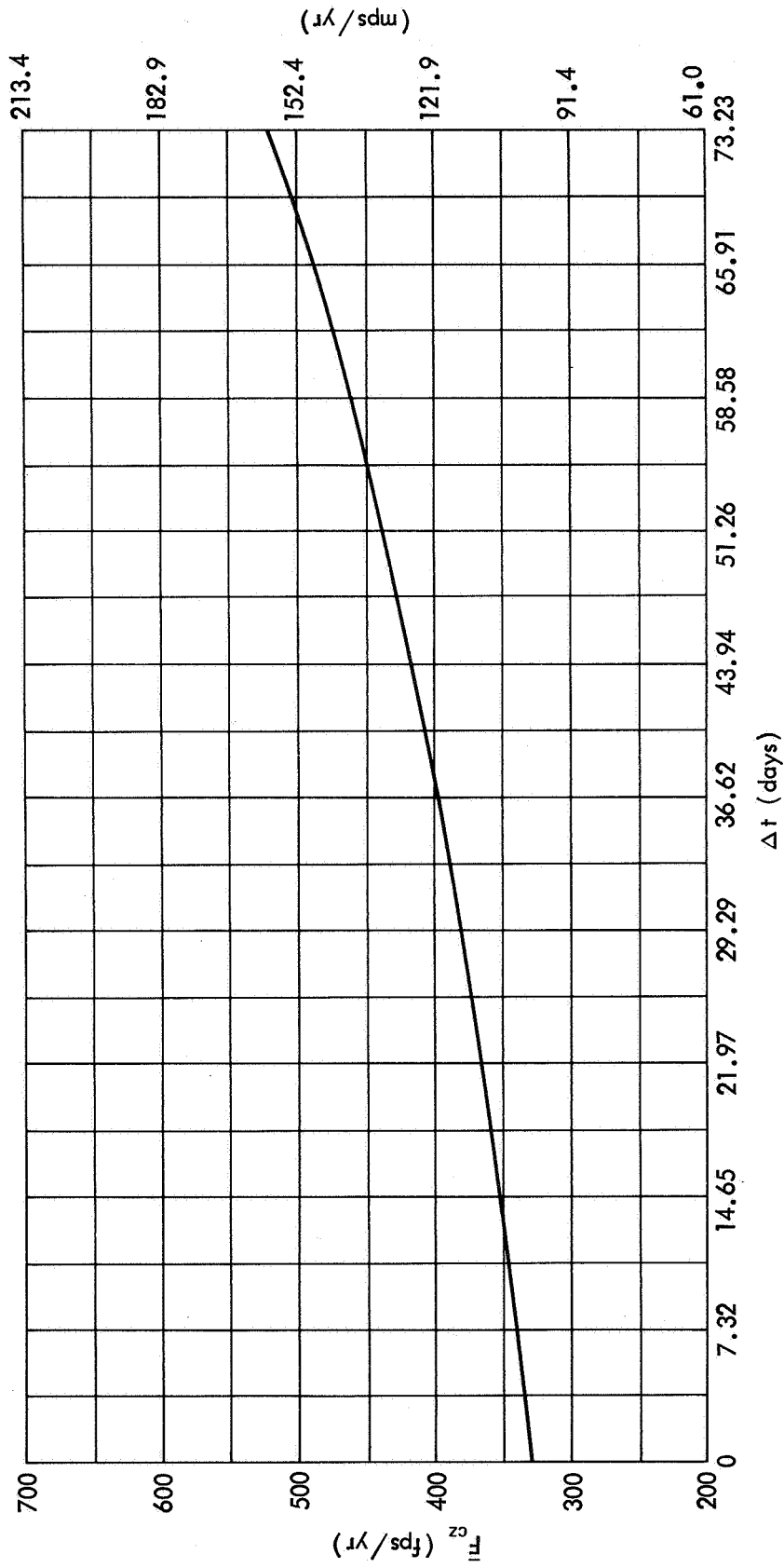


Figure 13—Average cost for period control vs. interval between control pulses.

Unfortunately, frequent control pulses of varying magnitude would be required to implement this scheme. Many measurements of $\dot{\xi}$ and ξ would also be needed. Therefore, a more practical stationkeeping technique has been devised that eases the satellite tracking requirements and reduces the frequency of the control pulses.

In the forthcoming publication by Farquhar and Kamel,* the following stationkeeping procedure is proposed:

(1) Track the satellite for an interval (an hour may be adequate) sometime before and after each control pulse to obtain estimates for $\dot{\xi}$, ξ , and η . (The time between pulses is typically 2 to 4 days.)

(2) For some constant value F_1 , compute the time t_1 when either $F = F_1$ or $F = -F_1$, where $F = \dot{\xi} + \lambda\xi - k\eta$ (λ and k are constants).

(3) Apply a thrust impulse at time t_1 . If $F = F_1$, the impulse is directed along the negative ξ -axis. If $F = -F_1$, the impulse is directed along the positive ξ -axis. All control impulses are equal in magnitude. (Stability is achieved by allowing the time interval between impulses to vary.)

Use of the method outlined above will cause the satellite to follow a limit-cycle motion in the neighborhood of the L_2 point. With the proper choice of F_1 and the impulse magnitude $\Delta\dot{\xi}$ the satellite will be captured in a one-sided limit cycle as shown in Figure 14. Two-sided limit cycles are also possible, but are usually not desired because the fuel costs are higher.

The average stationkeeping cost for a one-sided limit cycle with $\xi_{\min} = 15$ km is given in Figure 15.** In theory, this cost could be lowered by choosing a smaller value for ξ_{\min} . However, in actual practice the optimum value of ξ_{\min} is a function of the accuracies of the nominal path solution and of the estimates for $\dot{\xi}$, ξ , and η . Preliminary results from a digital computer simulation of the limit-cycle motion when nonlinear and time-varying effects are included in the equations of motion (See Appendix A) indicate that the satellite will spend most of its time in one-sided limit cycles when $\xi_{\min} \geq 15$ km.

The control parameters λ and k that are contained in the switching function $F = \dot{\xi} + \lambda\xi - k\eta$ are determined from stability and response considerations. In Figure 16, the damping effect of the parameter k on the transient response is illustrated. Notice that the stability of the one-sided limit cycle is jeopardized when k becomes too large.

*Farquhar and Kamel, op. cit.

**The nominal time interval between control pulses refers to the steady state condition.

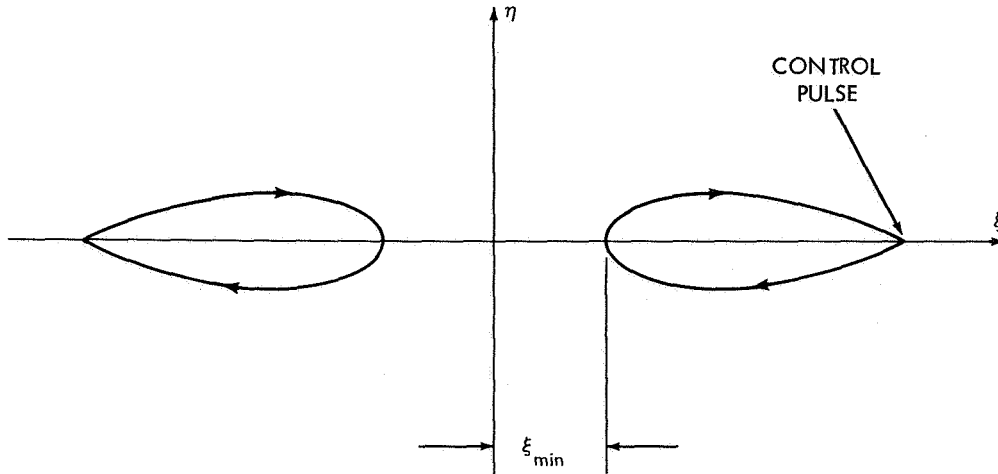


Figure 14—One-sided limit cycles (steady-state condition).

The important constant F_1 is given by*

$$F_1 = \frac{\Delta \dot{\xi}}{2} [1 + \lambda Q] \quad (7)$$

Graphs of the dependence of $\Delta \dot{\xi}$ and Q on the nominal limit-cycle period are shown in Figures 17 and 18.

5. Modification of Control Scheme for Electrical Propulsion

For various reasons, it may be desirable to use an electrical propulsion device to control a halo satellite. However, because these devices normally operate at very low thrust levels, long periods of thrusting would be required. Therefore, the impulsive control techniques described above could not be applied without some modification.

One way to modify the impulsive controls is to simply replace the impulses with finite constant-thrust periods. When the impulsive period control is so altered, its phase-plane representation is changed to the form shown in Figure 19 (cf. with Figure 11). It can be shown that the magnitude of the constant-thrust acceleration for this case is**

$$F_{cz} = A_H \omega_z^2 \left[\frac{\sin \left(\frac{\pi \epsilon}{2 \omega_{xy}} \right)}{\sin \left(\phi - \frac{\pi \epsilon}{2 \omega_{xy}} \right)} \right] \quad (8)$$

*The derivation of this formula and other theoretical results relating to the stationkeeping technique that is described in this section can be found in Farquhar and Kamel, op. cit.

**Farquhar and Kamel, op. cit.

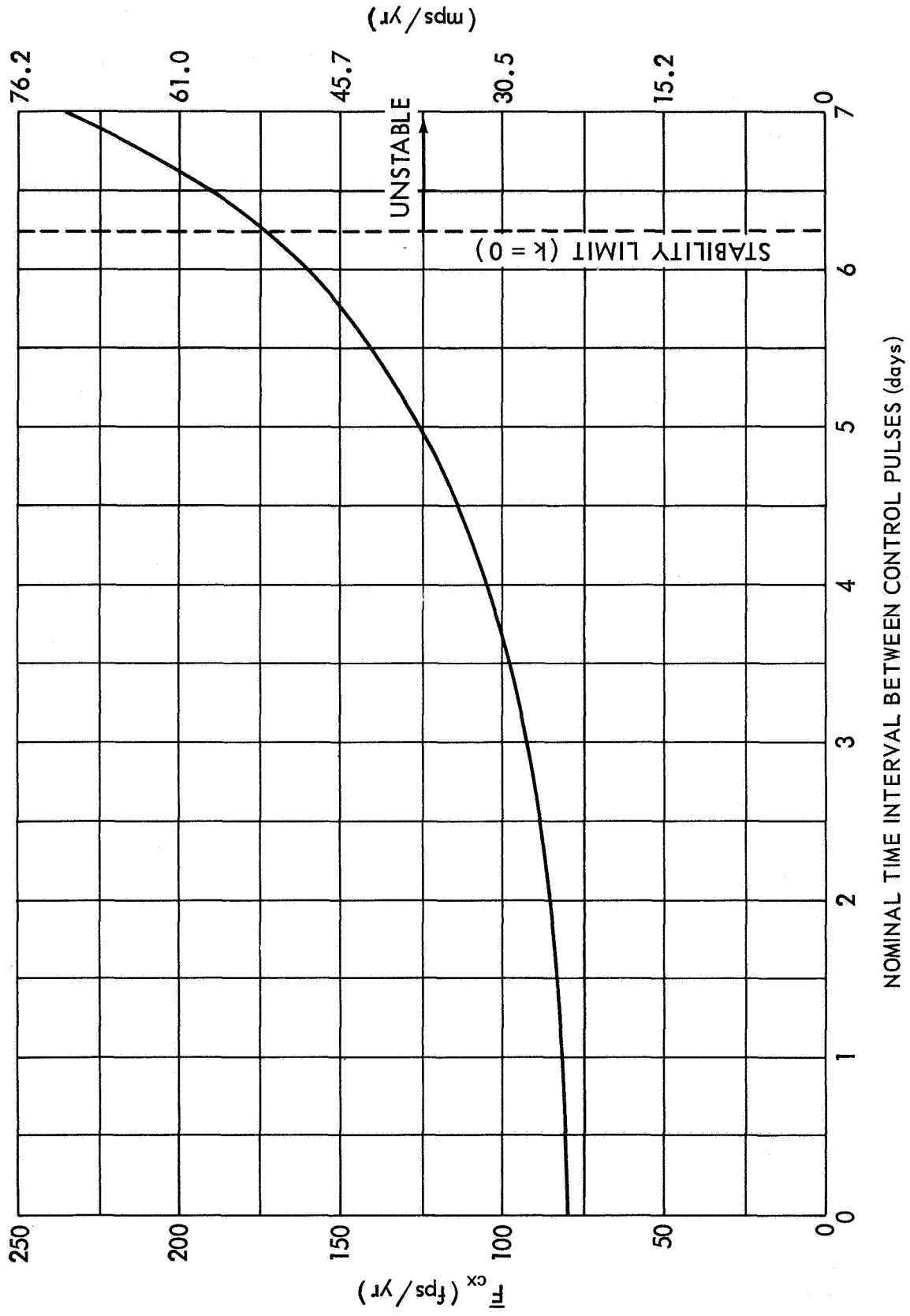
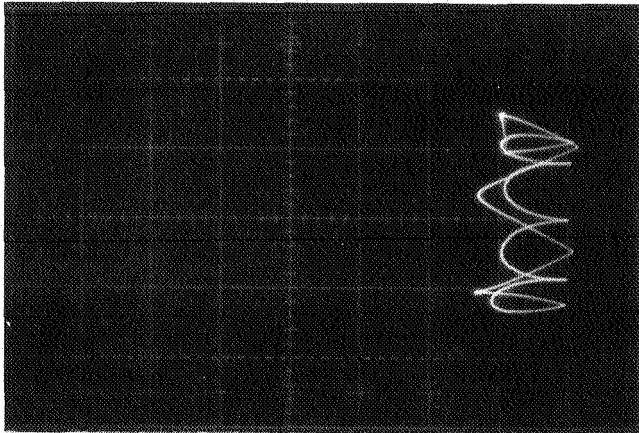
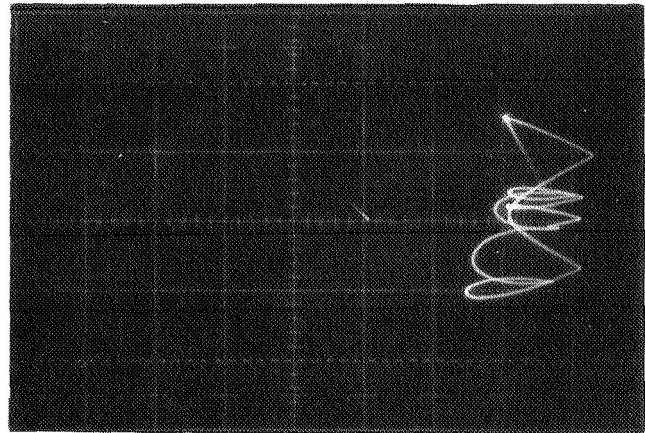


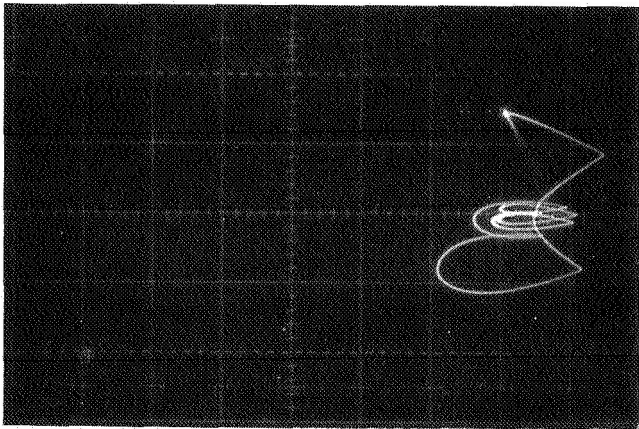
Figure 15—Average stationkeeping cost for one-sided limit cycle ($\xi_{min} = 15$ km).



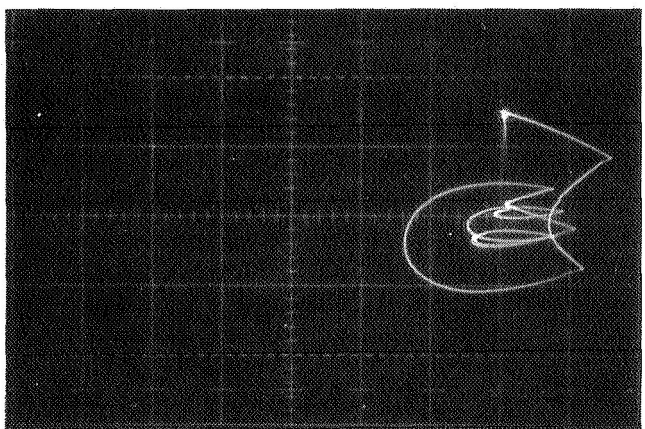
k=0



k=1



k=2



k=3

Figure 16—Transient response for one-sided limit cycle ($\lambda = 2.5$, $\xi_{\min} = 15$ km)
 η vs. ξ (analog computer simulation of linearized equations of motion).

where $\omega_{xy} = 1.865485$, $\omega_z = 1.794291$, $\epsilon = 0.0736493$, and the fraction of time that the engine is turned on is $2\phi/\pi$. If $A_H = 3500$ km and $\phi = \pi/3$, Equation (8) gives $F_{cz} = 6.04 \times 10^{-7}$ g.* For an analysis of the stationkeeping technique when the impulses are replaced by constant-thrust periods, see Reference 4.

*It is useful to know that $1 \text{ fps/yr} \approx 1 \times 10^{-9}$ g.

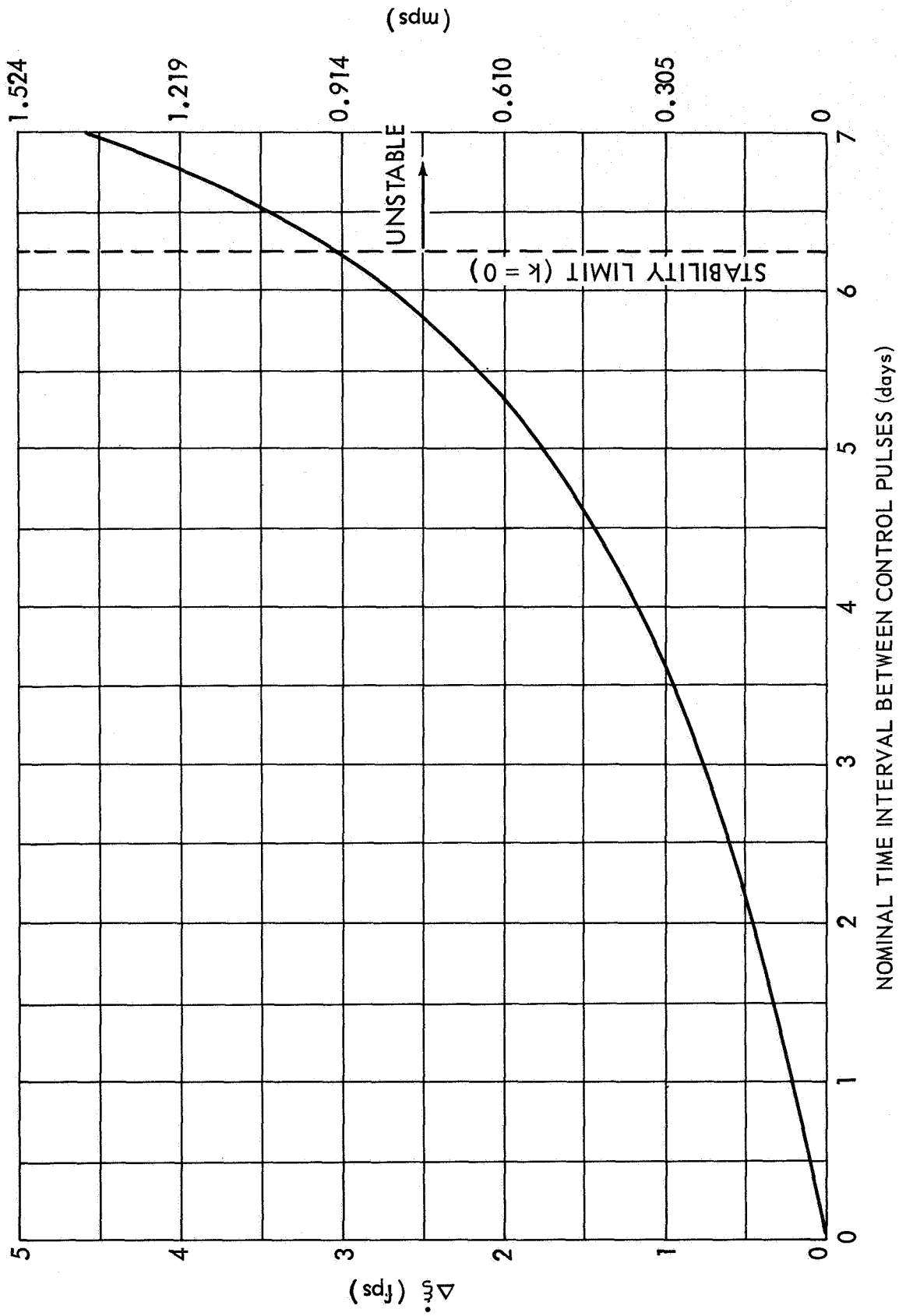


Figure 17—Impulse magnitude vs. nominal limit-cycle period ($\xi_{\min} = 15$ km).

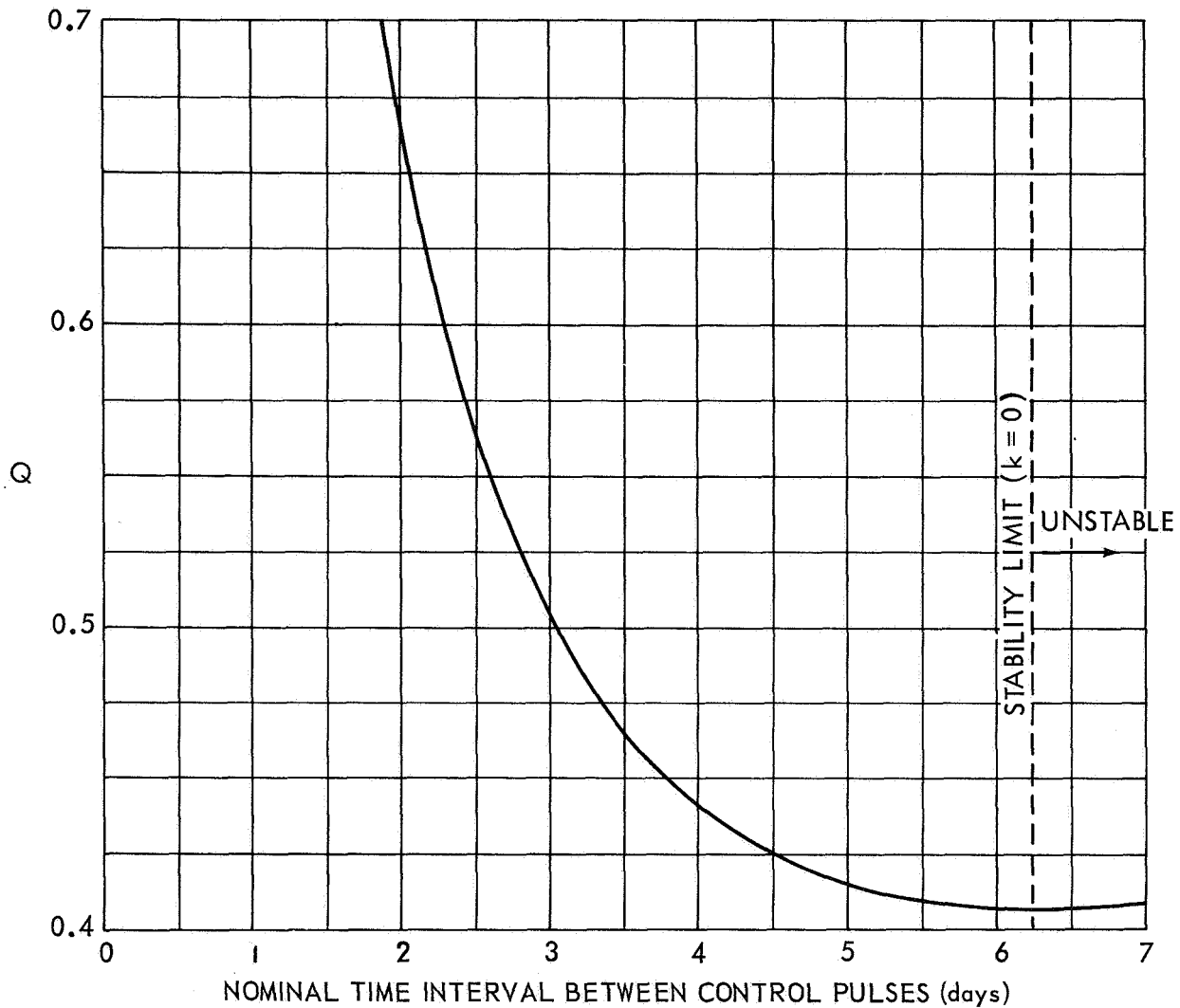


Figure 18—Q vs. nominal limit-cycle period.

C. Transfer Trajectories

In this section, the ΔV requirements for some transfer trajectories between an earth parking orbit and the vicinity of the L_2 point are presented. The results given here were obtained by employing a restricted three-body model and numerically integrating the equations of motion. Only trajectories which lie in the moon's orbital plane have been considered. Although the ΔV requirements were calculated for trajectories terminating at L_2 , they closely approximate the corresponding values for transfers to small-amplitude halo orbits around L_2 .

A typical two-impulse trajectory between the earth parking orbit and L_2 is depicted in Figure 20. The variation in ΔV as a function of the transfer time for this mode is given in Figure 21. Notice that the ΔV curve for the impulse at L_2 is starting to flatten out at $t = 108$ hours. Thus, it appears that only very small savings can be realized by extending the transfer time beyond 108 hours.

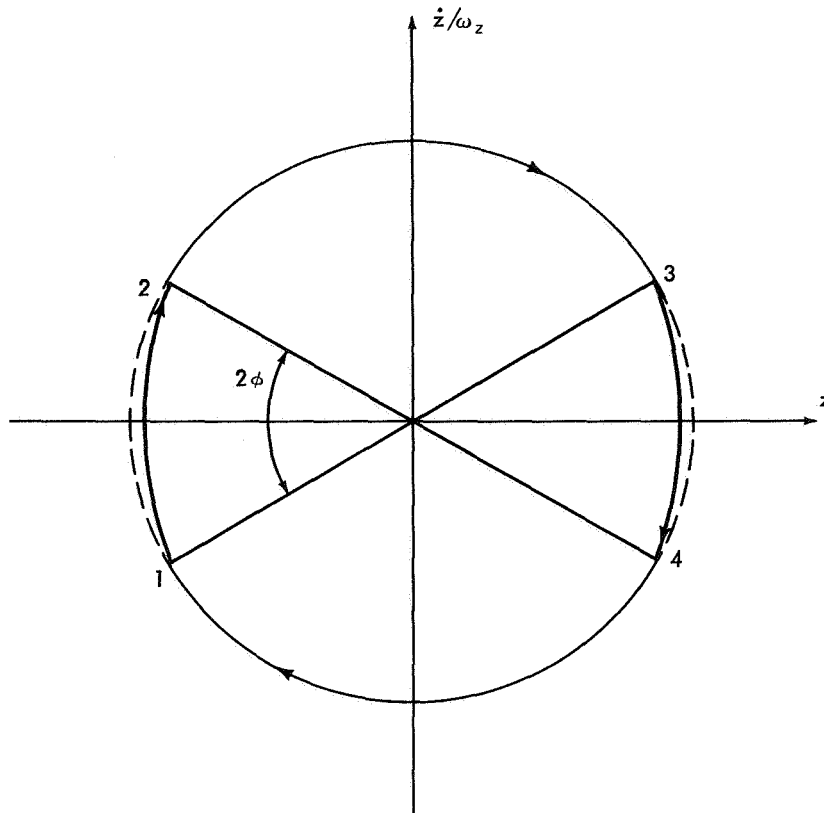


Figure 19—Phase-plane representation of z-axis period control
(continuous thrusting from points 1 to 2 and 3 to 4).

Fortunately, it is possible to reduce the ΔV costs below those for the two-impulse transfer by using a powered lunar swingby (Reference 3). This three-impulse transfer mode is illustrated in Figure 22. The total transfer time for this mode is almost 9 days, but the reduction in ΔV is appreciable.

Trajectories that start at L_2 and terminate in the earth parking orbit are just mirror images of the trajectories shown in Figures 20 and 22. The ΔV costs for the corresponding inbound and outbound transfers are identical.

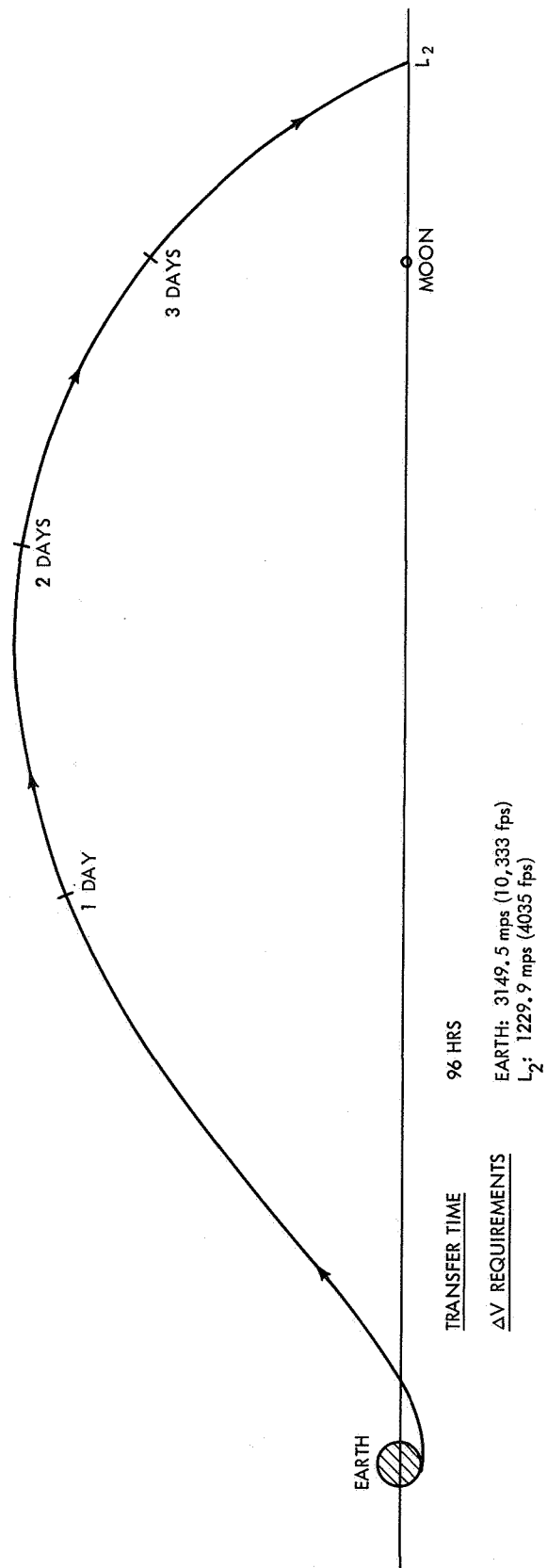


Figure 20—Two-impulse transfer from 185.2 km (100 n.mi.) earth parking orbit to L₂ point.

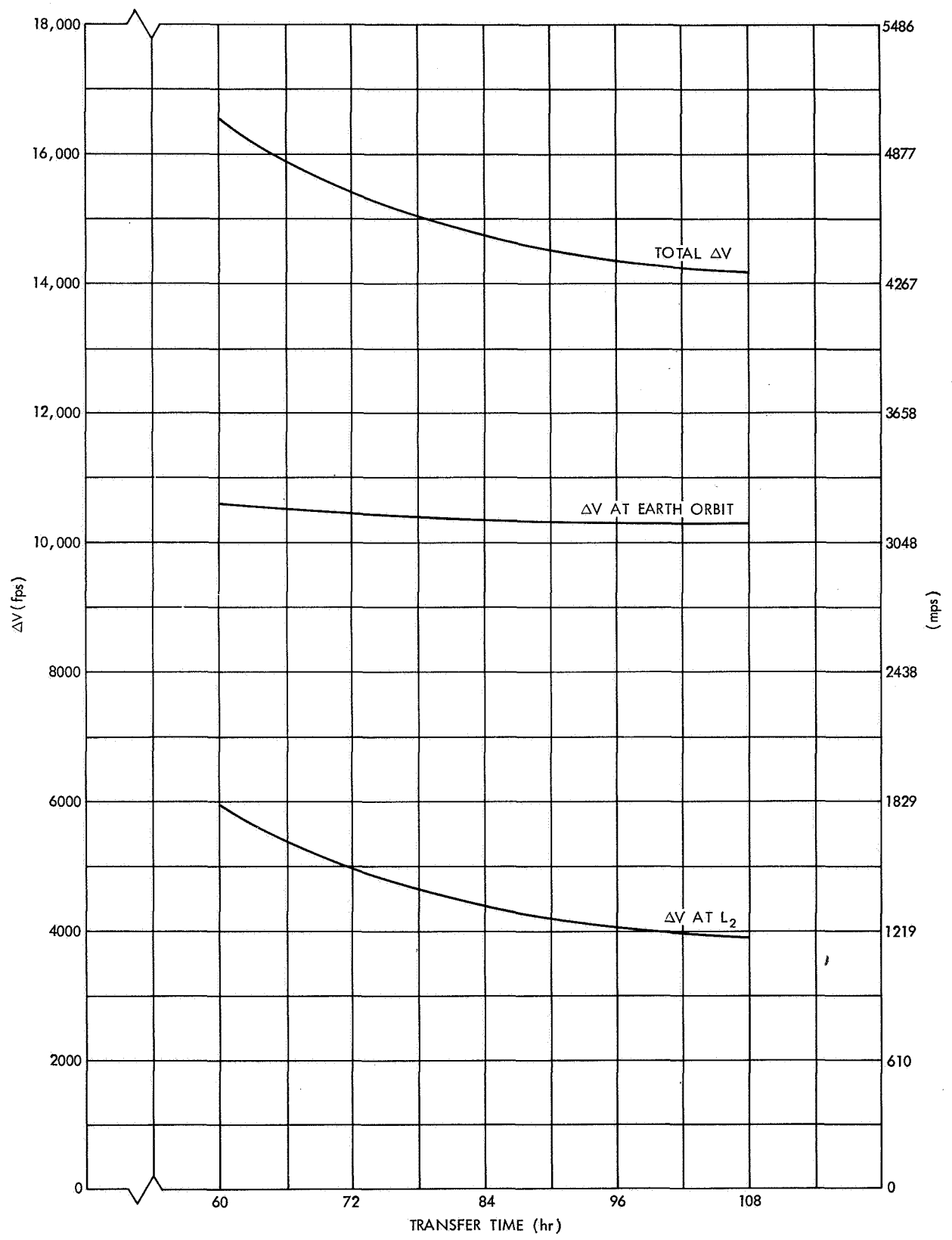


Figure 21— ΔV cost for two-impulse transfer from 185.2 km (100 n.mi.) earth parking orbit to L₂ point.

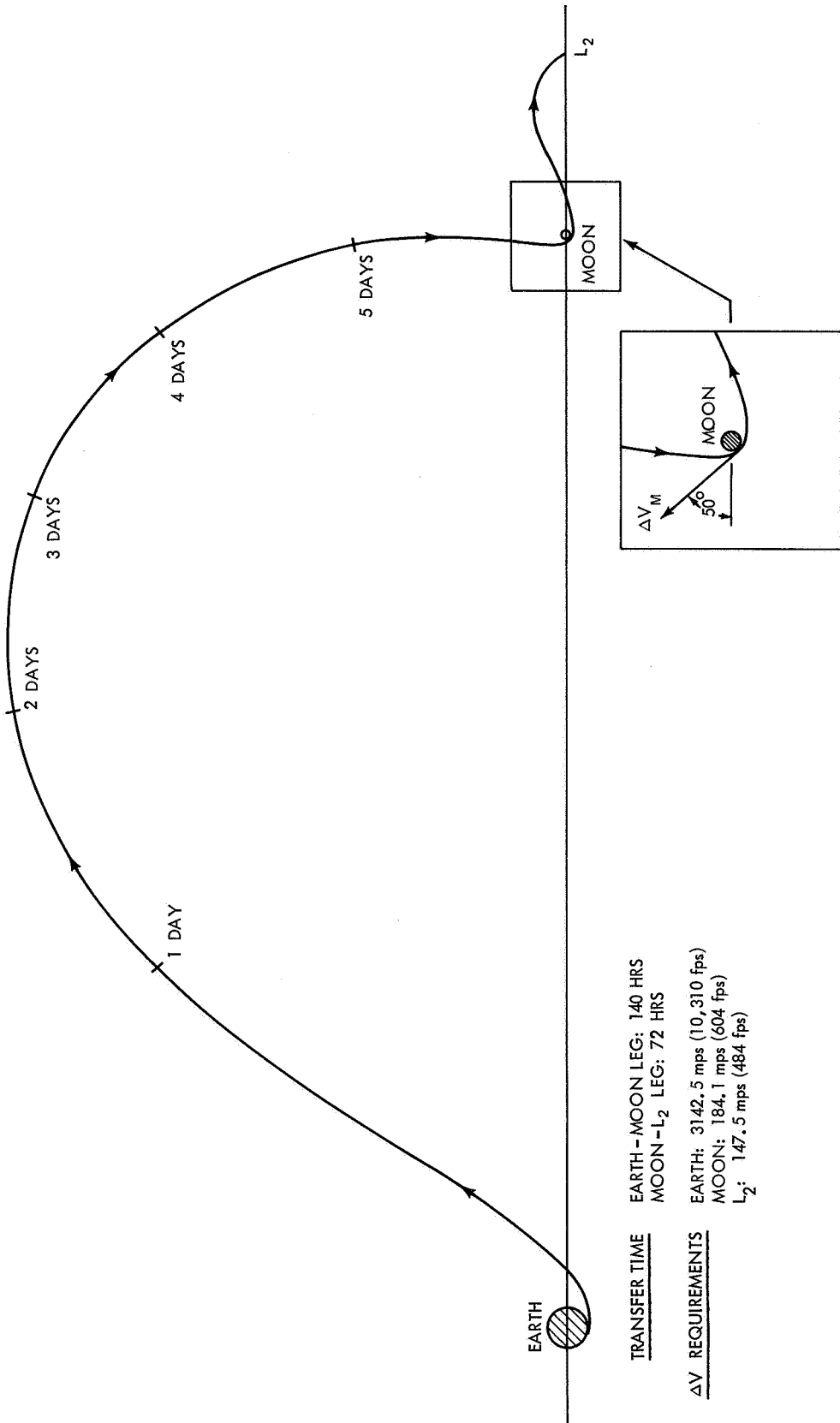


Figure 22—Three-impulse transfer from 185.2 km (100 n.mi.) earth parking orbit to L_2 point [perilune is 111.12 km (60 n.mi.)].

CHAPTER III

LUNAR FAR-SIDE COMMUNICATIONS LINK

Because a far-side communications link is not available, lunar-surface exploration (manned and unmanned) has been limited to the moon's near side. If maximum scientific return from the costly spacecraft that have been developed for lunar exploration is to be received, then this undesirable restriction should be removed. The role of halo satellites in eliminating the lunar far-side communications constraint is treated in this chapter.

A. Synchronous Halo Monitor (SHALOM)

The main geometrical features of the halo-satellite method for establishing an uninterrupted lunar far-side communications link are illustrated in Figures 1 and 23. With the control techniques given in Section II-B, the relay satellite could remain in the halo orbit where it would always be visible from both the earth and the far side of the moon. Because of properties that are similar to synchronous satellites of the earth (24-hour satellites), the halo communications satellite might well be termed a synchronous halo monitor (SHALOM). The quasi-stationary characteristic of SHALOM* greatly simplifies the acquisition and tracking problems for an antenna on the moon's far side. As a matter of fact, a halo orbit with a radius of 3500 km would always lie within the 11.1-deg beamwidth of a fixed lunar-surface antenna even when the latitudinal and longitudinal oscillations of the moon** are taken into account.

Another scheme for providing lunar far-side communications coverage would use two or more relay satellites in a lunar polar orbit (References 5 and 6).† This method

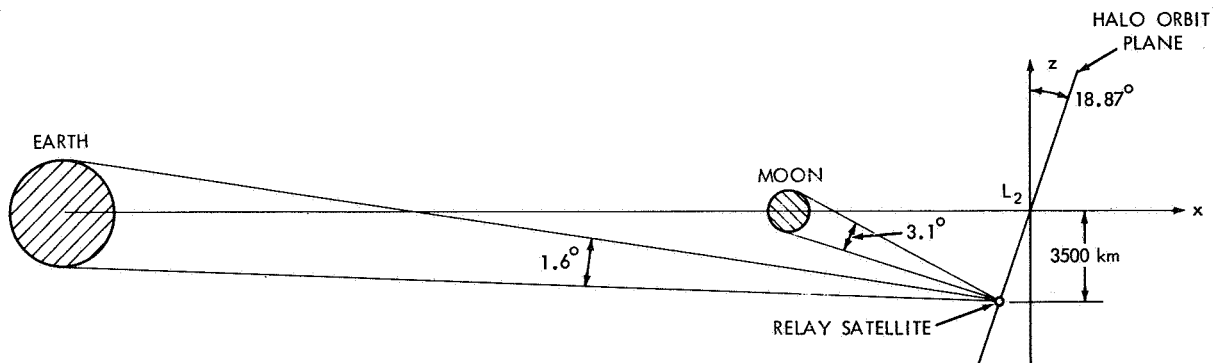


Figure 23—Halo-satellite geometry (not to scale).

*The relay satellite would take about 2 weeks to complete one circuit of the halo path.

**The latitudinal oscillation is about ± 6.73 deg and the longitudinal oscillation is approximately ± 7.75 deg. These oscillations are usually called lunar librations.

†Also see McNeely, J. T., and Ellis, W. H., "Circumlunar Communications Using Two Satellites in Lunar Polar Orbit", NASA-MSO Internal Note 68-FM-149, June 20, 1968.

would have shorter communications distances than the halo-satellite technique, but would be less attractive in other respects. Some of the advantages of SHALOM over the polar-orbiting satellite system are summarized in Table 1.

B. Importance in Anticipated Unmanned Lunar Program

The curtailment of the Apollo Program and the ensuing gap in manned lunar exploration has created a need for an automated lunar program. These unmanned missions can supplement Apollo results by gathering data from the entire lunar surface, particularly sites that are considered to be too risky for manned landings (e.g., the moon's far side). Clearly, SHALOM will be a key element in this program.

1. Support for Emplaced Stations and Roving Vehicles on Moon's Far Side

A widely spaced network of emplaced scientific stations on the moon is needed to answer many of the fundamental questions concerning the structure and composition of the lunar interior. The acquisition of seismic data would have the highest priority, but other geophysical observations (e.g., measurements from strainmeters, triaxial magnetometers, and heat-flow measurements) would also be enhanced by obtaining global measurements. When the network measurements are augmented with data collected from automated rovers and lunar orbiters, a fairly complete geophysical picture of the moon should emerge.

A halo comsat could support the stations and rovers on the far side of the moon. The continuous communications capability would be of great value since even small gaps in the data would seriously degrade some of the geophysical experiments. This continuous communications link would also be needed for remote control of lunar rovers. A summary of these services and other supporting functions of SHALOM is given in Table 2.

2. Selenodesy Experiment

A more accurate determination of the gravitational field of the moon would be of value to future manned lunar missions as well as lunar science. One method for gaining this improvement would be to obtain accurate Doppler tracking measurements of a low-altitude polar orbiter from the front and back sides of the moon. The backside tracking data would, of course, be collected from SHALOM. For additional selenodesy payoff, the polar orbiter should carry a radar altimeter and a gravity-gradient measuring instrument.

3. International Cooperation

The early development of a halo relay satellite would offer an uncommon opportunity for a joint Soviet-American lunar mission. Although the Soviets are engaged in an extensive lunar exploration program (Reference 7), they do not as yet appear to have plans for a far-side communications satellite. With an American halo comsat and a Russian sample-return vehicle (such as Luna-16) or surface rover (such as Luna-17), the first far-side landing could become a reality.

Table 1—Comparison of two proposed techniques for lunar far-side communications.

Criterion	Relay Satellite in Halo Orbit	Relay Satellite System in 11,112 km (6000 n. mi.) Lunar Polar Orbit
Number of satellites required	One satellite would give continuous coverage.	Three satellites spaced 120 deg apart in the polar orbit would provide uninterrupted coverage about 90% of the time.
Tracking and acquisition requirements (lunar surface antenna)	Quasi-stationary feature simplifies this problem. No tracking would be required when using an antenna with a beamwidth that is greater than 11.1 deg.	Steerable antenna required for tracking. A different relay satellite must be acquired every 12 hours.
Orbit-control requirements	Average cost for stationkeeping and period control is about $\Delta V = 132.0$ mps/yr (433 fps/yr). Control implementation is very simple.	Average cost for orbit stabilization and maintenance of proper spacing between satellites is roughly $\Delta V = 22.9$ mps/yr (75 fps/yr). The degree of difficulty of the control implementation has not been assessed. Without orbit stabilization, satellites would impact with moon in 8 months.
Attitude-control requirements	Control strategy is simplified by commonality of antenna pointing requirements. A spacecraft antenna with a beamwidth of 5 deg would provide full coverage of the earth and moon.	Control strategy is complicated by diverse antenna pointing requirements (satellite to earth and satellite to lunar surface).
Approximate ΔV requirement for orbit insertion	335.3 mps (1100 fps).	579.1 mps (1900 fps).

Table 2—Lunar far-side mission support tasks for halo communications satellite.

1. Relay spacecraft telemetry data to earth and command signals to spacecraft during lunar landing and take-off operations.
2. Continuously monitor scientific data from emplaced stations on moon's far side.
3. Relay television signals from roving vehicle to earth-based control center. Control commands from earth are also relayed to rover.
4. Track lunar orbiters when they are hidden from earth stations.
5. Provide a real-time, two-way communications link between earth stations and a manned spacecraft that is occulted by the moon.

As a possible landing site for a far-side mission, consider the crater Tsiolkovsky (see Figures 24-27). This crater is one of the most spectacular features on the far side of the moon and has been studied in great detail (e. g., see Reference 8). The exceptionally smooth crater floor of Tsiolkovsky (see Figure 27) is ideally suited for automated landings and long-range traverses of roving vehicles.

This type of cooperative space project has several noteworthy features:

- (1) Hardware-interface problems would be minimal,
- (2) Military and commercial space interests would not be involved,
- (3) Both nations would have a part in the first landing on the moon's far side, and
- (4) The lunar far-side communications capability could be shared with nations other than the Soviet Union.

C. Spacecraft Considerations

A number of preliminary design studies of halo communications satellites have already been completed (References 3, 9, and 10). The findings of these studies, together with the orbit-control results of Section II-B, provide a basis for estimating overall spacecraft-weight and launch-vehicle requirements. Some pertinent data for a typical halo spacecraft are given in Table 3.

The communications performance of the halo comsat can be demonstrated by a link calculation for television signals from a lunar-surface rover to the relay satellite, presented in Table 4. This particular link was chosen for this calculation because it is the most stringent requirement for the communications system.

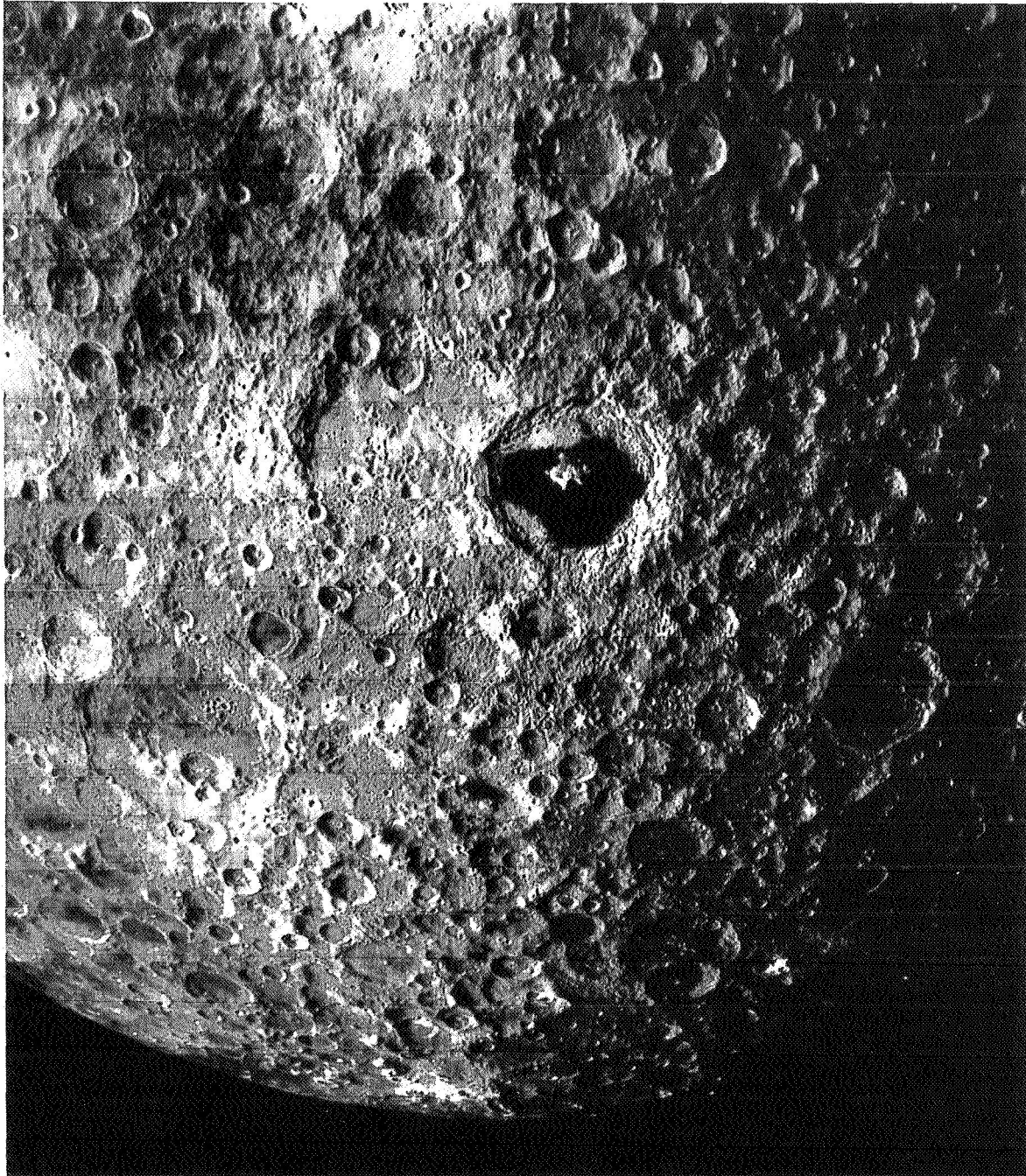


Figure 24—The southwestern area of the moon's far side. Tsiolkovsky is the conspicuous dark-floored crater (Lunar Orbiter photo). Framelet width is 55 km.

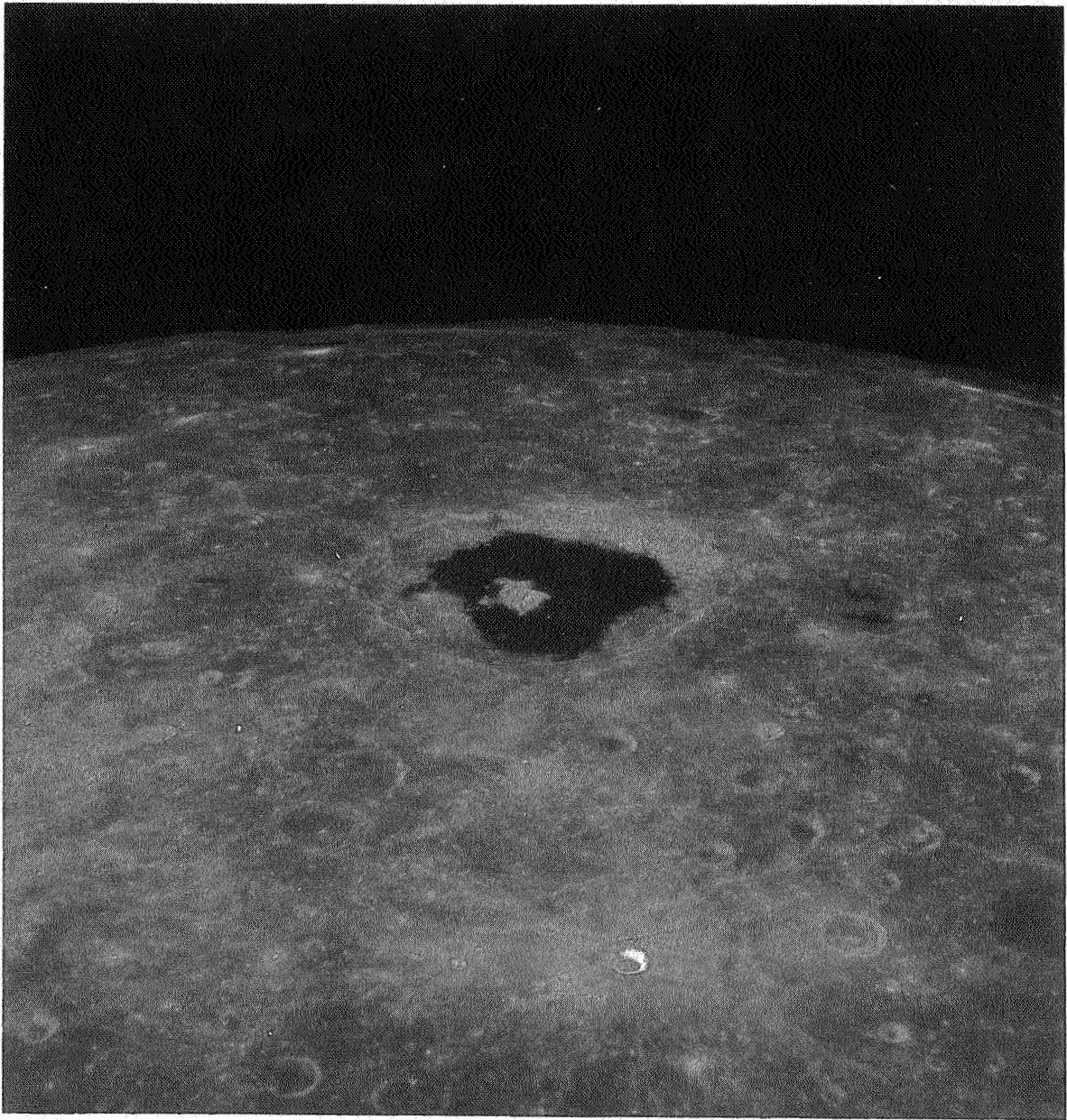


Figure 25—An oblique view of Tsiolkovsky (Apollo-8 photo).

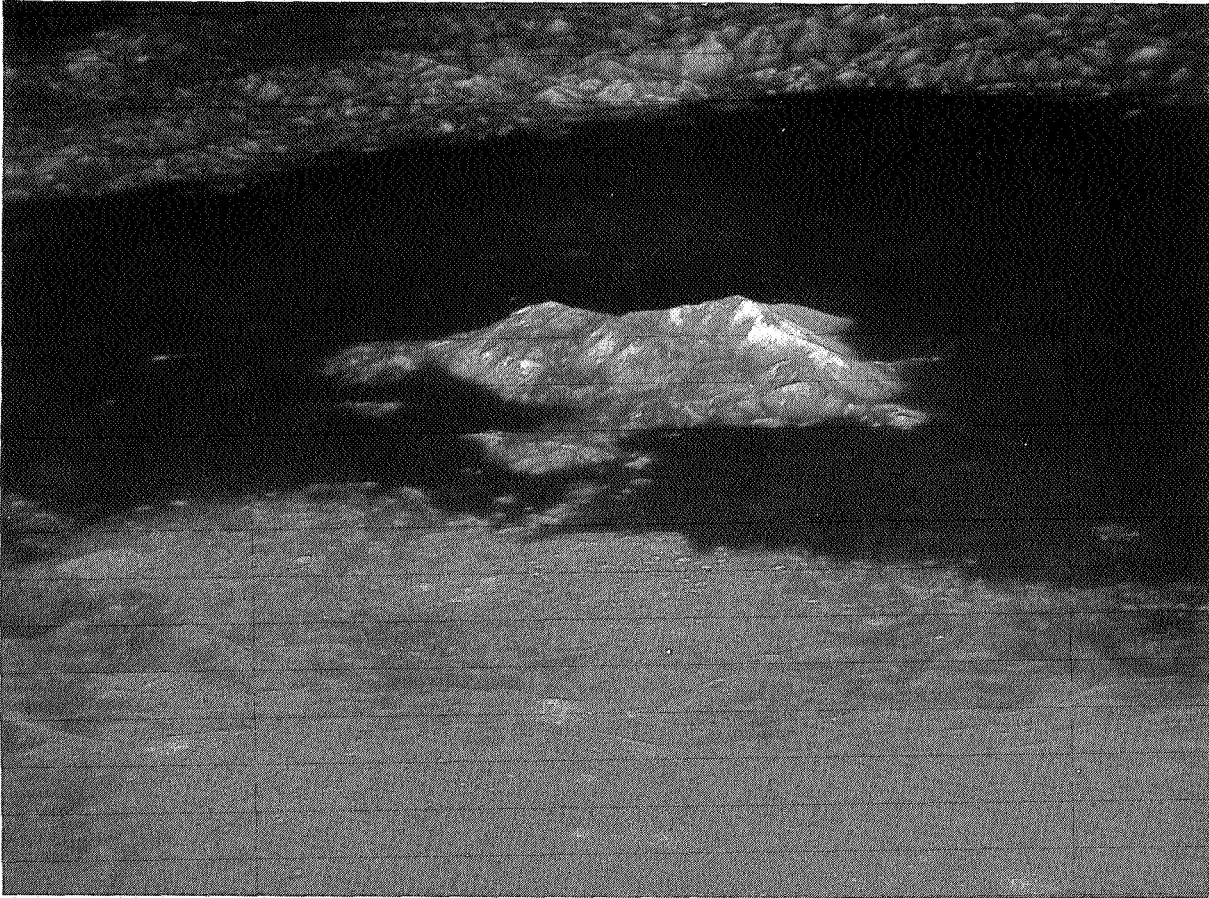


Figure 26—The central peak of the Tsiolkovsky Crater (Apollo-8 photo).

D. Complete Lunar Communications Network

If the radius of the halo orbit were enlarged to about 3700 km, the orbit would always be in view from the L_1 point (see Figure 2) as well as the earth. Therefore, if a second relay satellite were stationed at L_1 , a point-to-point communications system covering most of the lunar surface could be established. (This system was originally proposed in Reference 11.) However, this two-satellite system would not provide adequate coverage for the moon's polar and limb regions. Since these particular regions are of high scientific interest (especially Mare Orientale on the western limb), dependable communications support should be made available.

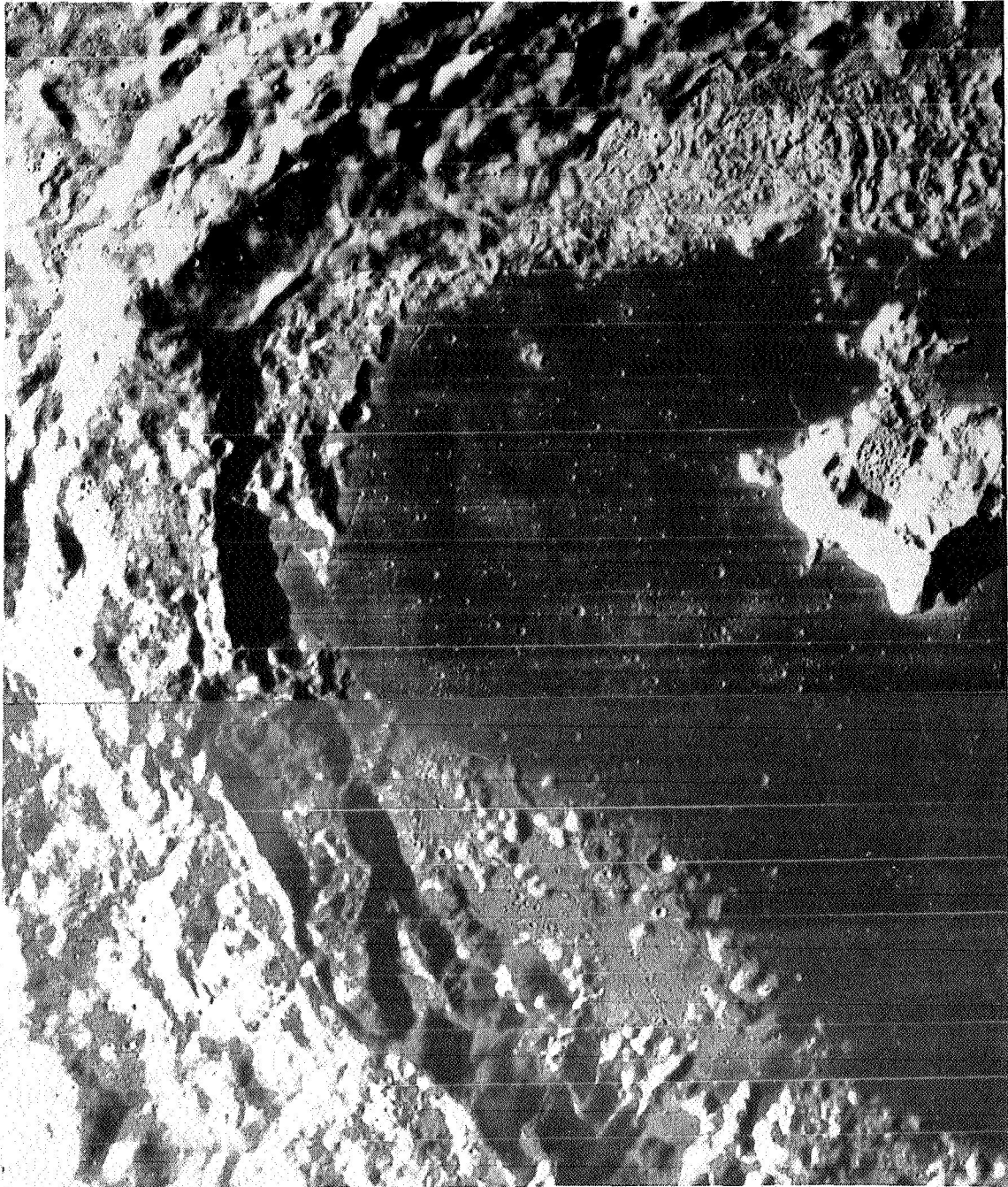


Figure 27—Close-up view of the western half of Tsiolkovsky. Most of the crater's floor has been flooded by a dark material whose freshness is indicated by the absence of large craters and the sparse distribution of small ones (Lunar Orbiter photo). Framelet width is 7 km.

Table 3—Preliminary spacecraft design data for SHALOM.

Operational Lifetime	3 years	
Radius of Halo Orbit	3500 km	
Launch Vehicle	TAT(9C)/DELTA/ TE 364-4	
Spacecraft Weight (at Translunar Injection)	408.2 kg	(900 lb)
ΔV Requirements		
	mps	(fps)
Midcourse Corrections	30.48	100
Halo Injection	335.28	1100
Stationkeeping (one pulse every 3 days)	85.34	280
Period Control (one pulse every 7.32 days)	310.90	1020
Attitude Control	22.86	75
Total	784.86	2575
Fuel Weight (Hydrazine $I_{sp} = 230$ sec)	119.7 kg	(264 lb)

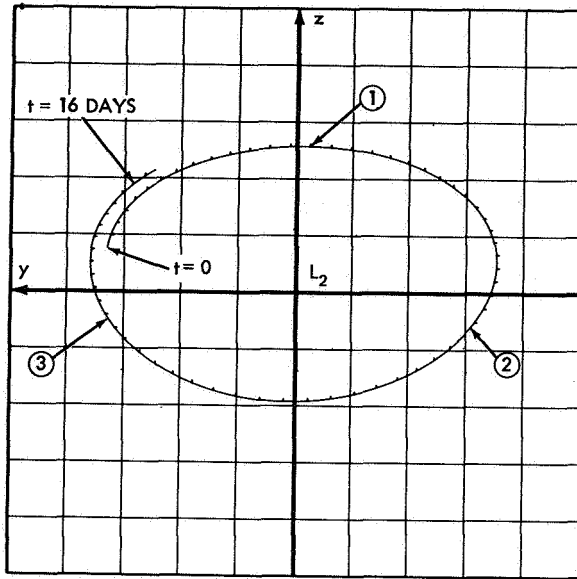
A very large halo orbit would provide coverage for the poles and limbs, yet still retain many of the desirable features of SHALOM (see Figures 6-8). Three relay satellites are spaced at 4.85-day intervals in this orbit as shown in Figure 28. Because the nominal trajectory for the relay-satellite network is shifted upward along the z-axis, coverage is poorest for the south polar region. Approximate maximum and minimum values of the relay-satellite elevation angles from different lunar sites are given in Table 5. Notice that there would be infrequent periods when none of the three relay satellites would be visible from the south pole. However, if required, this deficiency could be eliminated by using a four-satellite network.*

A final point may be made concerning the potential utility of the three-satellite communications network: it may also be very useful as a navigation aid for vehicles on the moon's far side. This service would be most important when real-time data is required (e.g., during lunar landing operations).

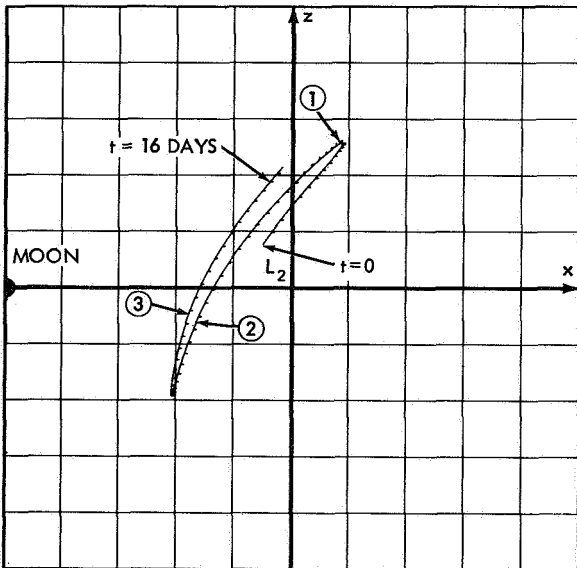
*It may also be possible to communicate directly with an earth station during these periods.

Table 4—Communications link calculation for television signals from lunar rover to SHALOM.

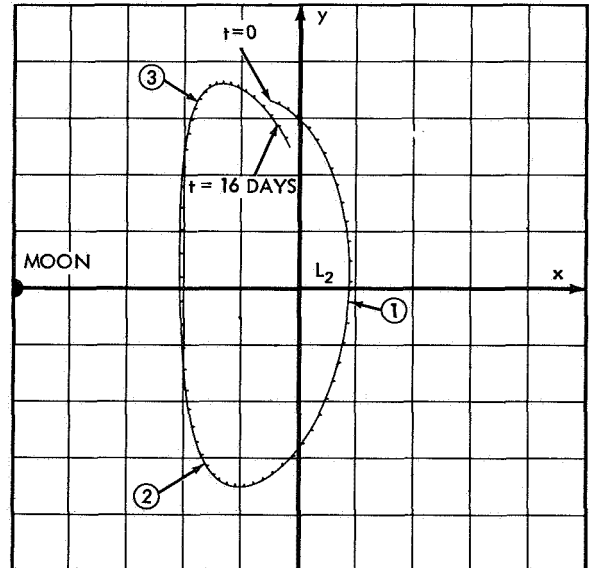
Modulation	FM with an index of 1.7
Video Bandwidth (500 lines at 1/2 frame per second)	200 kHz
Frequency (S-Band)	2.3 GHz
Required Postdetection Signal-to-Noise Ratio	25.0 dB
Required Predetection Bandwidth (B_{IF})	60.3 dB > 1 Hz
Bandwidth Ratio	5.4
Required Predetection Signal-to-Noise Ratio (S/N_o)	11.3 dB
Receiver Noise Temperature	570° K
Receiver Noise Spectral Density (N_o)	-201.0 dBw/Hz
Receiver Circuit Losses (L_R)	1.0 dB
Receiver Antenna Diameter	3.6 m (11.8 ft)
Receiver Antenna Beamwidth	2.65°
Receiver Antenna Gain (G_R)	36.2 dB
Transmitter Power (20 watts) (P_T)	13.0 dBw
Transmitter Circuit Losses (L_T)	1.4 dB
Transmitter Antenna Diameter	0.8 m (2.6 ft)
Transmitter Antenna Beamwidth	12°
Transmitter Antenna Gain (G_T)	23.0 dB
Transmitter Antenna Pointing Loss (L_P)	0.5 dB
Space Loss (L_S)	195.9 dB
Performance Margin (M)	2.8 dB
$M = P_T + G_T + G_R - L_T - L_P - L_R - L_S - N_o - B_{IF} - (S/N_o)$	



AS SEEN FROM MOON



PROJECTION IN PLANE PERPENDICULAR TO MOON'S ORBITAL PLANE



PROJECTION IN MOON'S ORBITAL PLANE

Figure 28—Typical halo trajectory segment for relay-satellite network relative to mean L_2 point. Time interval between tick marks is 6 hours, and the grid size is 12,900 km. Relay satellites are located at ①, ②, and ③. (Network is shown at time of minimum coverage for south polar region.)

Table 5—Approximate relay-satellite elevation angles with lunar librations taken into account.

Station Location	Favorable Libration		Unfavorable Libration	
	Maximum Elevation Angle	Minimum Elevation Angle	Maximum Elevation Angle	Minimum Elevation Angle
North Pole	30°	22°	14°	7°
South Pole	34°	11°	18°	-4°
Limb	39°	30°	25°	16°

CHAPTER IV

HALO-ORBIT SPACE STATION IN SUPPORT OF AN EXPANDED LUNAR EXPLORATION PROGRAM

In the summer of 1969, the President's Space Task Group proposed a comprehensive Integrated Program Plan for lunar exploration in the 1980's and beyond (Reference 12). A key item in this plan is the establishment of a space station in the vicinity of the moon. The Integrated Program Plan specifies that this space station be placed in a 111,12 km (60 n. mi.) polar lunar orbit. It is the purpose of this chapter to demonstrate that it would be better to locate the lunar space station in a halo orbit around the trans-lunar libration point. *

A. Elements of Expanded Lunar Program

In order to achieve the goals and objectives of an expanded lunar exploration program, it will be necessary to increase the limited landing-site accessibility, staytime, payload and mobility capabilities of the Apollo program. The frequency of lunar missions will also be increased. The final phase of this strategy calls for the creation of a permanent or semipermanent lunar-surface base. To accomplish a lunar program of this magnitude at a reasonable cost, it appears that a fully reusable earth-moon transportation system should be developed. The principal hardware elements of the earth-moon transportation system are as follows:

(1) Nuclear orbit-to-orbit shuttle (NOOS) or chemical orbit-to-orbit shuttle (COOS)—a reusable vehicle that operates between an earth orbit and the halo orbit. (See References 14-16 for a description of the nuclear shuttle vehicle.)

(2) Halo-orbit space station (HOSS)—a small manned station that is located in a 3500-km halo orbit about L_2 .

(3) Propellant storage depot (PSD)—an unmanned facility that is stationed near the HOSS. (A preliminary design is described in Reference 17.)

(4) Space tug—a reusable chemical vehicle that operates between the HOSS and the lunar surface.

In a typical mission sequence, the orbit-to-orbit shuttle (OOS) will be used to transport personnel and cargo from an earth-orbital base to the HOSS. ** The OOS will follow a three-impulse trajectory such as the one illustrated in Figure 22. Upon arrival at the halo orbit, the men and supplies will be transferred to the HOSS and the propellant

*It is interesting to note that libration-point space stations supporting lunar surface operations were discussed by Arthur C. Clarke as early as 1961 (Reference 13).

**As in the Integrated Program Plan, another reusable shuttle vehicle that performs transfers between earth and earth orbit is used to replenish the earth-orbital base.

for the lunar space tugs will be stowed in the PSD. The OOS will then return to the earth orbit. Transfer of cargo and passengers to the lunar surface will be effected by the space tug. Typical trajectories between the HOSS and a 111.12 km (60 n.mi.) lunar orbit are shown in Figure 29.*

B. Role of Halo-Orbit Space Station (HOSS)

The primary task for a lunar space station is to provide operational support for all lunar-surface and orbital activities. Some of these support functions will be discussed here.

1. Communications and Control Center

A halo orbit is an ideal location for a lunar communications and control center. This is so because continuous communications coverage for all far-side lunar operations would be available directly from the HOSS without dependence on relay satellites. Uninterrupted direct contact between the HOSS and the earth is also maintained. Moreover, with relay satellites at the L_1 point and in a large halo orbit as shown in Figure 28, the HOSS will always be able to communicate with any point on the moon or in orbit about it.** This type of communications and control network has the added advantage of being quasi-stationary with respect to the lunar surface. Finally, it should be noted that direct coverage of near-side lunar operations is already obtainable from earth stations.

The continuous communications coverage of the lunar far side by the HOSS will be especially beneficial when a lunar astronomical observatory is established, since it is quite likely that this observatory will be located on the far side of the moon. In the 1967 Summer Study of Lunar Science and Exploration (Reference 18), the Astronomy Working Group recommended a near-equatorial far-side observatory site. The Astronomy Working Group also stated a preference for a crater with a diameter of approximately 100 km and a rim height greater than 1 km above a fairly flat crater floor. An area of about 30 by 60 km that is free of cliffs, mountains, canyons, etc., is also desired for radio astronomy. It appears that the criteria listed above are nicely satisfied at the crater Tsiolkovsky (Figures 24-27).

A summary of some of the most important communications and control functions of the HOSS is presented in Table 6. Routine functions such as monitoring of scientific data from emplaced stations and tracking of unmanned orbiters should probably be handled by unmanned relay satellites. Therefore, these tasks are not listed in Table 6.

*As previously mentioned, in Section II-C, for trajectory calculations the halo-orbit terminus is well approximated by the L_2 point.

**The radius of the halo orbit for the space station must be at least 3700 km to maintain contact with the relay satellite at L_1 .

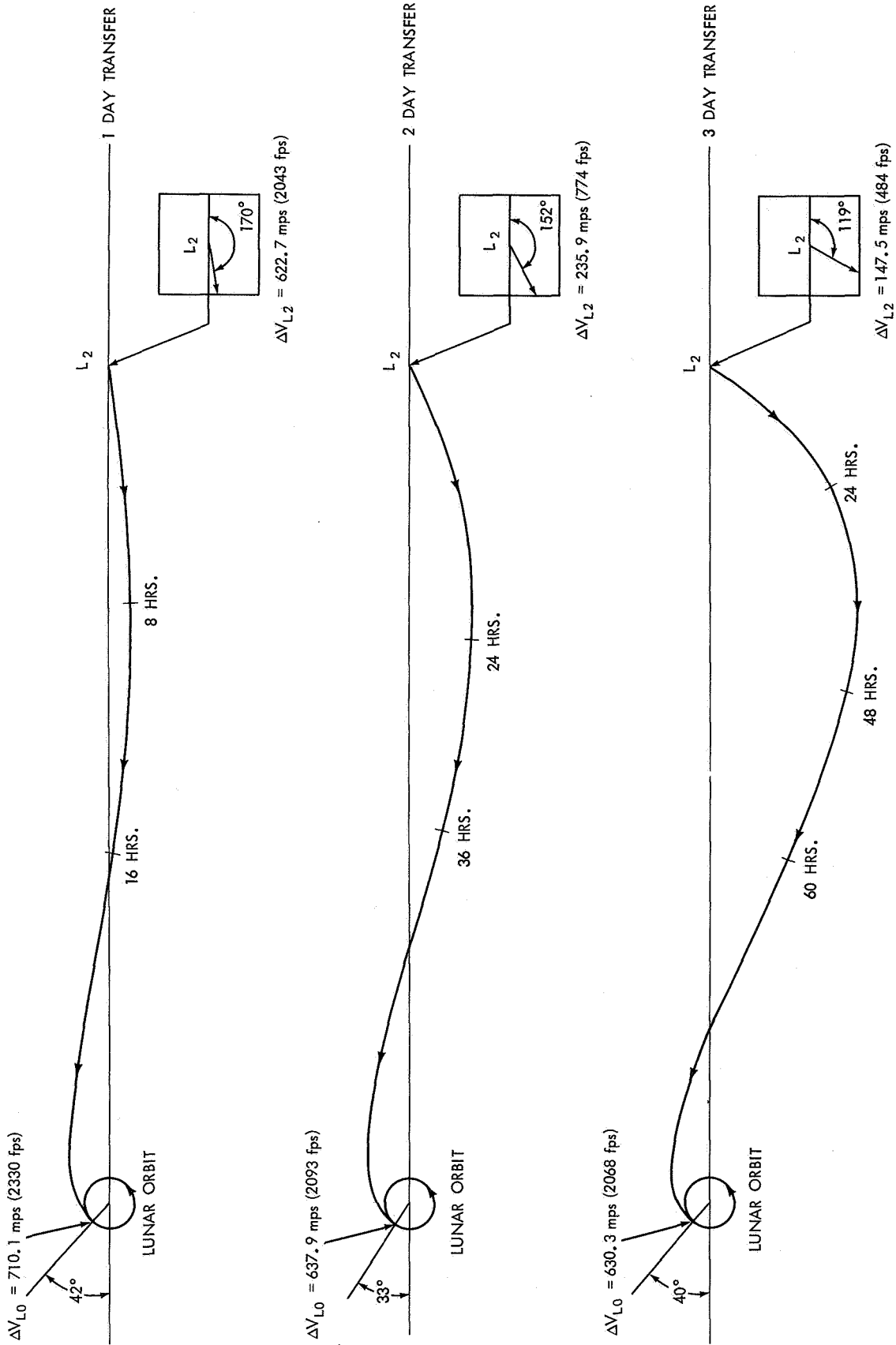


Figure 29—Two-impulse transfers from the L₂ point to a 111.12 km (60 n.mi.) lunar orbit.
(All transfers lie in moon's orbital plane.)

Table 6—Communications and control functions of the HOSS.

1. Control rendezvous and docking operations of OOS, PSD, and space tugs.
2. Monitor and control rendezvous, ascent, and descent trajectories of unmanned space tugs.
3. Assist in navigation and control of unmanned lunar-surface vehicles. (Vehicles on moon's near side may be controlled from earth.)
4. Provide earth data link and point-to-point communications service for moon's far side (polar and limb regions would use relay satellites).
5. Furnish communications and navigational support for manned surface expeditions.
6. Control unmanned remote-manipulator vehicles (Reference 19) in the lunar vicinity. These vehicles require continuous communications and minimal transmission delay times for efficient operation. They would be used mainly for satellite maintenance and repair.
7. Provide capability to command, control, and monitor all elements of the lunar program as required.

2. Lunar Logistics Depot

The HOSS will be the principal logistics staging point for all lunar missions. Here, OOS payloads will be broken down into smaller packages and then transported to the lunar surface by space tugs. Most rendezvous, docking, and refueling operations involving the OOS, PSD, and space tugs will take place in the vicinity of the HOSS.

The HOSS will also serve as a hangar for all lunar elements when they are not in use. These elements would include space tugs, remote-manipulator vehicles, relay satellites, and possibly even lunar-surface mobility aids. Extensive maintenance and repair services will be provided by the HOSS. This type of assistance would greatly increase the reliability and useful life of the listed elements.

There are two inherent advantages associated with the halo-orbit location for the logistics staging point:

(1) The quasi-stationary characteristic of the halo orbit with respect to the earth-moon line and the lunar surface permits considerable flexibility in the scheduling of lunar shuttle operations. For instance, the launch window for transfers between the halo orbit and the lunar surface is infinite.

(2) The ΔV requirements for transfers between the halo orbit and the lunar surface are almost identical for any landing site, since plane changes can be made quite cheaply at the halo orbit. The difference in ΔV cost is usually less than 61 mps (200 fps).

3. Comparison with Lunar-Orbit Space Station (LOSS) Alternative

Current versions of the Integrated Program Plan advocate a 111.12 km (60 n. mi.) polar lunar orbit for the lunar space station. The rationale for the selection of a polar inclination for the LOSS seems to be that a polar LOSS would pass over the entire lunar surface every 14 days.* Although the use of a polar orbit would permit space tug landings at any point on the moon with little or no plane change, the nominal surface staytime would probably be constrained to 14-day intervals. Otherwise, a plane change would be required when the tug returns to the LOSS. The ΔV penalty for this plane change as a function of surface staytime is given in Figure 30.** It should be noted that the results in Figure 30 were obtained by using a near-optimal three-impulse transfer.†

The selection of a low-altitude orbit for the LOSS has evidently been motivated by a desire to carry out an extensive program of orbital science (e.g., surface mapping, particles and fields experiments) from the LOSS. However, this reasoning is highly questionable. A recent study (Reference 20) of the scientific uses of a lunar orbital base has concluded that:

"... scientifically, there is no strong justification for a lunar orbital base, and that such a base should not be established unless there are compelling non-scientific reasons for doing so. . . The orbital science, except for photography, can be performed as well, or better, from an unmanned, non-returning spacecraft."

The present author agrees with this conclusion, and, therefore, scientific uses of the LOSS or HOSS will not be considered here.

The utility of the HOSS as a communications and control center for an advanced lunar program was previously described. The LOSS, on the other hand, would be particularly ill-suited for this role, for the following main reasons:

(1) A lunar-surface base would not have any direct contact with the LOSS for periods as long as 11 days. Moreover, the line-of-sight contact time would only be about 10 minutes per orbit even when the LOSS passes over the base site.

(2) Continuous direct contact between the LOSS and the earth would only be available for two 3-day periods each month. At other times, line-of-sight contact would be interrupted during every orbit.

(3) The LOSS would be almost completely dependent on satellite and/or earth relay links for control of certain critical lunar operations (e.g., a surface-rescue mission).

*The orbit plane for the lunar polar orbit is essentially fixed in inertial space with the moon's rotation accounting for the 14-day period.

**Faust, N. L., "Launch and Polar Orbit Transfer Velocity Requirements for the LM-B (Space Tug)" NASA-MSD Internal Note 70-FM-37, March 9, 1970.

†In the three-impulse transfer, the first impulse is used to inject the spacecraft into an intermediate elliptical orbit. At apolune, a second impulse is applied to rotate the orbit plane. The third impulse, at perilune, inserts the spacecraft into the target orbit. For plane changes less than about 20 deg, the optimal solutions degenerate into two-impulse transfers.

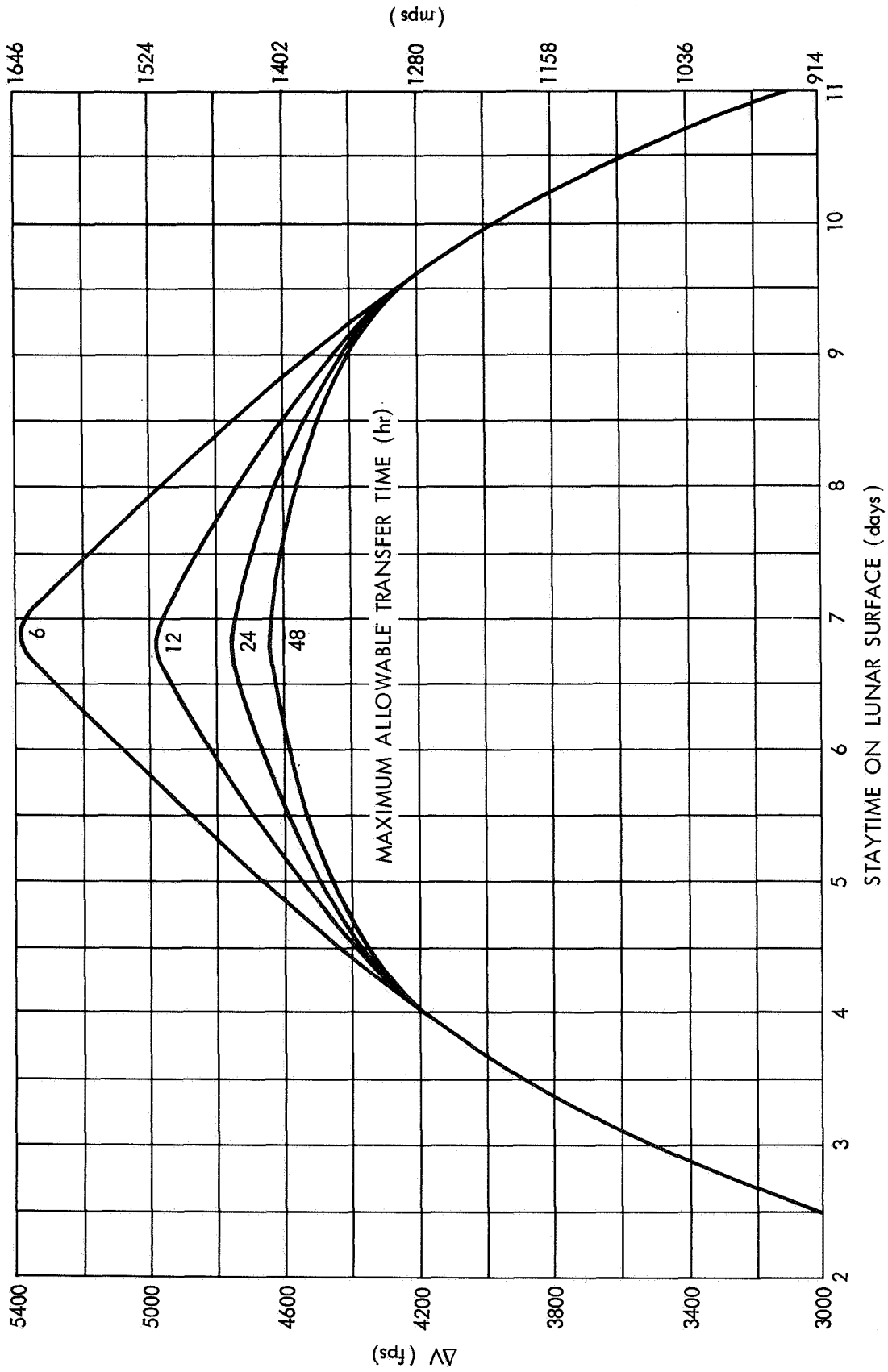


Figure 30—Plane-change ΔV penalty for a transfer between a 111.12 km (60 n.mi.) polar lunar orbit and an equatorial landing site*. (A near-optimal three-impulse transfer has been assumed.)

*Faust, op. cit.

Furthermore, two simultaneous relay links would usually be required and switchovers would occur every hour.

The use of a HOSS instead of a LOSS would also permit greater flexibility in the scheduling of shuttle operations. As already pointed out above, transfers between the HOSS and any point on the lunar surface could take place at any time without incurring an additional ΔV penalty. In contrast, an unrestricted launch window for transfers between the LOSS and a particular lunar site would, in general, involve costly plane changes. However, for transfers between the lunar space station and an earth parking orbit, the issue is not as clear-cut. Since plane changes must be minimized for economical OOS transfer, launch opportunities are limited by certain varying geometrical factors. For a LOSS, the following factors apply (References 14-16 and 21):

- (1) moon's position,
- (2) nodal regression of the earth parking orbit,
- (3) orientation of the LOSS orbit with respect to the earth-moon line.

Transfers to the HOSS would not be subjected to the third constraint, but the transfer times would be somewhat longer than those required for the LOSS.

Another oft-stated argument in favor of a LOSS is that it would be an ideal location for a rescue space tug. However, as can be seen in Figure 30, the plane-change ΔV penalty can become rather high when a surface rescue mission is needed at an inopportune time. Notice that the ΔV cost is not very sensitive to the maximum allowable transfer time. For a rescue tug stationed at a HOSS, the tradeoffs are quite different, as is apparent from Figure 31. A comparison of Figures 30 and 31 shows that, from a ΔV standpoint, neither concept has a clear advantage for all rescue situations. However, the ΔV comparison does not tell the whole story. As will be shown in the next section, the nominal design for the HOSS tug will have two stages: a first stage, used solely for the transfer from the HOSS to lunar orbit, and a second stage, for the lunar landing and subsequent return to the HOSS. Therefore, extra ΔV capability for a particular rescue situation could be obtained by simply using a modified first stage.

Finally, the stationkeeping requirements of the two space station concepts should be considered. The instability of the halo orbit may appear to be a serious drawback to the HOSS concept until it is realized that, without orbit control, the LOSS would impact with the lunar surface in about 4 months (a real LOSS). Furthermore, the stationkeeping cost for orbital stabilization of the LOSS would be about 121.9 mps/yr (400 fps/yr),* which is about four times the cost for stabilization of the HOSS (see Figure 15).

In Reference 12, Dr. George E. Mueller claimed that a LOSS would "provide a highly stable, safe, and flexible operations base". However, in view of the foregoing discussion, there is some doubt concerning the validity of this claim.

*One control pulse is assumed every 2 weeks.

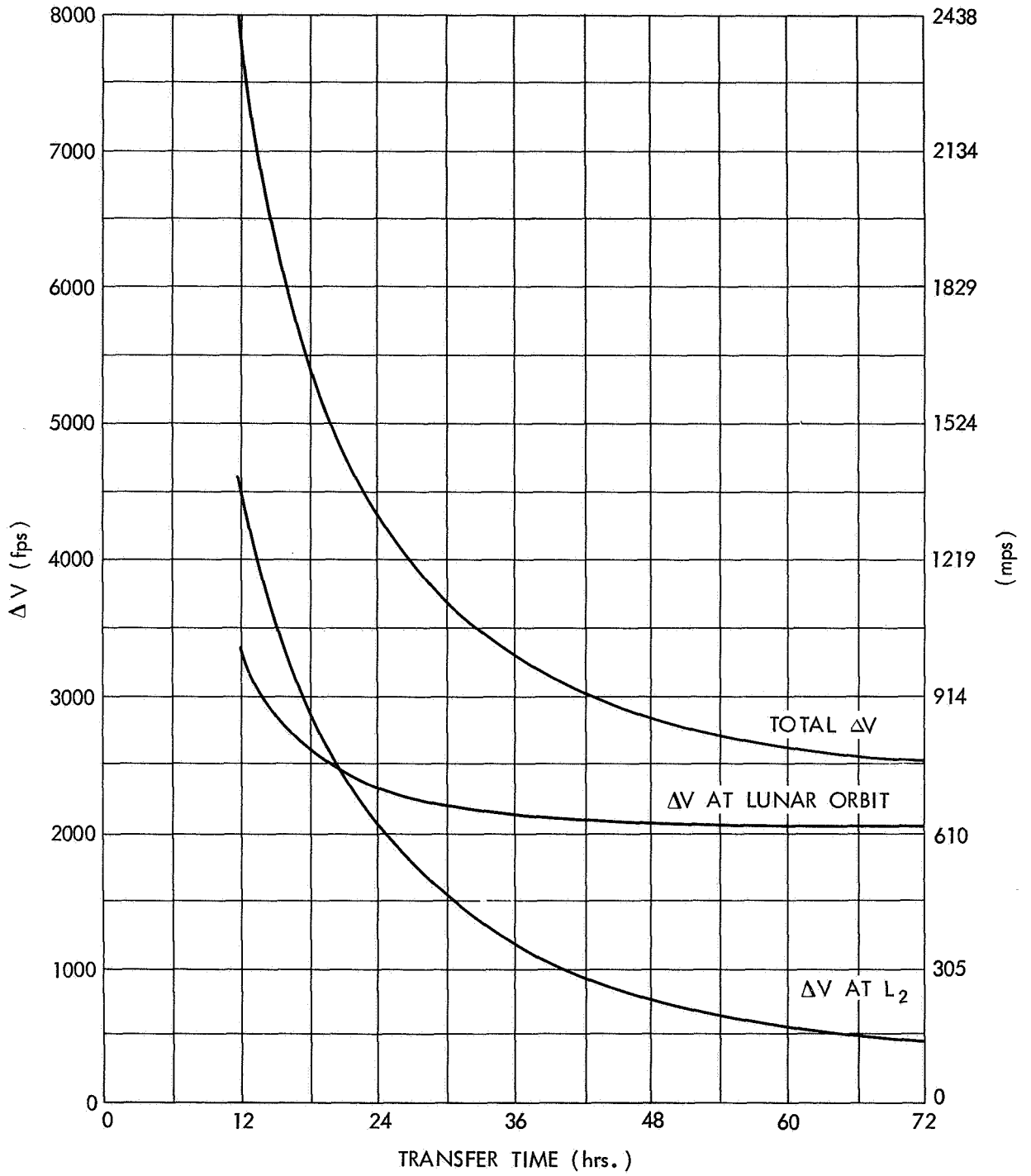


Figure 31— ΔV requirement for a two-impulse transfer between the L_2 point and a 111.12 km (60 n.mi.) lunar orbit. [An equatorial lunar orbit has been assumed. A polar lunar orbit could require as much as 61 mps (200 fps) additional ΔV .]

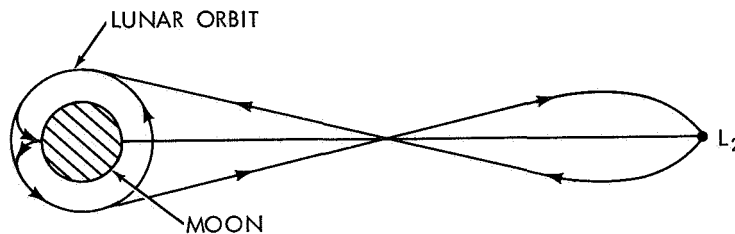
C. Lunar Transportation System Performance

Some of the operational advantages of using a HOSS instead of a LOSS were given above. In this section it will be shown that the use of a HOSS would also have a favorable effect on the overall performance of the reusable lunar shuttle system.

1. Space Tug

As previously noted, the space tug is used to ferry crew members and supplies between the lunar space station and the lunar surface. Although a tug based at a LOSS would almost certainly be a single-stage vehicle, a two-stage tug might be more efficient for transfers between a HOSS and the moon. Therefore, a comparison of the performance of one- and two-stage HOSS tugs is performed here.

The two assumed mission modes for the HOSS-based space tug are outlined in Figure 32. Notice that none of the operational flexibility of the halo-orbit rendezvous technique is sacrificed by using the two-stage mode.



SINGLE-STAGE MODE:

1. TUG DEPARTS FROM L₂ AND BRAKES TO 111.12 km (60.7 mi.) LUNAR ORBIT. [$\Delta V \approx 777$ mps (2550 fps) FOR 72-HR. TRANSFER].
2. TUG DESCENDS TO LUNAR SURFACE AND LEAVES PAYLOAD m_{sd} . [$\Delta V \approx 2012$ mps (6600 fps)].
3. TUG ASCENDS TO LUNAR ORBIT WITH PAYLOAD m_{sa} . [$\Delta V \approx 1890$ mps (6200 fps)].
4. TUG LEAVES LUNAR ORBIT AND RETURNS TO L₂. [$\Delta V \approx 777$ mps (2550 fps) FOR 72-HR. TRANSFER].

TWO-STAGE MODE:

1. FIRST STAGE IS USED TO EFFECT TUG TRANSFER FROM L₂ TO LUNAR ORBIT.
2. STAGES ARE THEN SEPARATED AND FIRST STAGE RETURNS TO L₂ WHILE SECOND STAGE DESCENDS TO LUNAR SURFACE AND LEAVES PAYLOAD m_{sd} .
3. SECOND STAGE ASCENDS TO LUNAR ORBIT AND RETURNS TO L₂ WITH PAYLOAD m_{sa} .

Figure 32—Mission modes for lunar space tug.

The performance of each mode can be determined by applying the standard rocket equations:

$$\frac{W_G}{W_G - W_P} = \exp \left[\frac{\Delta V}{I g} \right] \equiv K \quad (9)$$

$$W_G = W_{ST} + M_C + M_S \quad (10)$$

$$\lambda = W_P / W_{ST} \quad (11)$$

with the definitions

ΔV = velocity increment

I = specific impulse

g = gravitational acceleration at earth's surface

W_G = gross weight of vehicle

W_P = stage propellant weight*

W_{ST} = total stage weight

M_C = fixed module weight

M_S = payload

λ = mass fraction. **

Equations 9 to 11 can be used to obtain an expression for the total required propellant weight, W_{PT} . The normalized propellant weight W_{PT}/M_S will be the basic measure of performance for a given mission mode.

The principal definitions for the two-stage mode are given in Figure 33. A derivation of the performance function W_{PT}/m_{sd} for this mode is presented in Appendix D. Notice that Equation D-6 can be applied to the single-stage case by taking $\Delta V_d = 2789$ mps (9150 fps).

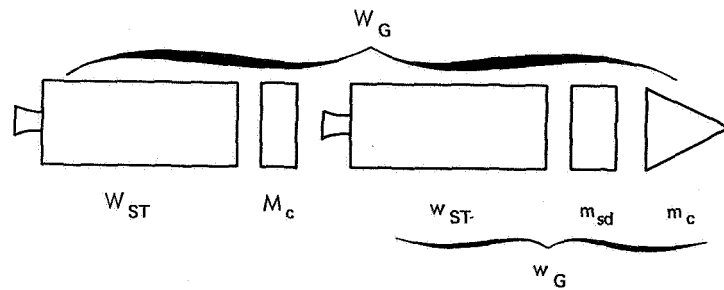
Quantitative results can be obtained from the equations of Appendix D only by making certain assumptions that reduce the number of independent parameters.

(1) $I_1 = I_2 = 444$ sec (H_2/O_2 combination).

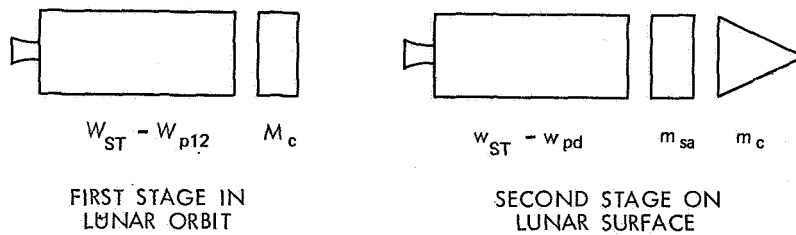
(2) No payload is returned from the lunar surface (i.e., $m_{sa} = 0$). Therefore, $k_2 = 0$.

*It is worth noting that the stage inert weight is given by $W_i = [(1 - \lambda)/\lambda] W_P$

**Typical values of the mass fraction are 0.80 to 0.90 (chemical rockets) and 0.70 to 0.80 (nuclear rockets).



INITIAL CONFIGURATION AT HOSS



FIRST STAGE IN LUNAR ORBIT

SECOND STAGE ON LUNAR SURFACE

CONFIGURATION JUST BEFORE RETURN TO HOSS

W_G : TOTAL GROSS WEIGHT
 m_{sd} : PAYLOAD DELIVERED TO LUNAR SURFACE
 m_{sa} : PAYLOAD RETURNED FROM LUNAR SURFACE
 FIRST STAGE:
 W_{ST} : STAGE WEIGHT
 M_c : FIXED MODULE WEIGHT
 W_{p12} : WEIGHT OF PROPELLANT USED TO BRAKE BOTH STAGES INTO LUNAR ORBIT

SECOND STAGE:
 w_G : GROSS WEIGHT
 w_{ST} : STAGE WEIGHT
 m_c : FIXED MODULE WEIGHT
 w_{pd} : WEIGHT OF PROPELLANT USED DURING LUNAR DESCENT

Figure 33—Stage definitions for two-stage space tug.

(3) Constant values are used for the ratios k_1 and α . Nominal values can be obtained by using preliminary space tug data.* Representative weights for the cargo version of the lunar space tug are:

$$w_p = 27,216 \text{ kg (60,000 lb)}$$

$$m_{sd} = 20,412 \text{ kg (45,000 lb) (includes cargo module).}$$

$$m_c = 3765 \text{ kg (8300 lb) [intelligence module } \sim 2268 \text{ kg (5000 lb), landing gear } \sim 1497 \text{ kg (3300 lb)]}$$

$$M_c = 567 \text{ kg (1250 lb).}$$

With this data, the ratios are approximately $k_1 = 0.185$ and $\alpha = 0.01$. These values will be used here.

With the assumptions listed above, the relative performance of the two mission modes can now be evaluated. The results, as functions of the mass fractions, are graphed in Figures 34 and 35. From these graphs, it can be seen that a performance improvement is gained by using the two-stage mission mode. The insensitivity of the performance function to the mass fraction for the first stage (λ_1) should also be noted.

2. Nuclear Orbit-to-Orbit Shuttle (NOOS)

The OOS operates between the earth-orbital base and the lunar space station. In addition to carrying personnel and cargo between the two stations, the OOS must deliver the propellant for the lunar space tugs. This subsection will consider the NOOS, and the COOS will be examined in the next subsection.

Three mission modes will be investigated here. The first mode calls for staging at a LOSS and is described in Figure 36. The other two modes utilize HOSS staging and involve either a one- or a two-stage space tug for transfers between the HOSS and the moon. The HOSS modes are outlined in Figure 37. Stage definitions for the NOOS with a single-stage tug are given in Figure 38, and the performance function for this mode is derived in Appendix E.

The assumptions for the tug stages that were listed in the previous subsection are retained here (i. e., $I = 444$ sec, $k_1 = 0.185$, $k_2 = 0$, and $\alpha = 0.01$). For the NOOS stage, the principal assumptions are

(1) $I = 825$ sec (H_2 propellant).

(2) No payload is returned from the lunar space station (i. e., $M_{sa} = 0$). Therefore, $\alpha_2 = 0$.

(3) $\alpha_1 = 0.111$. This value was determined by assuming the nominal weights

$$M_c = 4536 \text{ kg (10,000 lb)}$$

$$M_{sd} = 40,824 \text{ kg (90,000 lb) (includes cargo module).}$$

*"Space Tug", NASA-MSC Project Description Document, National Aeronautics and Space Administration, Manned Spacecraft Center, Advanced Missions Program Office, Houston, Texas, April 24, 1970.

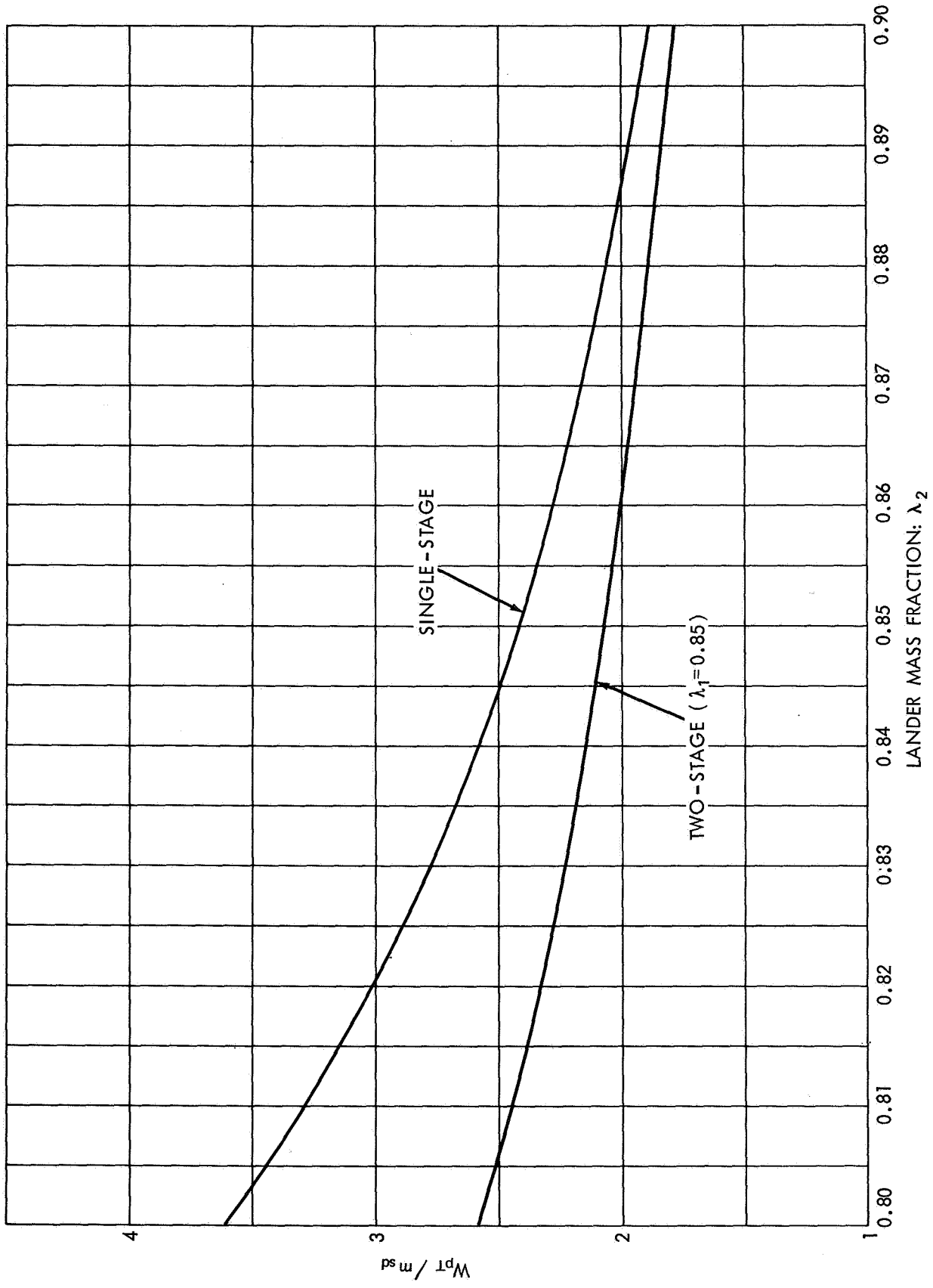


Figure 34—Normalized propellant weight for HOSS-based space tug as a function of the mass fraction for the landed stage.

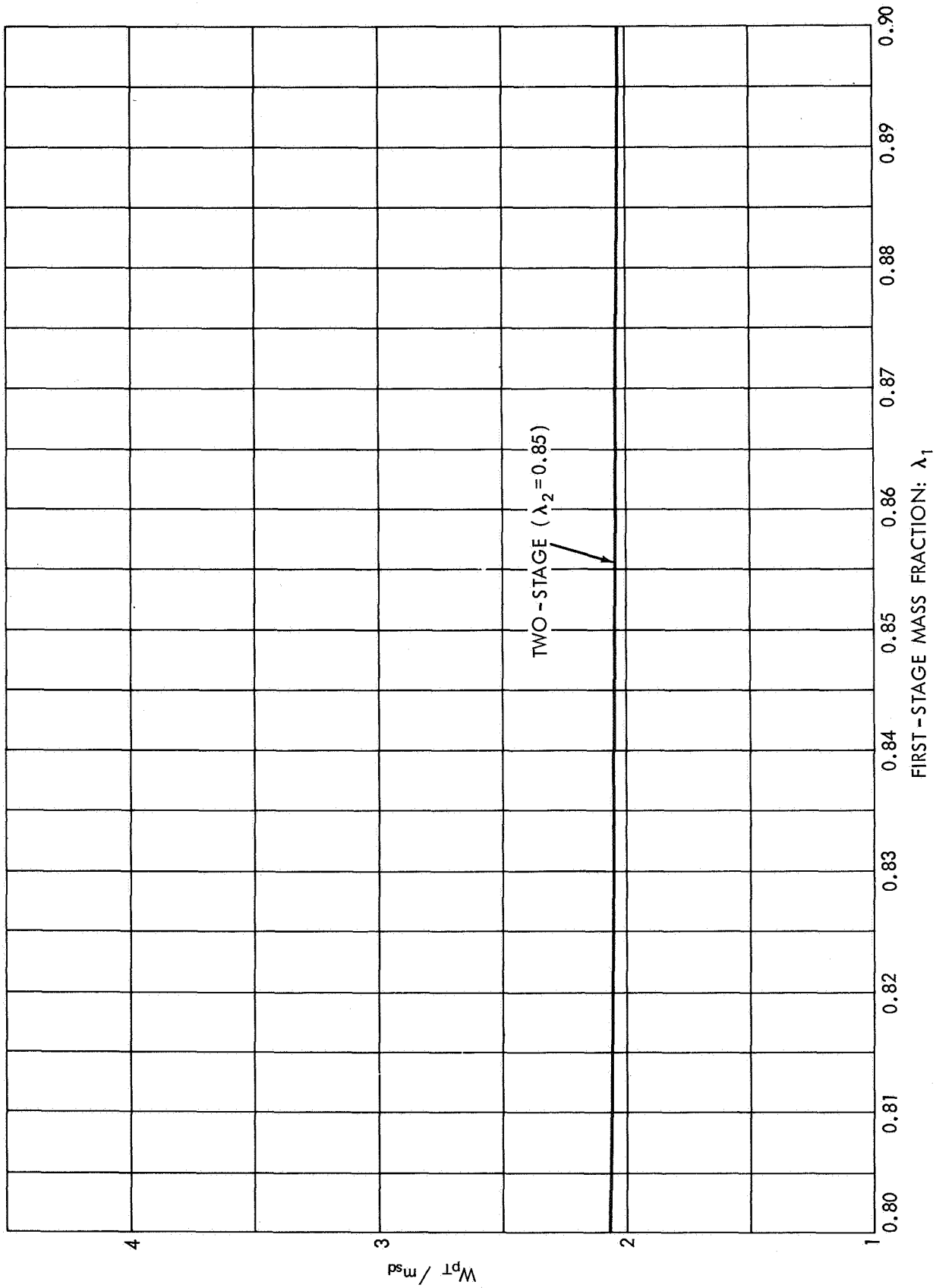
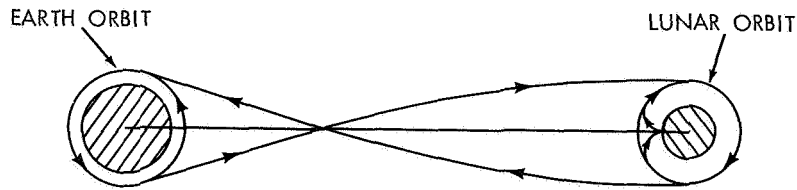


Figure 35—Normalized propellant weight for HOSS-based space tug as a function of the mass fraction for the first stage.



1. NOOS DEPARTS FROM 185.2 km (100 n.mi.) EARTH ORBIT AND BRAKES TO 111.12 km (60 n.mi.) LUNAR ORBIT. [FOR 108-HR TRANSFER, $\Delta V \approx 3139$ mps (10,300 fps) AT EARTH ORBIT AND $\Delta V \approx 914$ mps (3000 fps) AT LUNAR ORBIT].
2. NOOS DELIVERS PAYLOAD M_{sd} TO LOSS AND TRANSFERS TUG PROPELLANT w_p TO PSD.
3. NOOS TAKES PAYLOAD M_{sa} FROM LOSS AND RETURNS TO EARTH ORBIT. (ΔV costs are same as in ①).
4. PROPELLANT w_p IS TRANSFERRED FROM PSD TO SPACE TUG.
5. TUG DESCENDS TO LUNAR SURFACE AND LEAVES PAYLOAD m_{sd} [$\Delta V \approx 2012$ mps (6600 fps)].
6. TUG RETURNS TO LOSS WITH PAYLOAD m_{sa} [$\Delta V \approx 1890$ mps (6200 fps)].

NOTES:

1. ΔV COSTS FOR THE NOOS AT LUNAR ORBIT ARE FOR A 2-DAY LAUNCH WINDOW. AN UNFAVORABLE ALIGNMENT OF LUNAR POLAR ORBIT COULD REQUIRE AS MUCH AS 457 mps (1500 fps) ADDITIONAL ΔV EVEN WITH A 3-IMPULSE MANEUVER (Reference 22).
2. IT IS ASSUMED THAT $m_{sd} = \beta M_{sd}$, WHERE β HAS THE RANGE $0 \rightarrow 1$. THIS ACCOUNTS FOR THE PAYLOAD THAT STAYS AT THE LOSS.

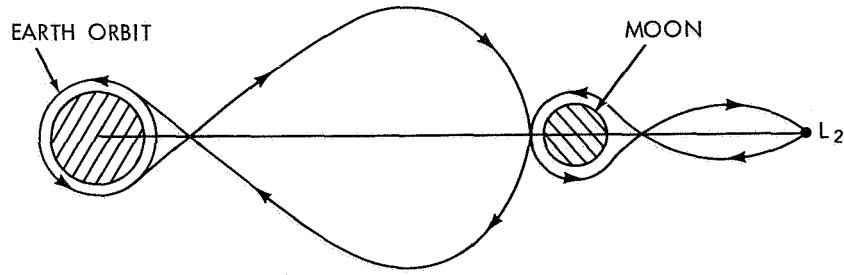
Figure 36—Mission mode for nuclear lunar shuttle system with LOSS rendezvous.

The performances of the candidate mission modes are compared in Figures 39 to 41. Notice that the LOSS rendezvous mode is rather sensitive to the NOOS mass fraction. As expected from the results of the previous subsection, a performance gain is registered if a two-stage space tug is used with the HOSS rendezvous mode. Furthermore, the use of a two-stage tug not only improves the overall performance of the lunar shuttle system with HOSS staging, but, as shown in Figure 42, it causes a considerable reduction in the stage weight for the lunar lander.

The sensitivity of the performance function to variations in the module ratios α_1 and k_1 is shown in Figures 43 and 44. It can be seen that even rather large variations in the module ratios would not significantly alter the relative performance results of Figures 39 to 41. Note that the relative changes in the performance functions are smaller than their absolute differences.

3. Chemical Orbit-to-Orbit Shuttle (COOS)

Two possible mission modes for a lunar shuttle system with a COOS are investigated here; one mode uses LOSS staging, while the other employs HOSS staging. Because



1. NOOS DEPARTS FROM 185.2 km (100 n.mi.) EARTH ORBIT AND BRAKES TO THE HOSS NEAR L_2 . [FOR 212-HR. TRANSFER, $\Delta V \approx 3139$ mps (10,300 fps) AT EARTH ORBIT AND $\Delta V \approx 335$ mps (1100 fps) FOR THE TWO REMAINING IMPULSES NEEDED TO ARRIVE AT THE HOSS].
2. NOOS DELIVERS PAYLOAD M_{sd} TO HOSS AND TRANSFERS TUG PROPELLANT w_p TO PSD.
3. NOOS TAKES PAYLOAD M_{sa} FROM HOSS AND RETURNS TO EARTH ORBIT. (ΔV costs are same as in ①).
4. PROPELLANT w_p IS TRANSFERRED FROM PSD TO SPACE TUG.
5. TWO POSSIBLE MISSION MODES FOR SPACE TUG OPERATIONS BETWEEN THE HOSS AND THE LUNAR SURFACE ARE DESCRIBED IN FIGURE 32.

NOTE: IT IS ASSUMED THAT $m_{sd} = \beta M_{sd}$, WHERE β HAS THE RANGE $0 \rightarrow 1$. THIS ACCOUNTS FOR THE PAYLOAD THAT STAYS AT THE HOSS.

Figure 37—Mission mode for nuclear lunar shuttle system with HOSS rendezvous.

of the lower specific impulse for a chemical stage, a two-stage COOS is used in both modes. The changes in the lunar shuttle modes when the NOOS is replaced by a two-stage COOS are described in Figure 45. Stage definitions for the two-stage COOS are given in Figure 46, and the performance function for the complete lunar shuttle system with this vehicle is derived in Appendix F.

As in the previous subsection, the assumptions for the tug stages are retained. For the COOS, the main assumptions are

- (1) $I_1 = I_2 = 444$ sec (H_2/O_2 combination).
- (2) No payload is returned from the lunar space station (i. e., $m_{sa} = 0$). Therefore, $\alpha_2 = 0$.
- (3) $\alpha_1 = 0.111$ and $\gamma = 0.01$.

The optimum ΔV split between the first and second stages of the COOS is obtained from Figure 47. Overall performances for the two mission modes are compared in Figures 48 to 51. Note the sensitivity of the LOSS rendezvous mode to a plane change at the lunar polar orbit.

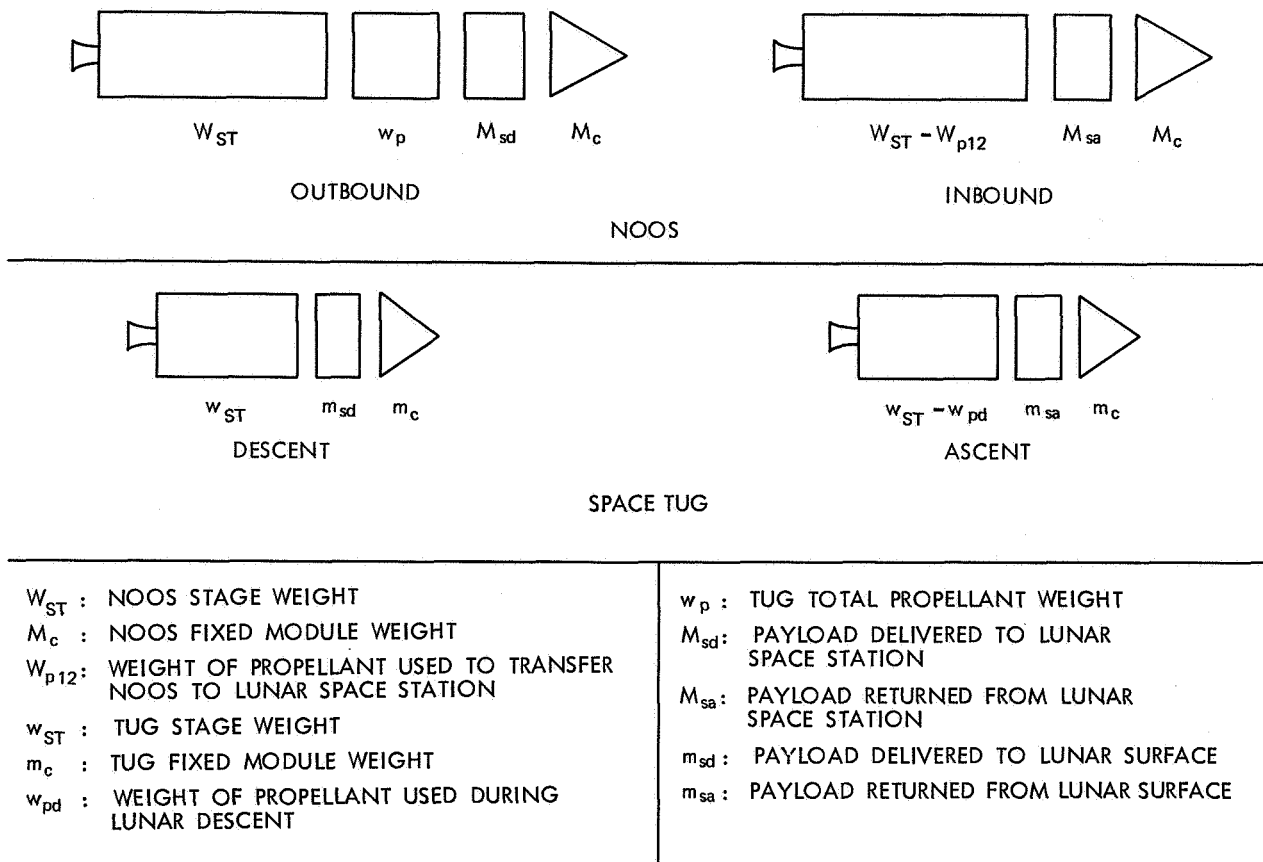


Figure 38—Stage definitions for nuclear lunar shuttle system with single-stage space tug.

4. Final Comments

The previous performance results, although based on idealized analyses, lead to three conclusions:

- (1) When using HOSS staging, the lunar space tug should be a two-stage vehicle.
- (2) For a lunar shuttle system with a NOOS, the HOSS rendezvous mode seems to have a slight performance advantage over the LOSS mode.
- (3) For a lunar shuttle system with a COOS, significant performance gains can be achieved by using HOSS staging.

When the nuclear and chemical lunar shuttle systems are compared, it should be noted that the performance estimates for the nuclear shuttle given in Figures 39 to 41 may be somewhat optimistic because

- (1) The effective specific impulse of the nuclear stage is reduced by inefficient cooldown impulses (References 14-16).

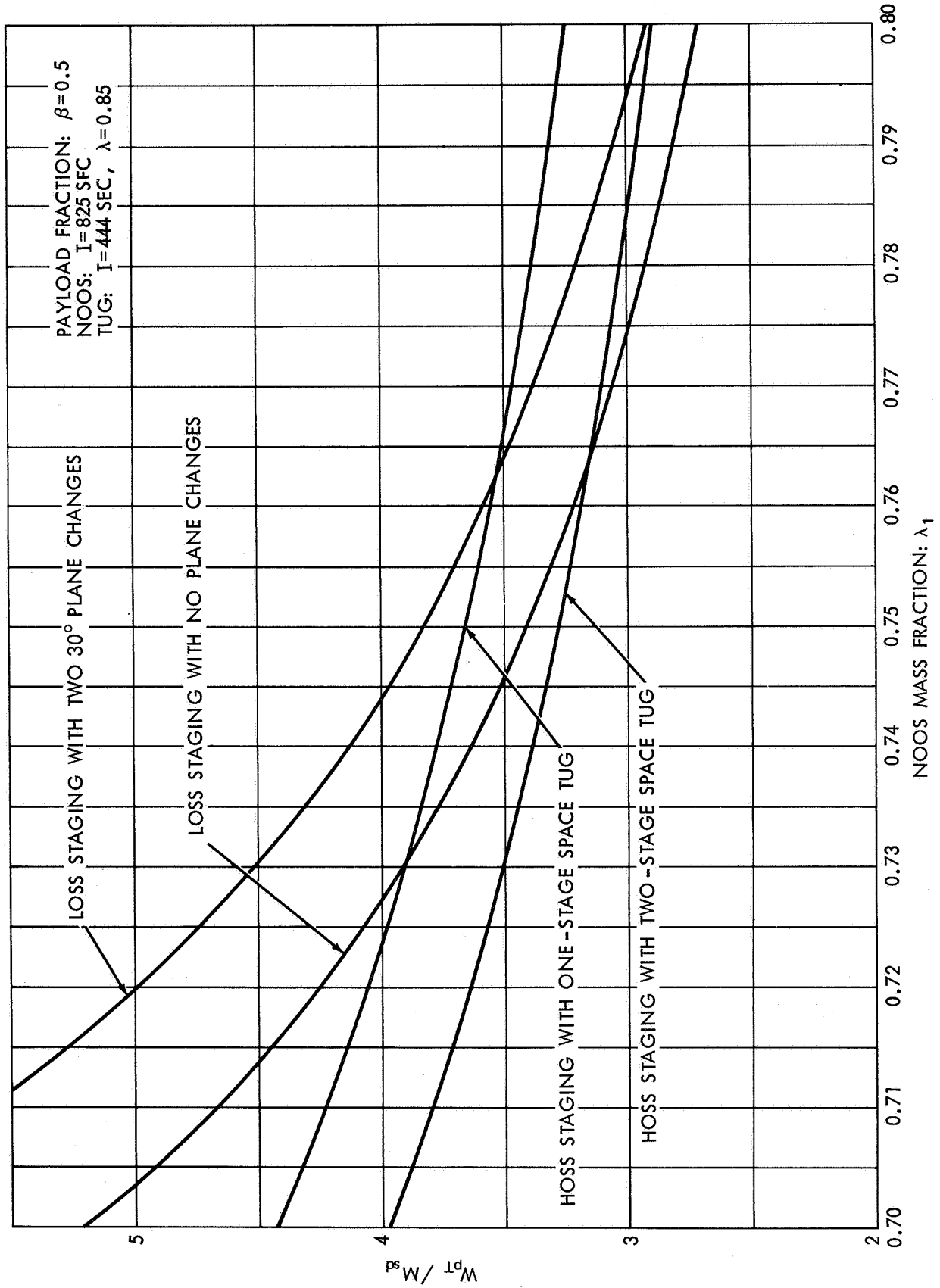


Figure 39—Normalized propellant weight for nuclear lunar shuttle system as a function of the mass fraction for the NOOS.

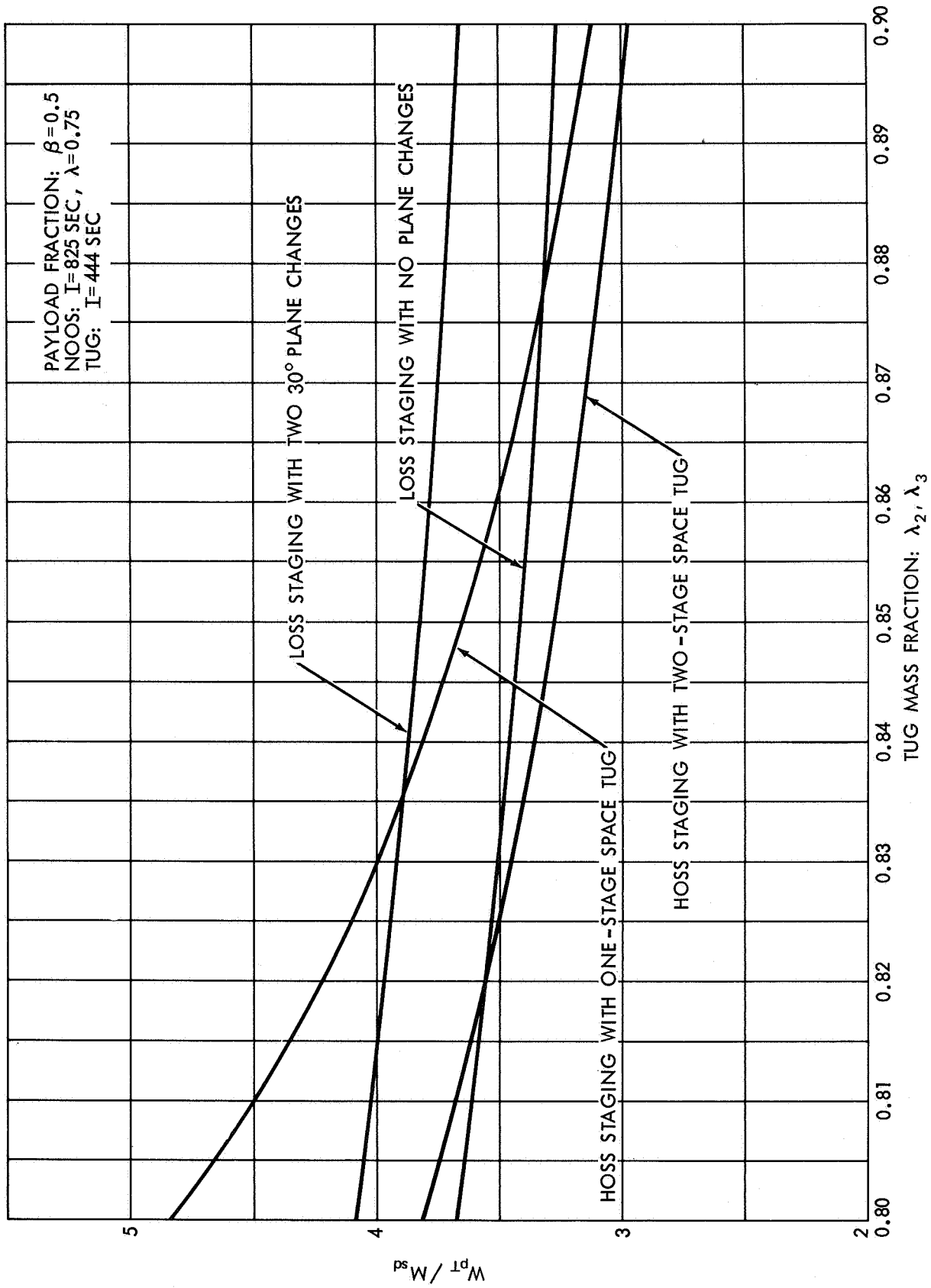


Figure 40—Normalized propellant weight for nuclear lunar shuttle system as a function of the mass fraction for the space tug.

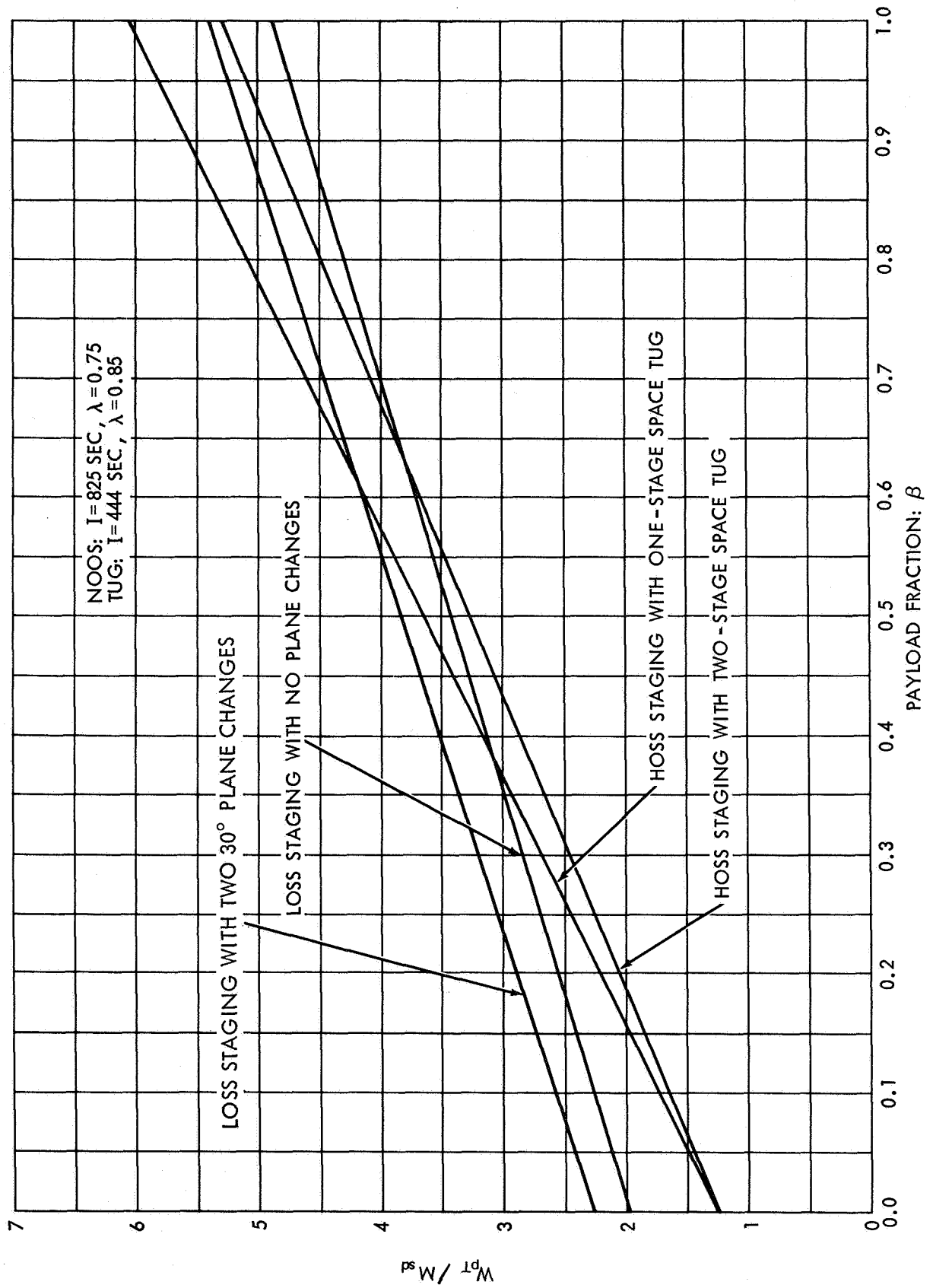


Figure 41—Normalized propellant weight for nuclear lunar shuttle system as a function of the payload fraction.

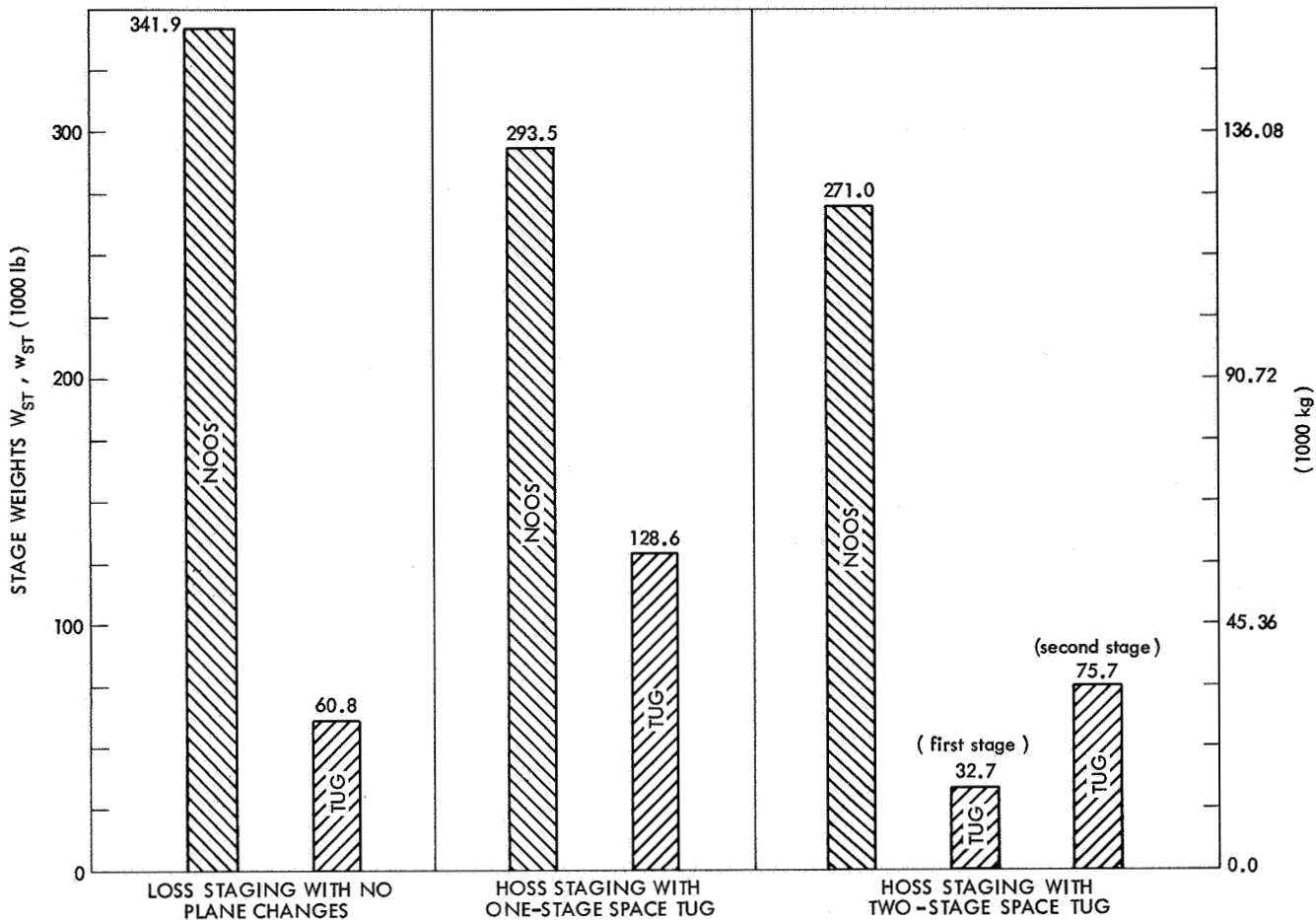


Figure 42—Stage weights for nuclear lunar shuttle system. Nominal case: $\beta = 0.5$; $M_{sd} = 40,824$ kg (90,000 lb); NOOS: $I = 825$ sec, $\lambda = 0.75$; Tug: $I = 444$ sec, $\lambda = 0.85$.

(2) A linear scaling law has been assumed. Actually, the mass fraction of the nuclear stage decreases substantially as its size decreases. *

Finally, it is recommended that more rigorous analyses of lunar shuttle modes using HOSS rendezvous be conducted. Mission modes that utilize propellants produced on the moon's surface might also be included in these studies. **

D. Use of HOSS as a Launching Platform for Unmanned Planetary Probes

The upper stage of the HOSS-based space tug could also be used to boost unmanned spacecraft into transplanetary trajectories. Of course, the unmanned probe must first

*Osias, D. J., "Performance Comparison of Nuclear and Chemical Lunar Shuttles," Bellcomm Memorandum B70-08028, Bellcomm, Inc., Washington, D.C., August 14, 1970.

**London, H. S., "Comparison of Several Lunar Shuttle Modes," Bellcomm Memorandum B69-09071, Bellcomm, Inc., Washington, D.C., September 29, 1969.

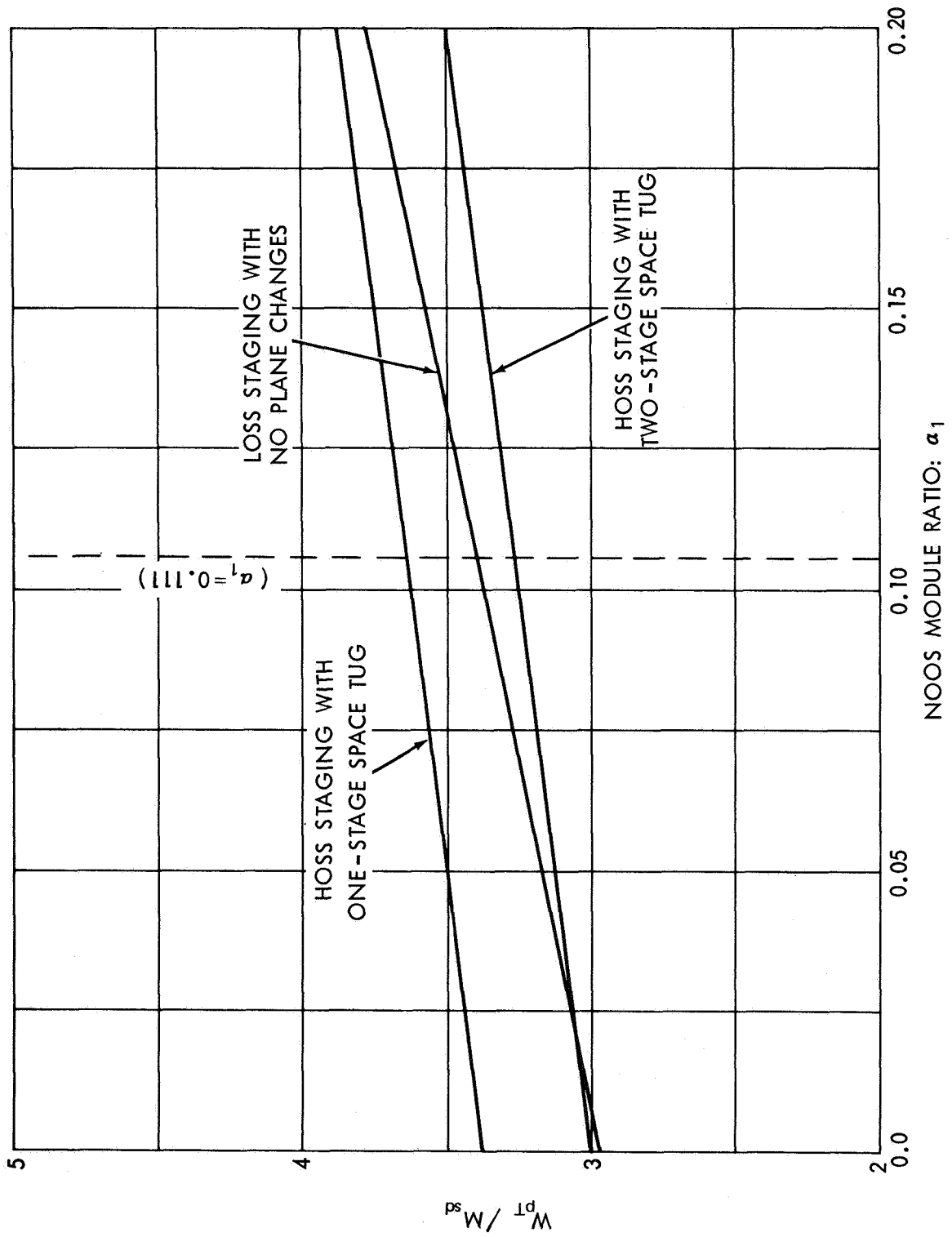


Figure 43—Performance function sensitivity to NOOS module ratio. $\beta = 0.5$; NOOS: $l = 825$ sec, $\lambda = 0.75$; Tug: $l = 444$ sec, $\lambda = 0.85$, $k_1 = 0.185$.

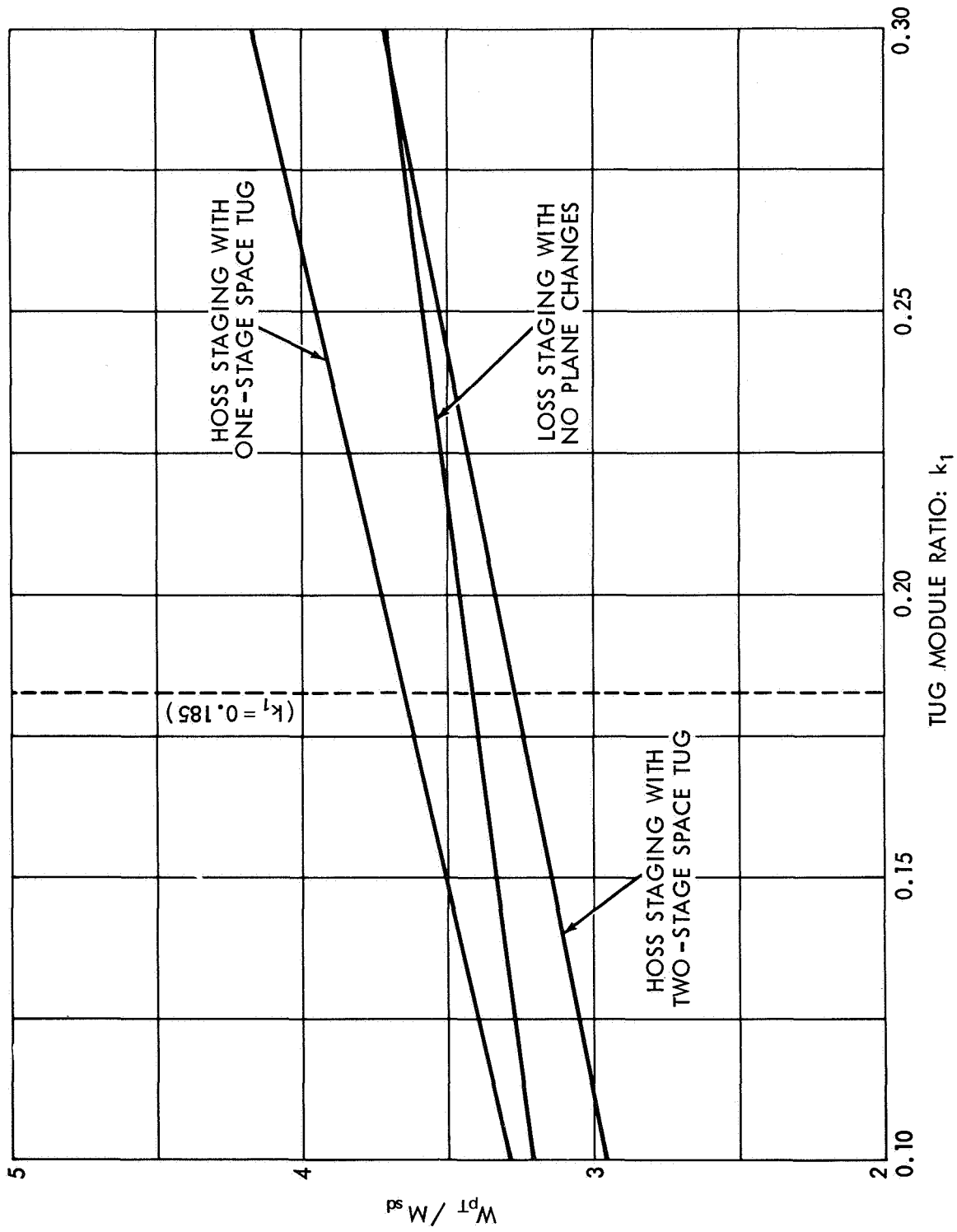
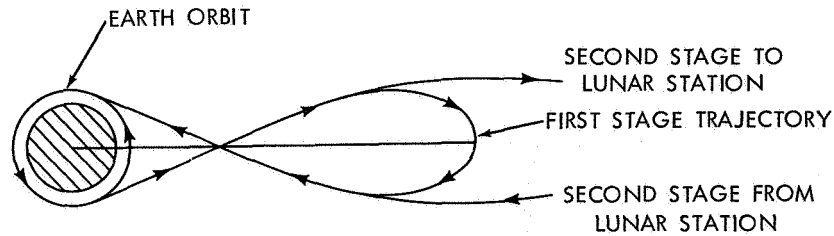


Figure 44—Performance function sensitivity to tug module ratio. $\beta = 0.5$; NOOS: $l = 825 \text{ sec}$, $\lambda = 0.75$, $\alpha_1 = 0.111$; Tug: $l = 444 \text{ sec}$, $\lambda = 0.85$.



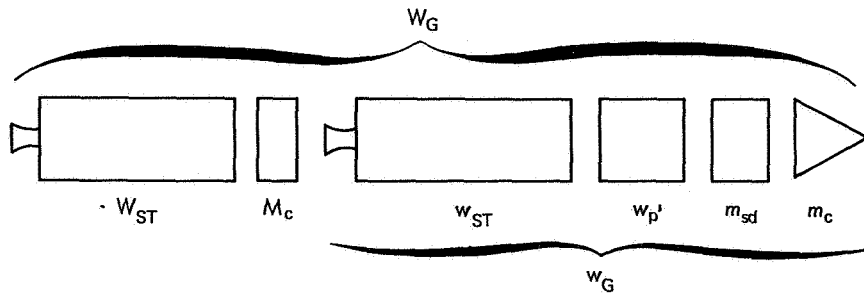
1. FIRST STAGE IS USED TO BOOST COOS FROM 185.2 km (100 n.mi.) PARKING ORBIT INTO HIGHLY ELLIPTICAL EARTH ORBIT. [$\Delta V \approx 2286$ mps (7500 fps) FOR LOSS STAGING AND $\Delta V \approx 1981$ mps (6500 fps) FOR HOSS STAGING].
2. FIRST STAGE SEPARATES IMMEDIATELY AFTER BURNOUT AND SECOND STAGE PROVIDES REMAINING ΔV REQUIRED FOR TRANSLUNAR INJECTION. [$\Delta V \approx 853$ mps (2800 fps) FOR LOSS STAGING AND $\Delta V \approx 1158$ mps (3800 fps) FOR HOSS STAGING].
3. FIRST STAGE DEBOOSTS ITSELF INTO ORIGINAL EARTH PARKING ORBIT. [$\Delta V \approx 2286$ mps (7500 fps) FOR LOSS STAGING AND $\Delta V \approx 1981$ mps (6500 fps) FOR HOSS STAGING].
4. MISSION MODE THEN PROCEEDS AS OUTLINED IN FIGURES 36 OR 37.

NOTE: FIGURE 47 HAS BEEN USED TO DETERMINE THE ΔV SPLIT BETWEEN THE FIRST AND SECOND STAGES.

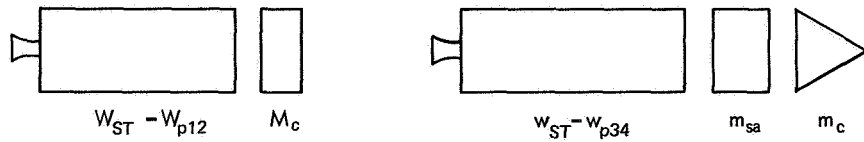
Figure 45—Modification of mission mode for lunar shuttle system when NOOS is replaced by two-stage COOS.

be transported to the HOSS with other shuttle vehicles. The transfer from earth orbit would be accomplished with the OOS. Subsequent maneuvers are described in Figure 52. Note the unusual use of a powered earth swingby.

The performance for a typical HOSS-based space tug is given in Figure 53. These results not only disclose a substantial payload dividend, but they also show that there is not a very large performance difference between the reusable and expendable tug modes.



INITIAL CONFIGURATION IN EARTH PARKING ORBIT



FIRST STAGE IN ELLIPTICAL EARTH ORBIT

SECOND STAGE AT LUNAR SPACE STATION

CONFIGURATION JUST BEFORE RETURN TO EARTH PARKING ORBIT

W_G : TOTAL GROSS WEIGHT
 m_{sd} : PAYLOAD DELIVERED TO LUNAR SPACE STATION
 m_{sa} : PAYLOAD RETURNED FROM LUNAR SPACE STATION
 $w_{p'}$: PROPELLANT DELIVERED TO PSD (for Tug)
 FIRST STAGE:
 W_{ST} : STAGE WEIGHT
 M_c : FIXED MODULE WEIGHT
 W_{p12} : WEIGHT OF PROPELLANT USED TO BOOST BOTH STAGES INTO ELLIPTICAL EARTH ORBIT

SECOND STAGE:
 w_G : GROSS WEIGHT
 w_{ST} : STAGE WEIGHT
 m_c : FIXED MODULE WEIGHT
 w_{p34} : WEIGHT OF PROPELLANT USED TO ARRIVE AT LUNAR SPACE STATION

Figure 46—Stage definitions for two-stage COOS.

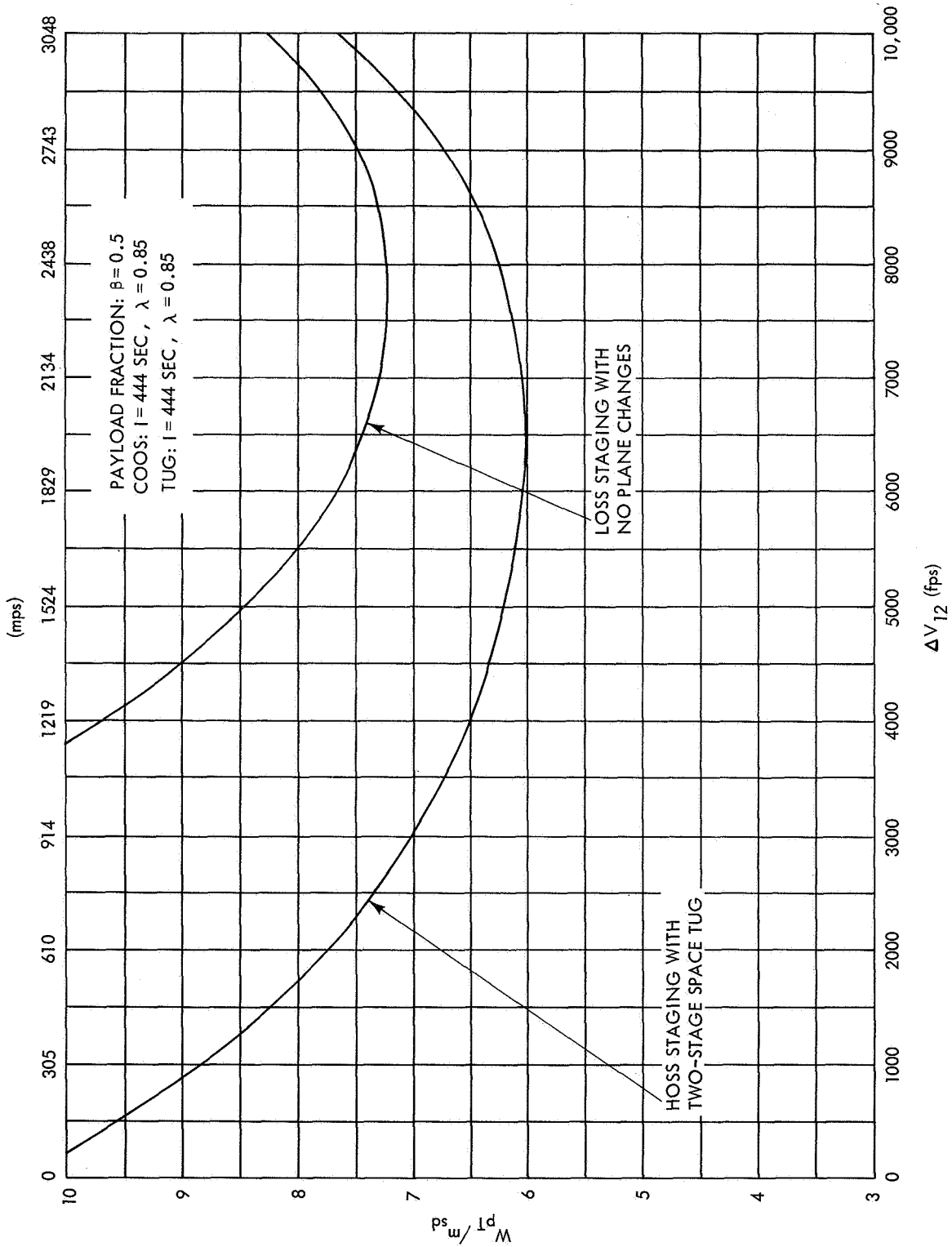


Figure 47—Normalized propellant weight for chemical lunar shuttle system as a function of the ΔV increment for the first stage of the COOS.

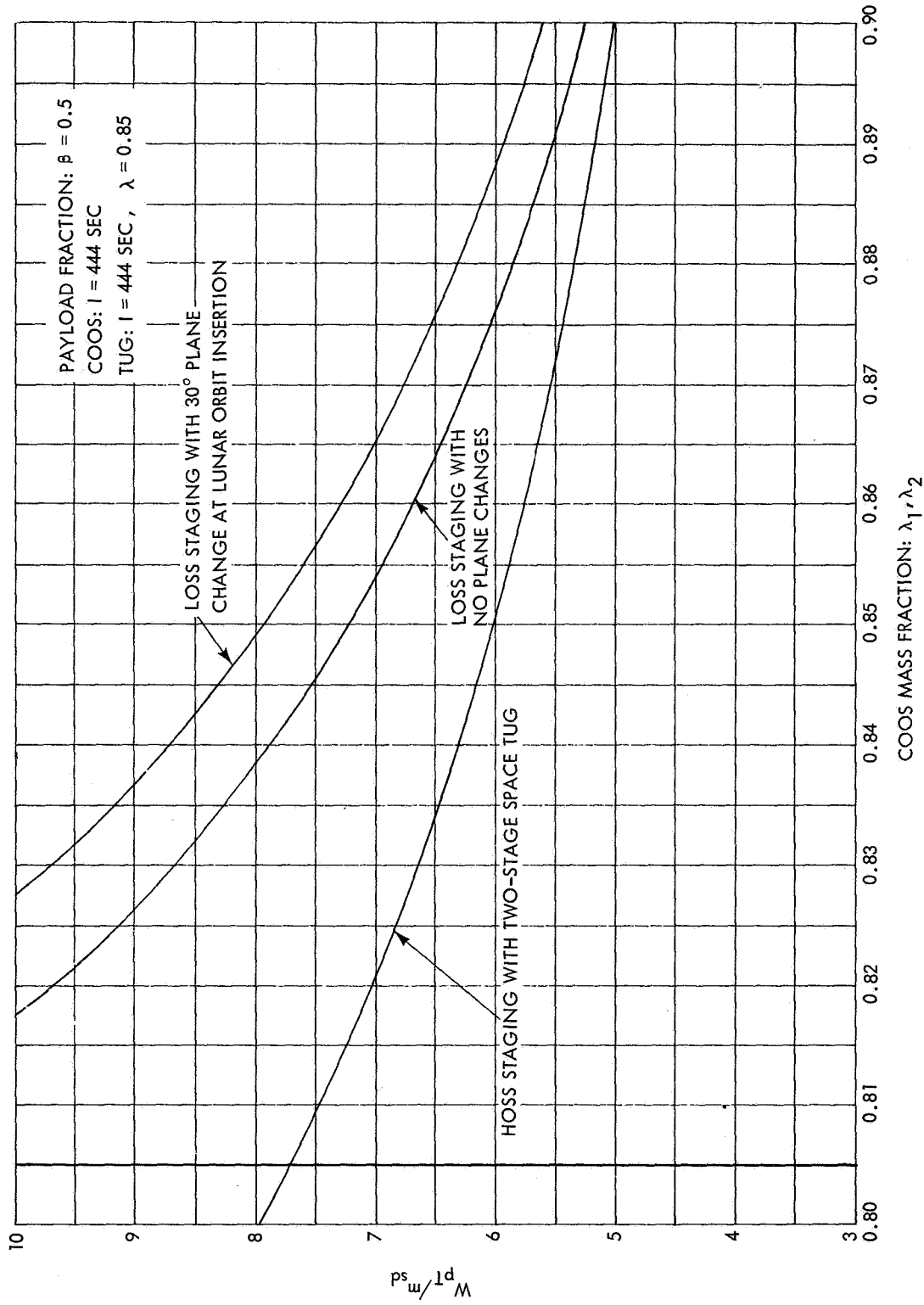


Figure 48—Normalized propellant weight for chemical lunar shuttle system as a function of the mass fraction for the COOS.

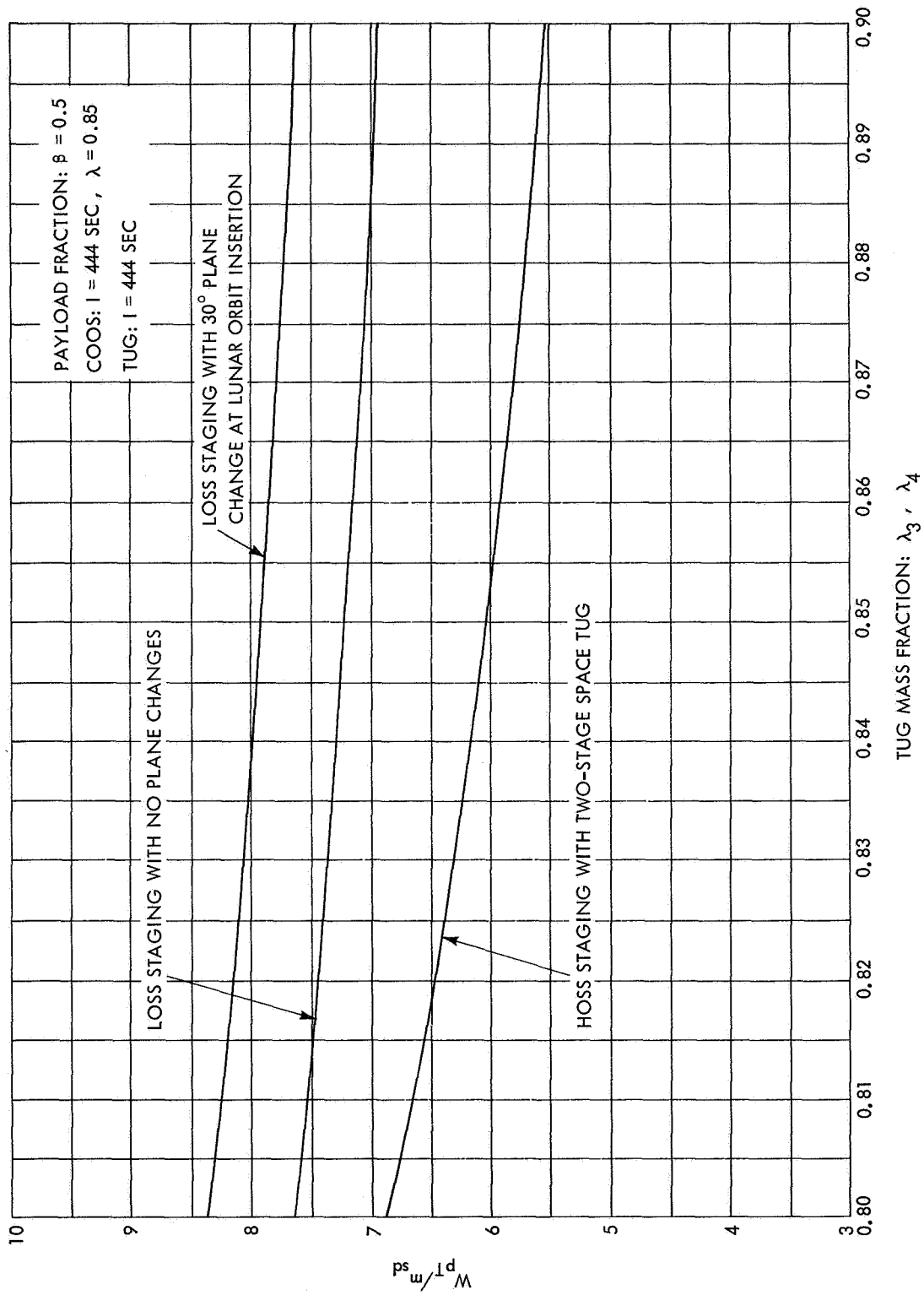


Figure 49—Normalized propellant weight for chemical lunar shuttle system as a function of the mass fraction for the space tug.

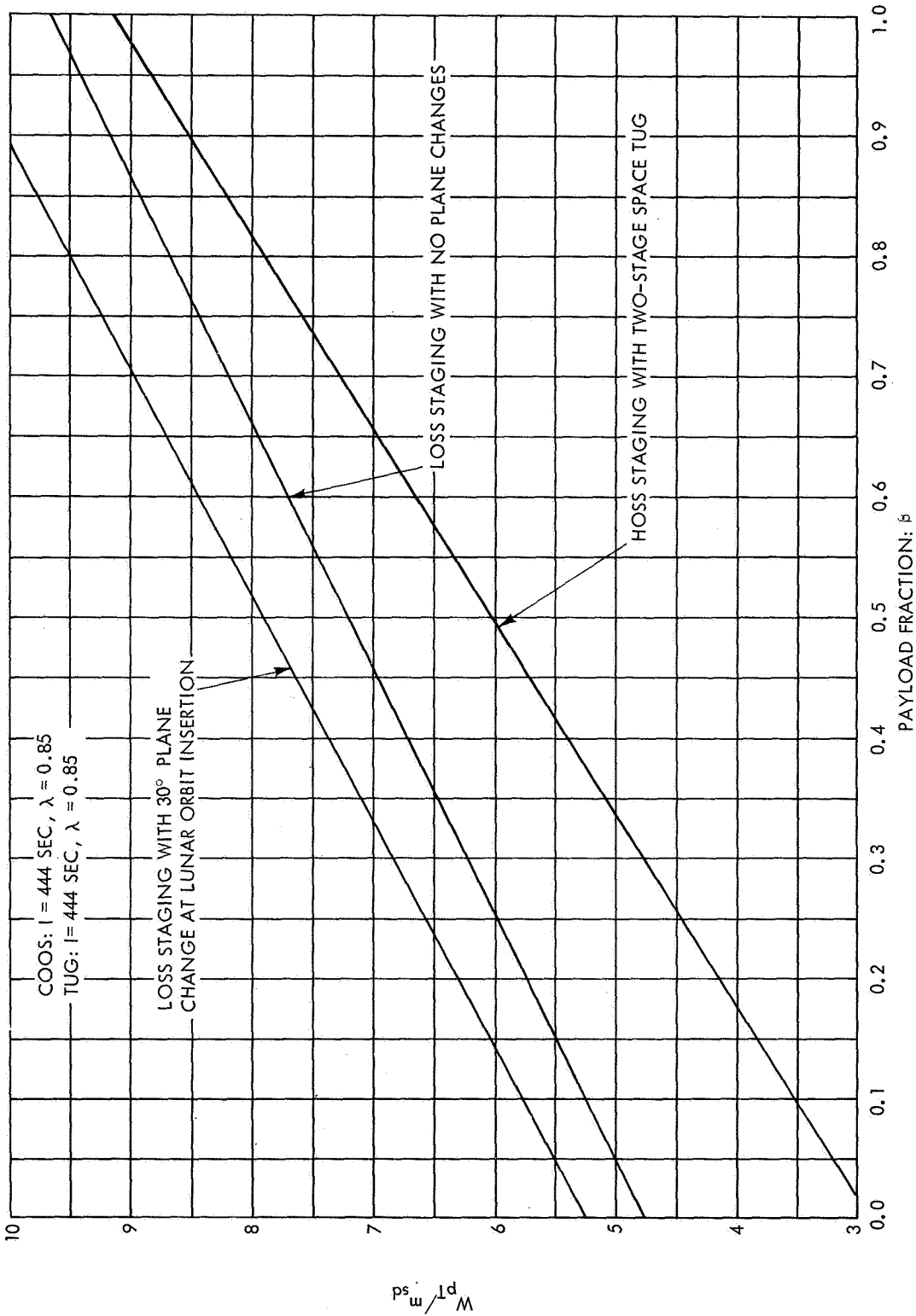


Figure 50—Normalized propellant weight for chemical lunar shuttle system as a function of the payload fraction.

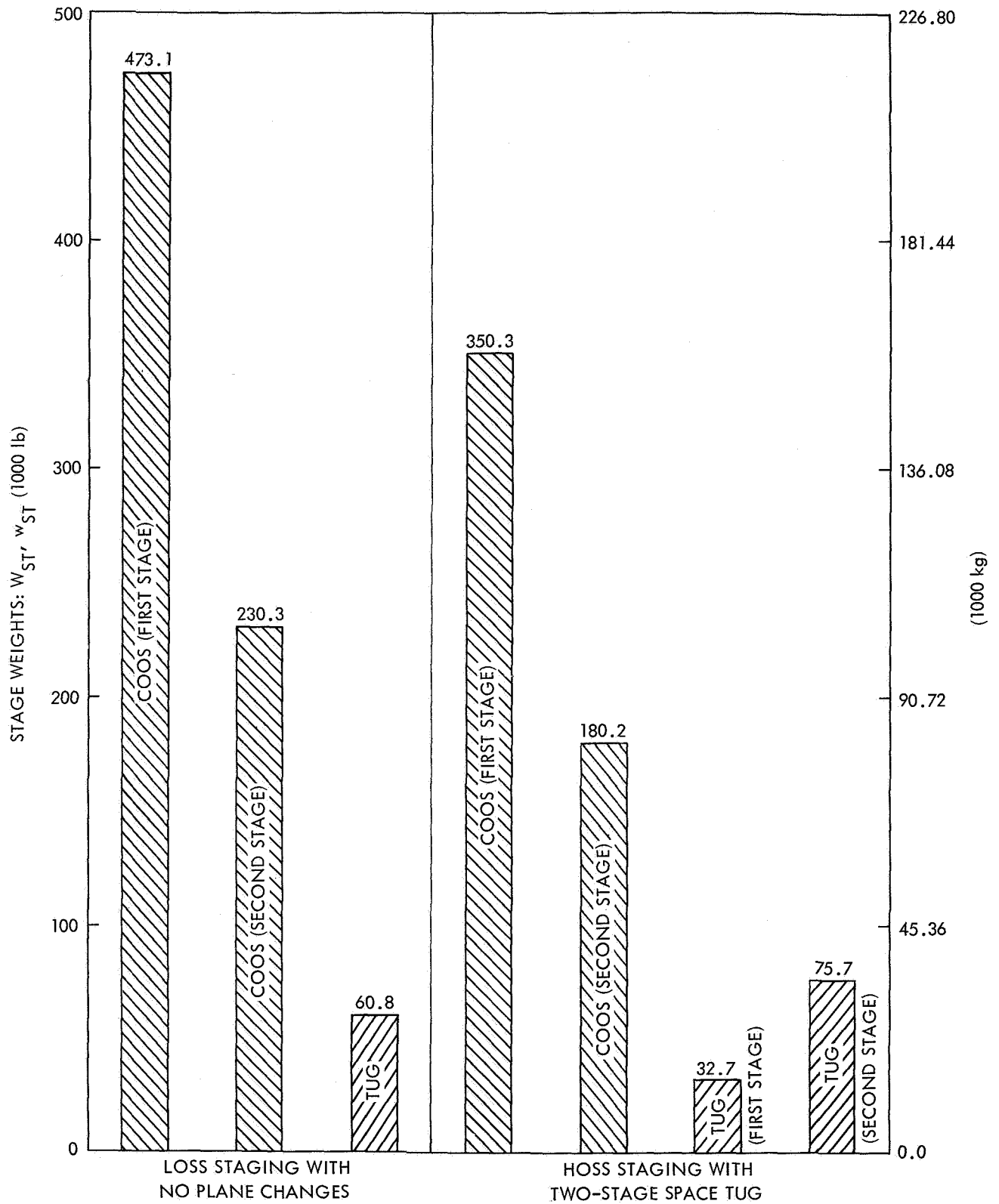
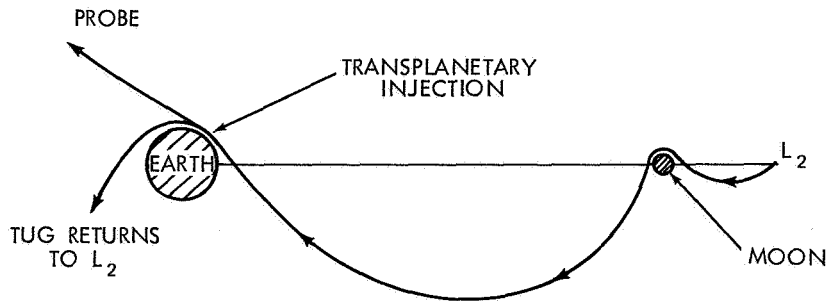


Figure 51—Stage weights for chemical lunar shuttle system. Nominal case: $\beta = 0.5$; $m_{sd} = 40,824$ kg (90,000 lb); COOS: $l = 444$ sec, $\lambda = 0.85$; Tug: $l = 444$ sec, $\lambda = 0.85$.



1. TUG ENTERS TRANS-EARTH TRAJECTORY BY APPLYING IMPULSES AT L_2 AND AT PERILUNE. $[\Delta V \approx 335 \text{ mps (1100 fps)}]$.
 2. NEAR PERIGEE, TUG SUPPLIES ΔV NEEDED FOR TRANSPLANETARY INJECTION OF UNMANNED PROBE

$$\Delta V \approx \sqrt{V_\infty^2 + \frac{2\mu}{r_p}} - V_p$$

WHERE μ IS THE EARTH'S GRAVITATIONAL PARAMETER
 r_p IS THE PERIGEE RADIUS
 V_p IS THE ORIGINAL VELOCITY NEAR PERIGEE
 (almost equal to escape velocity)
 V_∞ IS THE HYPERBOLIC EXCESS VELOCITY
 3. IMMEDIATELY AFTER BOOST PHASE, TUG SEPARATES FROM UNMANNED PROBE AND DEBOOSTS ITSELF INTO A TRANSLUNAR TRAJECTORY. ΔV COSTS ARE ASSUMED TO BE SAME AS IN ②. (Actual ΔV costs would be somewhat higher due to lunar phasing requirements).
 4. TUG RETURNS TO HOSS BY USING TWO-IMPULSE MANEUVER DESCRIBED IN ①. $[\Delta V \approx 335 \text{ mps (1100 fps)}]$.
- NOTE: STEPS ③ AND ④ ARE DELETED FOR AN EXPENDABLE TUG

Figure 52—Mission mode for transplanetary injection of unmanned probe using earth swingby.

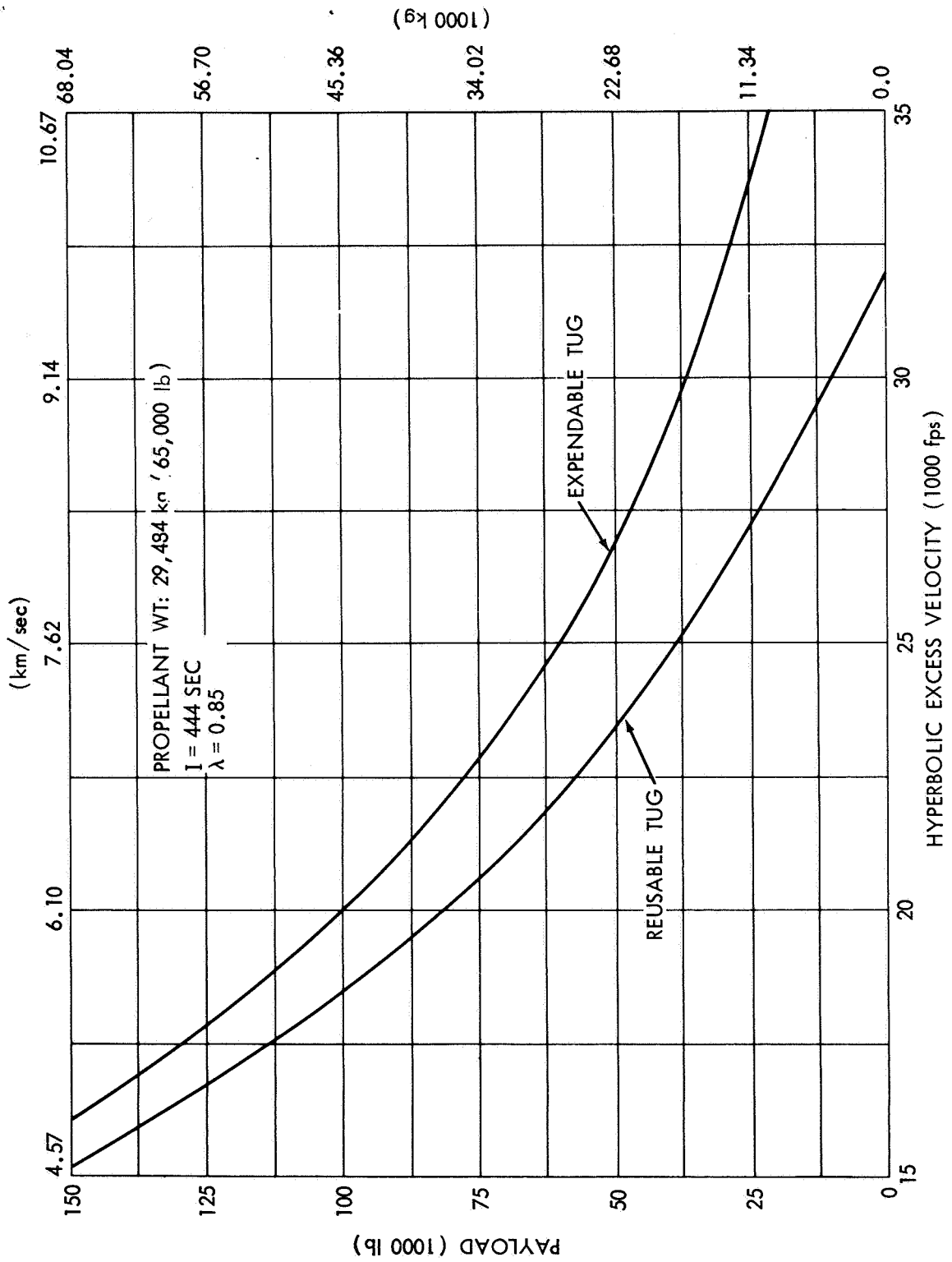


Figure 53—Planetary injection capability of HOSS-based space tug.

CHAPTER V

CONCLUSIONS AND RECOMMENDATIONS

There does not seem to be any major technical obstacle to establishing and maintaining a satellite in a halo orbit. It has been shown that the fuel expenditure required for stationkeeping and orbit control is quite reasonable. Moreover, the simplicity of the single-axis stabilization technique presented in Chapter II should dispel any doubts about the feasibility of implementing the theoretical control laws.

The importance of halo relay satellites in extending communications coverage to earth-occulted sites on the moon has also been demonstrated. With a halo comsat it would be possible to obtain backside tracking data from lunar orbiters. It would also be possible to operate an unmanned roving vehicle on the far side of the moon. These tasks could not be supported very efficiently with a lunar-orbit relay-satellite system.

Because of the many apparent advantages of a HOSS over a LOSS, it is recommended that the strategy for the lunar-program portion of the Manned Spaceflight Integrated Plan be reconsidered. Comprehensive studies should be initiated to determine the most efficient mission modes for a reusable earth-moon transportation system. Operational aspects as well as performance tradeoffs should be evaluated in these studies.

ACKNOWLEDGMENT

The author would like to thank Ted Edelbaum and Saul Serben for furnishing the computer program that was used to determine the ΔV requirements for transfer trajectories to the L_2 libration point.

Goddard Space Flight Center
National Aeronautics and Space Administration
Greenbelt, Maryland, January 26, 1971
311-07-21-01-51



REFERENCES

1. Farquhar, R. W., "Station-Keeping in the Vicinity of Collinear Libration Points with an Application to a Lunar Communications Problem", AAS Preprint 66-132, American Astronautical Society, July 1966.
2. Farquhar, R. W., "The Control and Use of Libration-Point Satellites", NASA Technical Report R-346, National Aeronautics and Space Administration, Washington, D.C., Sept. 1970.
3. "Final Report for Lunar Libration Point Flight Dynamics Study", General Electric Co., under Contract NAS-5-11551 with Goddard Space Flight Center, Greenbelt, Md., April 1969.
4. Farquhar, R. W., "Limit-Cycle Analysis of a Controlled Libration-Point Satellite", Journal of the Astronautical Sciences, Vol. 17, No. 5, March-April 1970, pp. 267-291.
5. Arndt, G. D., Batson, B. H., and Novosad, S. W., "An Analysis of the Telecommunications Performance of a Lunar Relay Satellite System", IEEE International Communications Conference Proceedings, Boulder, Colo., June 9-11, 1969, pp. 7-21 to 7-27.
6. Breland, G. W., et al., "Lunar Far Side Communications Analysis for Satellite Relay Systems", TRW Systems Group, under Contract NAS-9-8166, with Manned Spacecraft Center, Houston, Texas, April 1970.
7. "Soviets Plan Extensive Lunar Exploration", Aviation Week and Space Technology, Vol. 93, No. 14, Oct. 5, 1970, pp. 14-16.
8. Guest, J. E., and Murray, J. B., "Nature and Origin of Tsiolkovsky Crater, Lunar Farside", Planetary and Space Science, Vol. 17, No. 1, Jan. 1969, pp. 121-141.
9. "Project Linus", Department of Aerospace Engineering, University of Michigan, Ann Arbor, Mich., Dec. 1969. Available from Clearinghouse for Scientific and Technical Information, Springfield, Va., Document No. N70-17420.
10. Kurland, J. R., and Goodwin, C. H., "Analysis of a Communication Satellite for Lunar Far-Side Exploration", MIT CSR T-70-1, Massachusetts Institute of Technology, Center for Space Research, Cambridge, Mass., June 1970.
11. Farquhar, R. W., "Lunar Communications with Libration-Point Satellites", Journal of Spacecraft and Rockets, Vol. 4, No. 10, Oct. 1967, pp. 1383-1384.
12. Mueller, G. E., "An Integrated Space Program for the Next Generation", Astronautics and Aeronautics, Vol. 8, No. 1, Jan. 1970, pp. 30-51.
13. Clarke, A. C., A Fall of Moon Dust, New York: Harcourt, Brace and World, Inc., New York, 1961.

14. "Nuclear Flight System Definition Study, Phase-2 Final Report", McDonnell Douglas Astronautics Co., under Contract NAS-8-24714 with Marshall Space Flight Center, Huntsville, Ala., May 1970.
15. "Nuclear Flight System Definition Study, Phase-2 Final Report", Lockheed Missiles and Space Co., under Contract NAS-8-24715, with Marshall Space Flight Center, Huntsville, Ala., May 1970.
16. "Nuclear Flight System Definition Study, Phase-2 Final Report", North American Rockwell Corp., Space Division, under Contract NAS-8-24975 with Marshall Space Flight Center, Huntsville, Ala., Aug. 1970.
17. Schilb, L. L., "Orbiting Propellant Depot for Chemical Orbit-to-Orbit Shuttle", Aerospace Corp. Report No. TOR-0059(6758-01)-16, Aerospace Corp., El Segundo, Calif., Oct. 5, 1970.
18. "1967 Summer Study of Lunar Science and Exploration", NASA Special Publication 157, National Aeronautics and Space Administration, Washington, D.C., 1967.
19. Interian, A., and Kugath, D., "Remote Manipulators in Space", Astronautics and Aeronautics, Vol. 7, No. 5, May 1969, pp. 24-32.
20. Hartmann, W. K., and Sullivan, R. J., "Objectives of Permanent Lunar Bases", IIT Res. Inst. Report No. P-32, IIT Research Institute, Chicago, Ill., Jan. 1970. Available from Clearinghouse for Scientific and Technical Information, Springfield, Va., Document No. N70-28753.
21. Sugar, R. D., and Winneberger, R. A., "Mission Analysis of OOS/RNS Operations Between Earth Orbit and Lunar Orbit", Aerospace Corp. Report No. TOR-0066 (5759-07)-5, Aerospace Corp., El Segundo, Calif., June 22, 1970.
22. Webb, E. D., "Three-Impulse Transfer from Lunar Orbits", Space Flight Mechanics, Science and Technology Series, Vol. 11, New York: American Astronautical Society, 1967, pp. 541-553.

Appendix A

Nonlinear Equations of Motion

A complete derivation for the equations of motion of a satellite in the vicinity of the earth-moon L_2 point will be given in a forthcoming publication by Farquhar and Kamel.* Only the final results are presented here. In the Cartesian coordinate system (x, y, z) of Figure 2, with higher-order terms neglected the equations of motion can be written in the expanded form

$$\begin{aligned}
 \ddot{x} - 2(1 + \nu_z) \dot{y} = & [(1 + \nu_z)^2 + 2(1 + \rho)^{-3} B_L] x \\
 & + \dot{\nu}_z y - \nu_x \nu_z z \\
 & - \frac{3}{2} C_L (1 + \rho)^{-4} [2x^2 - (y^2 + z^2)] \\
 & + 2D_L (1 + \rho)^{-5} [2x^2 - 3(y^2 + z^2)] x \\
 & - \frac{5}{8} E_L (1 + \rho)^{-6} [8x^4 + 3(y^4 + z^4) - 24x^2(y^2 + z^2) + 6y^2 z^2] \\
 & - m^2 \left(\frac{a_s}{r_s} \right)^3 \left\{ \left[1 - 3 \left(\frac{x_s}{r_s} \right)^2 \right] x - 3 \left(\frac{x_s}{r_s} \right) \left(\frac{y_s}{r_s} \right) y \right. \\
 & \quad \left. - 3 \left(\frac{x_s}{r_s} \right) \left(\frac{z_s}{r_s} \right) z \right\}, \tag{A-1a}
 \end{aligned}$$

$$\begin{aligned}
 \ddot{y} + 2(1 + \nu_z) \dot{x} = & [(1 + \nu_z)^2 - (1 + \rho)^{-3} B_L + \nu_x^2] y \\
 & - \dot{\nu}_z x + \dot{\nu}_x z + 2\nu_x \dot{z} + 3C_L (1 + \rho)^{-4} xy \\
 & - \frac{3}{2} D_L (1 + \rho)^{-5} [4x^2 - (y^2 + z^2)] y
 \end{aligned}$$

*Farquhar and Kamel, *op. cit.*

$$\begin{aligned}
& + \frac{5}{2} E_L (1 + \rho)^{-6} [4x^2 - 3(y^2 + z^2)] xy \\
& + m^2 \left(\frac{a_s}{r_s} \right)^3 \left\{ 3 \left(\frac{x_s}{r_s} \right) \left(\frac{y_s}{r_s} \right) x - \left[1 - 3 \left(\frac{y_s}{r_s} \right)^2 \right] y \right. \\
& \quad \left. + 3 \left(\frac{y_s}{r_s} \right) \left(\frac{z_s}{r_s} \right) z \right\}
\end{aligned} \tag{A-1b}$$

$$\begin{aligned}
\ddot{z} = & [\nu_x^2 - (1 + \rho)^{-3} B_L] z - \nu_x (1 + \nu_z) x \\
& - \dot{\nu}_x y - 2\nu_x \dot{y} + 3C_L (1 + \rho)^{-4} xz \\
& - \frac{3}{2} D_L (1 + \rho)^{-5} [4x^2 - (y^2 + z^2)] z \\
& + \frac{5}{2} E_L (1 + \rho)^{-6} [4x^2 - 3(y^2 + z^2)] xz \\
& + m^2 \left(\frac{a_s}{r_s} \right)^3 \left\{ 3 \left(\frac{x_s}{r_s} \right) \left(\frac{z_s}{r_s} \right) x + 3 \left(\frac{y_s}{r_s} \right) \left(\frac{z_s}{r_s} \right) y \right. \\
& \quad \left. - \left[1 - 3 \left(\frac{z_s}{r_s} \right)^2 \right] z \right\}
\end{aligned} \tag{A-1c}$$

where

$$\left. \begin{aligned}
B_L &= 3.1904236569 \\
C_L &= 15.845108285 \\
D_L &= 91.700262028 \\
E_L &= 544.05732354
\end{aligned} \right\} \tag{A-2}$$

The m^2 terms in Equation A-1 are due to the direct solar perturbation. The effects of the indirect solar perturbation and the moon's orbital eccentricity are contained in the quantities of ρ , ν_z , and ν_x which represent variations in the earth-moon distance and the moon's angular rate. These quantities can be obtained from the lunar theory of De Pontecoulant (References A-1 and A-2) and are given by

$$(1 + \rho)^{-1} = 1 + e \cos \phi + e^2 \cos 2 \phi$$

$$\begin{aligned}
& + \frac{1}{6} m^2 + m^2 \cos 2 \xi + \frac{15}{8} m e \cos (2 \xi - \phi) \\
& - \frac{1}{8} e^3 \cos \phi + \frac{9}{8} e^3 \cos 3 \phi + \frac{19}{6} m^3 \cos 2 \xi \\
& - \frac{15}{16} m \left(\frac{a}{a'} \right) \cos \xi - \frac{5}{8} e \gamma^2 \cos (\phi - 2 \eta) \\
& + \frac{15}{4} m e^2 \cos 2 \xi + \frac{187}{32} m^2 e \cos (2 \xi - \phi) \\
& + \frac{35}{8} m e e' \cos (2 \xi - \phi - \phi') - \frac{15}{8} m e e' \cos (2 \xi - \phi + \phi') \\
& + \frac{5}{4} \left(\frac{a}{a'} \right) e' \cos (\xi + \phi') - \frac{7}{12} m^2 e \cos \phi \\
& + \frac{33}{16} m^2 e \cos (2 \xi + \phi) - \frac{105}{64} m e^2 \cos (2 \xi - 3 \phi) \\
& - \frac{3}{2} m^2 e' \cos \phi' + \frac{7}{2} m^2 e' \cos (2 \xi - \phi') \\
& - \frac{1}{2} m^2 e' \cos (2 \xi + \phi') + \frac{21}{8} m e e' \cos (\phi - \phi') \\
& - \frac{21}{8} m e e' \cos (\phi + \phi')
\end{aligned} \tag{A-3}$$

$$\begin{aligned}
\nu_z & = 2 e \cos \phi + \frac{5}{2} e^2 \cos 2 \phi \\
& + \frac{11}{4} m^2 \cos 2 \xi + \frac{15}{4} m e \cos (2 \xi - \phi) \\
& - \frac{e^3}{4} \cos \phi + \frac{13}{4} e^3 \cos 3 \phi + \frac{85}{12} m^3 \cos 2 \xi
\end{aligned}$$

$$\begin{aligned}
& -\frac{15}{8} m \left(\frac{a}{a'} \right) \cos \xi - \frac{5}{4} e \gamma^2 \cos (\phi - 2 \eta) \\
& + \frac{75}{8} m e^2 \cos 2 \xi + \frac{143}{16} m^2 e \cos (2 \xi - \phi) \\
& + \frac{35}{4} m e e' \cos (2 \xi - \phi - \phi') - \frac{15}{4} m e e' \cos (2 \xi - \phi + \phi') \\
& + \frac{5}{2} \left(\frac{a}{a'} \right) e' \cos (\xi + \phi') - \frac{3}{2} m^2 e \cos \phi \\
& + \frac{51}{8} m^2 e \cos (2 \xi + \phi) - \frac{105}{32} m e^2 \cos (2 \xi - 3 \phi) \\
& - 3 m^2 e' \cos \phi' + \frac{77}{8} m^2 e' \cos (2 \xi - \phi') \\
& - \frac{11}{8} m^2 e' \cos (2 \xi + \phi') + \frac{21}{4} m e e' \cos (\phi - \phi') \\
& - \frac{21}{4} m e e' \cos (\phi + \phi')
\end{aligned} \tag{A-4}$$

$$v_x = 3 m^2 \gamma \cos \xi \sin (\nu' - \Omega) \tag{A-5}$$

where

$$\phi = \left(1 - \frac{3}{4} m^2 - \frac{225}{32} m^3 \right) t + \epsilon - \tilde{\omega} \tag{A-6}$$

$$\xi = (1 - m) t + \epsilon - \epsilon' \tag{A-7}$$

$$\eta = \left(1 + \frac{3}{4} m^2 - \frac{9}{32} m^3 - \frac{273}{128} m^4 \right) t + \epsilon - \Omega_0 \tag{A-8}$$

$$\phi' = m t + \epsilon' - \tilde{\omega}' \tag{A-9}$$

$$\nu' = m t + \epsilon' + 2 e' \sin \phi' + \frac{5}{4} e'^2 \sin 2 \phi' \quad (\text{A-10})$$

$$\Omega = \Omega_0 - \left(\frac{3}{4} m^2 - \frac{9}{32} m^3 - \frac{273}{128} m^4 \right) t \quad (\text{A-11})$$

Auxiliary quantities for the direct solar perturbation can also be written in terms of the angle variables of Equations A-6 to A-11; thus,

$$\begin{aligned} \left(\frac{x_s}{r_s} \right) &= \cos \xi - 2 (e \sin \phi - e' \sin \phi') \sin \xi \\ &- \cos \xi \left\{ e^2 + e'^2 + \frac{1}{4} \gamma^2 - (e^2 \cos 2\phi + e'^2 \cos 2\phi') \right. \\ &- 2 e e' [\cos (\phi - \phi') - \cos (\phi + \phi')] \left. \right\} \\ &- \sin \xi \left\{ \frac{5}{4} e^2 \sin 2\phi - \frac{5}{4} e'^2 \sin 2\phi' + \frac{11}{8} m^2 \sin 2\xi \right. \\ &+ \left. \frac{15}{4} m e \sin (2\xi - \phi) - 3 m e' \sin \phi' \right\} \\ &+ \frac{1}{4} \gamma^2 \cos (2\eta - \xi) \end{aligned} \quad (\text{A-12})$$

$$\begin{aligned} \left(\frac{y_s}{r_s} \right) &= -\sin \xi - 2 (e \sin \phi - e' \sin \phi') \cos \xi \\ &+ \sin \xi \left\{ e^2 + e'^2 + \frac{1}{4} \gamma^2 - (e^2 \cos 2\phi + e'^2 \cos 2\phi') \right. \\ &- 2 e e' [\cos (\phi - \phi') - \cos (\phi + \phi')] \left. \right\} \\ &- \cos \xi \left\{ \frac{5}{4} e^2 \sin 2\phi - \frac{5}{4} e'^2 \sin 2\phi' + \frac{11}{8} m^2 \sin 2\xi \right. \\ &+ \left. \frac{15}{4} m e \sin (2\xi - \phi) - 3 m e' \sin \phi' \right\} \\ &- \frac{1}{4} \gamma^2 \sin (2\eta - \xi) \end{aligned} \quad (\text{A-13})$$

$$\left(\frac{z_s}{r_s}\right) = \gamma \sin (\nu' - \Omega) \quad (\text{A-14})$$

$$\left(\frac{a_s}{r_s}\right)^3 = 1 + 3e' \cos \phi' + \frac{3}{2}e'^2 (1 + 3 \cos 2\phi') \quad (\text{A-15})$$

The astronomical constants used in the above equations are

m = ratio of the mean motions of the moon and the sun ($m = 0.0748013263$)

e = moon's orbital eccentricity ($e = 0.054900489$)

e' = earth's orbital eccentricity ($e' = 0.0167217$)

(a/a') = modified ratio of the semimajor axes for the orbits of earth and the moon
 $[a/a' = 0.0025093523]$

γ = tangent of the mean inclination of the moon's orbit ($\gamma = 0.0900463066$)

ϵ, ϵ' = mean longitudes of the epochs of the mean motions of the moon and the sun

$\tilde{\omega}, \tilde{\omega}'$ = mean longitudes of the lunar and solar perigees

Ω_0 = longitude of the mean ascending node of the moon's orbit.

Numerical values for the last five constants can be found in Reference A-3.

REFERENCES

- A-1. De Pontecoulant, G., Théorie Analytique du Système du Monde, Vol. 4, Paris: Bachelier, 1846.
- A-2. Brown, E. W., An Introductory Treatise on the Lunar Theory, New York: Dover Publications, 1960.
- A-3. The American Ephemeris and Nautical Almanac, Washington: U.S. Government Printing Office.

Appendix B

Analytical Solution for Lissajous Nominal Path

A fourth-order analytical solution for the Lissajous nominal path will be derived in a forthcoming publication by Farquhar and Kamel.* This solution, with fourth-order terms excluded, is given below (there are 278 additional terms in the fourth-order solution). For convenience, the amplitudes A_y and A_z have been renormalized by dividing these quantities by the factor $\gamma_L m$. With this additional normalization, the nominal path can be written in the form

$$\begin{aligned}x_n &= m x_1 + m^2 x_2 + m^3 x_3 \\y_n &= m y_1 + m^2 y_2 + m^3 y_3 \\z_n &= m z_1 + m^2 z_2 + m^3 z_3\end{aligned}\tag{B-1}$$

where

$$\begin{aligned}x_1 &= 0.341763 A_y \sin T_1 \\y_1 &= A_y \cos T_1 \\z_1 &= A_z \sin T_2 \\x_2 &= 0.554904 \left(\frac{e}{m}\right) A_y \sin (\phi - T_1) \\&+ 0.493213 \left(\frac{e}{m}\right) A_y \sin (\phi + T_1) \\&- 0.09588405 A_y^2 \cos 2 T_1 \\&+ 0.128774 A_z^2 \cos 2 T_2 \\&- 0.268186 A_z^2 - 0.205537 A_y^2\end{aligned}\tag{B-2}$$

(B-3)

*Farquhar and Kamel, op. cit.

$$\begin{aligned}
y_2 = & - 1.90554 \left(\frac{e}{m} \right) A_y \cos (\phi - T_1) \\
& + 1.210699 \left(\frac{e}{m} \right) A_y \cos (\phi + T_1) \\
& - 0.055296 A_y^2 \sin 2 T_1 \\
& - 0.08659705 A_z^2 \sin 2 T_2
\end{aligned} \tag{B-4}$$

$$\begin{aligned}
z_2 = & 1.052082 \left(\frac{e}{m} \right) A_z \sin (\phi + T_2) \\
& + 1.856918 \left(\frac{e}{m} \right) A_z \sin (\phi - T_2) \\
& + 0.4241194 A_y A_z \cos (T_2 - T_1) \\
& + 0.1339910 A_y A_z \cos (T_2 + T_1)
\end{aligned} \tag{B-5}$$

$$\begin{aligned}
x_3 = & \left(\frac{e}{m} \right)^2 A_y [- 0.122841 \sin (2 \phi - T_1) \\
& + 0.643204 \sin (2 \phi + T_1)] \\
& + \left(\frac{e}{m} \right) A_z^2 [0.198388 \cos \phi - 0.387184 \cos (\phi - 2 T_2) \\
& + 0.335398 \cos (\phi + 2 T_2)] \\
& + \left(\frac{e}{m} \right) A_y^2 [0.173731 \cos \phi + 0.325999 \cos (\phi - 2 T_1) \\
& - 0.270446 \cos (\phi + 2 T_1)] \\
& + \left(\frac{e}{m} \right) A_y [- 1.10033 \sin (\phi - T_1 - 2 \xi) \\
& - 1.189247 \sin (\phi + T_1 - 2 \xi)]
\end{aligned}$$

$$\begin{aligned}
& + A_y A_z^2 [- 0.430448 \sin (2T_2 - T_1) \\
& \quad - 0.031302 \sin (2T_2 + T_1)] \\
& + A_y^3 [0.027808 \sin 3T_1] + C_1 A_y \sin T_1 \\
& + A_y [- 0.38856 \sin (T_1 - 2\xi) \\
& \quad + 0.455452 \sin (T_1 + 2\xi)] \tag{B-6}
\end{aligned}$$

$$\begin{aligned}
y_3 = & \left(\frac{e}{m}\right)^2 A_y [0.608685 \cos (2\phi - T_1) \\
& \quad + 1.407026 \cos (2\phi + T_1)] \\
& + \left(\frac{e}{m}\right) A_z^2 [- 0.116822 \sin \phi - 0.214742 \sin (\phi - 2T_2) \\
& \quad - 0.232503 \sin (\phi + 2T_2)] \\
& + \left(\frac{e}{m}\right) A_y^2 [- 0.109499 \sin \phi - 0.144553 \sin (\phi - 2T_1) \\
& \quad - 0.155751 \sin (\phi + 2T_1)] \\
& + \left(\frac{e}{m}\right) A_y [2.733367 \cos (\phi - T_1 - 2\xi) \\
& \quad - 3.848485 \cos (\phi + T_1 - 2\xi)] \\
& + A_y A_z^2 [- 1.191421 \cos (2T_2 - T_1) \\
& \quad - 0.000165 \cos (2T_2 + T_1)] \\
& + A_y^3 [- 0.027574 \cos 3T_1] \\
& + A_y [- 1.743411 \cos (T_1 - 2\xi) \\
& \quad + 0.741825 \cos (T_1 + 2\xi)] \tag{B-7}
\end{aligned}$$

$$\begin{aligned}
z_3 = & \left(\frac{e}{m}\right)^2 A_z [-0.536652 \sin(2\phi - T_2) \\
& + 1.103381 \sin(2\phi + T_2)] \\
& + \left(\frac{e}{m}\right) A_y A_z [-0.353754 \cos(\phi - T_2 - T_1) \\
& + 0.367360 \cos(\phi + T_2 + T_1) \\
& + 0.063629 \cos(\phi - T_2 + T_1) \\
& - 0.034729 \cos(\phi + T_2 - T_1)] \\
& + \left(\frac{e}{m}\right) A_z [-2.353465 \sin(\phi - T_2 - 2\xi) \\
& - 3.831413 \sin(\phi + T_2 - 2\xi)] \\
& + A_z^3 [0.017664 \sin 3T_2] \\
& + A_z A_y^2 [-0.86684 \sin(T_2 - 2T_1) \\
& - 0.044724 \sin(T_2 + 2T_1)] \\
& + A_z [-1.487917 \sin(T_2 - 2\xi) \\
& + 0.475507 \sin(T_2 + 2\xi)] \tag{B-8}
\end{aligned}$$

with

$$\begin{aligned}
C_1 = & 0.09210089 \left(\frac{e}{m}\right)^2 + 0.02905486 A_y^2 \\
& + 0.007644849 A_z^2 \tag{B-9}
\end{aligned}$$

$$T_1 = \omega_{xy} t + \theta_1 \tag{B-10}$$

$$T_2 = \omega_z t + \theta_2 \quad (\text{B-11})$$

$$\omega_{xy} = \frac{1.865485}{1 + m^2 \omega_{x2}} \quad (\text{B-12})$$

$$\omega_z = \frac{1.794291}{1 + m^2 \omega_{z2}} \quad (\text{B-13})$$

$$\begin{aligned} \omega_{x2} = & 0.1387811 \left(\frac{e}{m} \right)^2 + 0.04349909 A_y^2 \\ & - 0.04060812 A_z^2 \end{aligned} \quad (\text{B-14})$$

$$\begin{aligned} \omega_{z2} = & 0.5981779 \left(\frac{e}{m} \right)^2 - 0.03293845 A_y^2 \\ & + 0.03923249 A_z^2 \end{aligned} \quad (\text{B-15})$$

$$\gamma_L = 0.1678331476 \quad (\text{B-16})$$

and θ_1 , θ_2 are phase angles that are usually taken to be zero. The remaining quantities are defined in Appendix A.



Appendix C

Fuel Cost for z-Axis Period Control

Between impulses, the satellite will follow a Lissajous nominal path. The first-order approximation to this trajectory in the yz-plane can be written as

$$y_n = A_H \cos \omega_{xy} t \tag{C-1}$$

$$z_n = A_H \sin (\omega_{xy} t - \psi)$$

where $\psi = \psi_0 + \epsilon t$ and $\epsilon = \omega_{xy} - \omega_z = 0.0736493$. Since ϵ is small, the phase angle ψ can be approximated by an average value through each cycle. From Figure 11, it is easy to see that the magnitude of the control impulse is

$$|\Delta \dot{z}| = 2 \omega_z A_H \sin \psi_c \tag{C-2}$$

where ψ_c is the phase angle for the cycle that just misses the occulted zone. If occultation is to be prevented, impulses must be applied at intervals of

$$\Delta t = \frac{2 \psi_c}{\epsilon} \tag{C-3}$$

Therefore, the average control acceleration is given by

$$\overline{F_{cz}} = \frac{2 \omega_z A_H}{\Delta t} \sin \left(\frac{\epsilon \Delta t}{2} \right) \tag{C-4}$$

All that remains now is to determine a value of A_H that will guarantee nonoccultation.

As shown in Figure 10, higher-order nominal path corrections will sometimes cause the radius of the halo orbit to drop below its first-order approximation. So that the nominal trajectory will not enter the occulted zone, it is necessary to have $A_H > A'_m$. It is found empirically that

$$A'_m \cong A_m + \beta A_H + \gamma A_H^2 \tag{C-5}$$

where $\beta = 0.05$, $\gamma = 4$, and A_m is the radius of the occulted zone ($A_m = 0.008057202$ in normalized units).

An additional increase in A_H is required to account for the variation in the radius of the Lissajous nominal path. If r denotes this radius, it follows from Equation C-1 that

$$\begin{aligned} r^2 &= y_n^2 + z_n^2 \\ &= A_H^2 + \frac{1}{2} A_H^2 [(1 - \cos 2\psi) \cos 2\omega_{xy} t - (\sin 2\psi) \sin 2\omega_{xy} t] \end{aligned} \quad (C-6)$$

For a trajectory that just touches the enlarged occulted zone A'_m , it can be deduced from Equation C-6 that

$$A'_m = A_H (1 - \sin \psi_c)^{1/2} \quad (C-7)$$

If Equations C-5 and C-7 are combined to eliminate A'_m , the minimum value of A_H that will insure nonoccultation is found to be

$$A_H = \frac{1}{2\gamma} [b - (b^2 - 4\gamma A_m)^{1/2}] \quad (C-8)$$

where

$$b = [(1 - \sin \psi_c)^{1/2} - \beta]. \quad (C-9)$$

Appendix D

Derivation of Performance Function for a Two-Stage Space Tug

With the use of Equations 9 to 11 and Figures 32 and 33, the basic relations for the second stage can be written

$$\frac{w_G}{w_G - w_{pd}} = \exp \left[\frac{\Delta V_d}{I_2 g} \right] \equiv K_d \quad (D-1)$$

$$\frac{w_G - w_{pd} - (m_{sd} - m_{sa})}{w_G - w_p - (m_{sd} - m_{sa})} = \exp \left[\frac{\Delta V_a}{I_2 g} \right] \equiv K_a \quad (D-2)$$

$$w_G = \frac{w_p}{\lambda_2} + m_c + m_{sd} \quad (D-3)$$

with $\Delta V_d = 2012$ mps (6600 fps) and $\Delta V_a = 2667$ mps (8750 fps). Let

$$k_1 = \frac{m_c}{m_{sd}} \quad (D-4)$$

$$k_2 = \frac{m_{sa}}{m_{sd}} \quad (D-5)$$

and eliminate w_G and w_{pd} from Equations D-1 to D-3; then

$$\frac{w_p}{m_{sd}} = \left(\frac{\lambda_2}{\lambda_2 - f} \right) [(1 + k_1) f + (k_2 - 1) q] \quad (D-6)$$

where

$$f = \frac{K_a K_d - 1}{K_a K_d} \quad (D-7)$$

$$q = \frac{K_a - 1}{K_a} \quad (D-8)$$

For the first stage, the relations are

$$\frac{W_G}{W_G - W_{p12}} = \exp \left[\frac{\Delta V_{12}}{I_1 g} \right] \equiv K_{12} \quad (D-9)$$

$$\frac{W_G - W_{p12} - w_G}{W_G - W_p - w_G} = K_{12} \quad (D-10)$$

$$W_G = \frac{W_p}{\lambda_1} + M_c + w_G \quad (D-11)$$

with $\Delta V_{12} = 777$ mps (2550 fps). The elimination of W_G and W_{p12} from equations D-9 to D-11 yields

$$\frac{W_p}{w_G} = \left(\frac{\lambda_1}{\lambda_1 - F} \right) [(1 + \alpha) F - G] \quad (D-12)$$

where

$$\alpha = \frac{M_c}{w_G} \quad (D-13)$$

$$F = \frac{K_{12}^2 - 1}{K_{12}^2} \quad (D-14)$$

$$G = \frac{K_{12} - 1}{K_{12}} \quad (D-15)$$

A straightforward manipulation of the foregoing equations gives the performance function

$$\frac{W_{pT}}{m_{sd}} = \left(\frac{\lambda_1}{\lambda_1 - F} \right) [(1 + \alpha) F - G] \left[\frac{1}{\lambda_2} \left(\frac{W_p}{m_{sd}} \right) + (1 + k_1) \right]$$
$$+ \frac{W_p}{m_{sd}} \equiv h_T \tag{D-16}$$



Appendix E

Derivation of Performance Function for a Two-Stage Lunar Shuttle System

With the use of Equations 9 to 11 and Figures 36 to 38, the basic relations for the tug stage can be written

$$\frac{w_G}{w_G - w_{pd}} = \exp \left[\frac{\Delta V_d}{I_2 g} \right] \equiv K_d \quad (\text{E-1})$$

$$\frac{w_G - w_{pd} - (m_{sd} - m_{sa})}{w_G - w_p - (m_{sd} - m_{sa})} = \exp \left[\frac{\Delta V_a}{I_2 g} \right] \equiv K_a \quad (\text{E-2})$$

$$w_G = \frac{w_p}{\lambda_2} + m_c + m_{sd} \quad (\text{E-3})$$

For the LOSS mission mode, $\Delta V_d = 2012$ mps (6600 fps), and $\Delta V_a = 1890$ mps (6200 fps). For the HOSS mission mode, $\Delta V_d = 2789$ mps (9150 fps), and $\Delta V_a = 2667$ mps (8750 fps). Let

$$k_1 = \frac{m_c}{m_{sd}} \quad (\text{E-4})$$

$$k_2 = \frac{m_{sa}}{m_{sd}} \quad (\text{E-5})$$

and eliminate w_G and w_{pd} from Equations E-1 to E-3; then

$$\frac{w_p}{m_{sd}} = \left(\frac{\lambda_2}{\lambda_2 - f} \right) [(1 + k_1) f + (k_2 - 1) q] \equiv h_T \quad (\text{E-6})$$

where

$$f = \frac{K_a K_d - 1}{K_a K_d} \quad (\text{E-7})$$

$$q = \frac{K_a - 1}{K_a} \quad (\text{E-8})$$

For the NOOS stage, the relations are

$$\frac{W_G}{W_G - W_{p12}} = \exp \left[\frac{\Delta V_{12}}{I_1 g} \right] \equiv K_{12} \quad (\text{E-9})$$

$$\frac{W_G - W_{p12} - (M_{sd} - M_{sa}) - w_p}{W_G - W_p - (M_{sd} - M_{sa}) - w_p} = K_{12} \quad (\text{E-10})$$

$$W_G = \frac{W_p}{\lambda_1} + M_{sd} + w_p + M_c \quad (\text{E-11})$$

When the LOSS mission mode is employed, $\Delta V_{12} = 4054$ mps (13,300 fps). With the HOSS mission mode, $\Delta V_{12} = 3475$ mps (11,400 fps). Define

$$a_1 = \frac{M_c}{M_{sd}} \quad (\text{E-12})$$

$$a_2 = \frac{M_{sa}}{M_{sd}} \quad (\text{E-13})$$

$$m_{sd} = \beta M_{sd} \quad (0 \leq \beta \leq 1) \quad (\text{E-14})$$

and the foregoing equations will reduce to the overall performance function*

$$\frac{W_{pT}}{M_{sd}} = \left(\frac{\lambda_1}{\lambda_1 - F} \right) [(1 + \beta h_T) H + \alpha_1 F + \alpha_2 G] + \beta h_T \quad (\text{E-15})$$

where

$$F = \frac{K_{12}^2 - 1}{K_{12}^2} \quad (\text{E-16})$$

$$G = \frac{K_{12} - 1}{K_{12}} \quad (\text{E-17})$$

$$H = \frac{K_{12} - 1}{K_{12}^2} \quad (\text{E-18})$$

*This formula can be used for a two-stage HOSS-based tug if the function h_T is simply replaced with Equation D-16. However, it should be recalled that the same symbols have different meanings in Appendices D and E.



Appendix F

Derivation of Performance Function for a Lunar Shuttle System With a Two-Stage COOS

With the use of Equations 9 to 11 and Figures 45 and 46, the basic relations for the second stage of the COOS can be written

$$\frac{w_G}{w_G - w_{p34}} = \exp \left[\frac{\Delta V_{34}}{I_2 g} \right] \equiv K_{34} \quad (\text{F-1})$$

$$\frac{w_G - w_{p34} - (m_{sd} - m_{sa}) - w'_p}{w_G - w_p - (m_{sd} - m_{sa}) - w'_p} = \exp \left[\frac{\Delta V_{56}}{I_2 g} \right] \equiv K_{56} \quad (\text{F-2})$$

$$w_G = \frac{w_p}{\lambda_2} + m_{sd} + w'_p + m_c \quad (\text{F-3})$$

For the LOSS mission mode, $\Delta V_{34} = 1768$ mps (5800 fps), and $\Delta V_{56} = 4054$ mps (13,300 fps). For the HOSS mission mode, $\Delta V_{34} = 1494$ mps (4900 fps), and $\Delta V_{56} = 3475$ mps (11,400 fps). From Equations F-1 to F-3 and previous results from Appendices D and E, it can be shown that

$$\frac{w_p}{m_{sd}} = \left(\frac{\lambda_2}{\lambda_2 - f} \right) [(1 + \alpha_1) f + (\alpha_2 - 1) q + \beta (f - q) h_T] \equiv h \quad (\text{F-4})$$

where

$$\alpha_1 = \frac{m_c}{m_{sd}} \quad (\text{F-5})$$

$$\alpha_2 = \frac{m_{sa}}{m_{sd}} \quad (\text{F-6})$$

$$\beta = \frac{(m_{sd})_T}{m_{sd}} \quad (\text{F-7})$$

$$f = \frac{K_{34} K_{56} - 1}{K_{34} K_{56}} \quad (\text{F-8})$$

$$q = \frac{K_{56} - 1}{K_{56}} \quad (\text{F-9})$$

and $(m_{sd})_T$ is the payload delivered to the lunar surface. The function h_T is obtained from Equation D-16 for the HOSS mission mode or from Equation E-6 when LOSS staging is used. (Note that the same symbols have different meanings in Appendices D, E, and F).

For the first stage of the COOS, the relations are

$$\frac{W_G}{W_G - W_{p12}} = \exp \left[\frac{\Delta V_{12}}{I_1 g} \right] \equiv K_{12} \quad (\text{F-10})$$

$$\frac{W_G - W_{p12} - w_G}{W_G - W_p - w_G} = K_{12} \quad (\text{F-11})$$

$$W_G = \frac{W_p}{\lambda_1} + M_c + w_G \quad (\text{F-12})$$

with $\Delta V_{12} = 2286$ mps (7500 fps) for the LOSS mission mode and $\Delta V_{12} = 1981$ mps (6500 fps) for the HOSS mission mode. Finally, a little bit of algebra leads to the overall performance function

$$\frac{W_{pT}}{m_{sd}} = \left(\frac{\lambda_1}{\lambda_1 - F} \right) [(1 + \gamma) F - G] \left[\frac{h}{\lambda_2} + (1 + \alpha_1) + \beta h_T \right] + h + \beta h_T \quad (\text{F-13})$$

where

$$\gamma = \frac{M_c}{w_G} \quad (\text{F-14})$$

$$F = \frac{K_{12}^2 - 1}{K_{12}^2} \quad (\text{F-15})$$

$$G = \frac{K_{12} - 1}{K_{12}} \quad (\text{F-16})$$



NATIONAL AERONAUTICS AND SPACE ADMINISTRATION

WASHINGTON, D. C. 20546

OFFICIAL BUSINESS

PENALTY FOR PRIVATE USE \$300

FIRST CLASS MAIL



POSTAGE AND FEES PAID
NATIONAL AERONAUTICS AND
SPACE ADMINISTRATION

POSTMASTER: If Undeliverable (Section 158
Postal Manual) Do Not Return

"The aeronautical and space activities of the United States shall be conducted so as to contribute . . . to the expansion of human knowledge of phenomena in the atmosphere and space. The Administration shall provide for the widest practicable and appropriate dissemination of information concerning its activities and the results thereof."

— NATIONAL AERONAUTICS AND SPACE ACT OF 1958

NASA SCIENTIFIC AND TECHNICAL PUBLICATIONS

TECHNICAL REPORTS: Scientific and technical information considered important, complete, and a lasting contribution to existing knowledge.

TECHNICAL NOTES: Information less broad in scope but nevertheless of importance as a contribution to existing knowledge.

TECHNICAL MEMORANDUMS: Information receiving limited distribution because of preliminary data, security classification, or other reasons.

CONTRACTOR REPORTS: Scientific and technical information generated under a NASA contract or grant and considered an important contribution to existing knowledge.

TECHNICAL TRANSLATIONS: Information published in a foreign language considered to merit NASA distribution in English.

SPECIAL PUBLICATIONS: Information derived from or of value to NASA activities. Publications include conference proceedings, monographs, data compilations, handbooks, sourcebooks, and special bibliographies.

TECHNOLOGY UTILIZATION PUBLICATIONS: Information on technology used by NASA that may be of particular interest in commercial and other non-aerospace applications. Publications include Tech Briefs, Technology Utilization Reports and Technology Surveys.

Details on the availability of these publications may be obtained from:

SCIENTIFIC AND TECHNICAL INFORMATION OFFICE

NATIONAL AERONAUTICS AND SPACE ADMINISTRATION

Washington, D.C. 20546